

แอมเบอร์ไลท์เอ็กซ์เอดี-2 ที่มีหมู่ฟังก์ชันเพอร์ฟลูออโรสำหรับสกัดไอออนโลหะหนัก
ในน้ำสกัดที่ได้จากกากของเสียที่หล่อแข็งโดยปูนซีเมนต์



นางสาวมาริสตา วงษ์แก้ว

สถาบันวิทยบริการ จุฬาลงกรณ์มหาวิทยาลัย

วิทยานิพนธ์นี้เป็นส่วนหนึ่งของการศึกษาตามหลักสูตรปริญญาวิทยาศาสตรมหาบัณฑิต

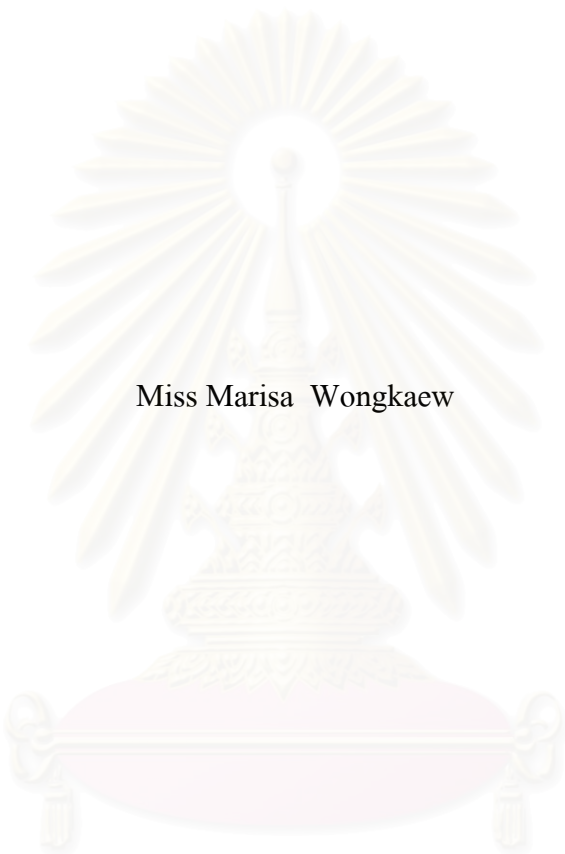
สาขาวิชาเคมี ภาควิชาเคมี

คณะวิทยาศาสตร์ จุฬาลงกรณ์มหาวิทยาลัย

ปีการศึกษา 2550

ลิขสิทธิ์ของจุฬาลงกรณ์มหาวิทยาลัย

PURPURIN FUNCTIONALIZED AMBERLITE XAD-2 FOR EXTRACTION OF HEAVY
METAL IONS IN LEACHATE FROM CEMENT-BASED STABILIZED WASTE



Miss Marisa Wongkaew

A Thesis Submitted in Partial Fulfillment of the Requirements
for the Degree of Master of Science Program in Chemistry

Department of Chemistry

Faculty of Science

Chulalongkorn University

Academic Year 2007

Copyright of Chulalongkorn University


Thesis Title PURPURIN FUNCTIONALIZED AMBERLITE XAD-2 FOR
EXTRACTION OF HEAVY METAL IONS IN LEACHATE FROM
CEMENT-BASED STABILIZED WASTE

By Miss Marisa Wongkaew


Field of Study Chemistry

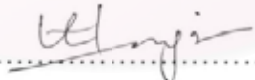
Thesis Advisor Assistant Professor Apichat Imyim, Ph.D.


Accepted by the Faculty of Science, Chulalongkorn University in Partial
Fulfillment of the Requirements for the Master's Degree



..... Dean of the Faculty of Science
(Professor Piamsak Menasveta, Ph.D.)


THESIS COMMITTEE


..... Chairman
(Associate Professor Sirirat Kokpol, Ph.D.)


..... Thesis Advisor
(Assistant Professor Apichat Imyim, Ph.D.)


..... Member
(Associate Professor Thawatchai Tuntulani, Ph.D.)


..... Member
(Assistant Professor Pakorn Varanusupakul, Ph.D.)


..... Member
(Panya Sunintaboon, Ph.D.)

มาริสา วงษ์แก้ว : แอมเบอร์ไลท์เอ็กซ์เอดี-2 ที่มีหมู่ฟังก์ชันเพอร์ฟูรินสำหรับสกัดไอออนโลหะหนักในน้ำสกัดที่ได้จากกากของเสียที่หล่อแข็งโดยปูนซีเมนต์. (PURPURIN FUNCTIONALIZED AMBERLITE XAD-2 FOR EXTRACTION OF HEAVY METAL IONS IN LEACHATE FROM CEMENT-BASED STABILIZED WASTE) อ.ที่ปรึกษา: ผศ.ดร.อภิชาติ อิ่มยิ้ม, 111 หน้า.

สังเคราะห์คีเลตเชิงเรซินชนิดใหม่โดยเชื่อมต่อกีเลตลิงลิแกนด์เพอร์ฟูรินบนสารรองรับของแข็งพอลิเมอร์แอมเบอร์ไลท์เอ็กซ์เอดี-2 ผ่านทางพันธะเอโซ (-N=N-) และติดตามหาลักษณะเฉพาะของผลิตภัณฑ์ที่สังเคราะห์ได้ด้วยกล้องจุลทรรศน์อิเล็กตรอนแบบส่องกราด การวิเคราะห์ปริมาณธาตุที่เป็นองค์ประกอบ ฟลูออรีนทรานสฟอร์มอินฟราเรดและรามานสเปกโทรสโกปีและการวิเคราะห์เชิงความร้อน ศึกษาภาวะที่เหมาะสมในการสกัดไอออนโลหะแคดเมียม โครเมียม และตะกั่ว ในเมทริกซ์สองชนิด คือ น้ำสกัดปูนซีเมนต์และน้ำปราศจากไอออนด้วยการสกัดแบบเบบท์และคอลัมน์ และวิเคราะห์ปริมาณไอออนโลหะด้วยเทคนิคเฟลมอะตอมมิคแอบซอร์บชันสเปกโทรเมตรี ผลการทดลองพบว่า พีเอช 4.0 คือ พีเอชที่เหมาะสมในการสกัดไอออนโลหะทั้งหมดในเมทริกซ์ทั้งสองชนิด การดูดซับไอออนโลหะทั้งหมดจะเข้าสู่สมดุลภายในเวลา 1 ชั่วโมง ไอออนแคดเมียมและตะกั่วที่ถูกดูดซับบนเรซินสามารถชะออกได้โดยใช้ 1% กรดไนตริก ภายในเวลา 10 นาที โดยมีร้อยละการกลับคืนของการชะมากกว่า 90% สำหรับการชะไอออนโครเมียมทำได้โดยใช้ 10% ไฮโดรเจนเปอร์รอกไซด์ในโซเดียมไฮดรอกไซด์ 0.1 โมลาร์ ภายในเวลา 30 นาที โดยมีร้อยละการกลับคืนของการชะมากกว่า 80% ความจุในการดูดซับไอออนแคดเมียม โครเมียม และตะกั่วบนคีเลตเชิงเรซินมีค่าเท่ากับ 75.0, 68.2, 82.7 ไมโครโมลต่อกรัมเรซิน สำหรับเมทริกซ์ที่เป็นน้ำปราศจากไอออน และ 54.1, 46.5 และ 55.7 ไมโครโมลต่อกรัมเรซิน สำหรับน้ำสกัดเมทริกซ์ ตามลำดับ การทดลองนี้มีข้อจำกัดสำหรับการสกัดในระบบคอลัมน์ อย่างไรก็ตามสามารถเพิ่มประสิทธิภาพของการสกัดได้โดยใช้ระบบการวนสารละลายผ่านคอลัมน์ วิธีการสกัดแบบเบบท์โดยใช้คีเลตเชิงเรซินที่สังเคราะห์ได้ใหม่นี้ มีความแม่นยำสูง โดยให้ร้อยละการกลับคืนของไอออนแคดเมียมและตะกั่วเท่ากับ 86.5 และ 89.9% ตามลำดับ และเมื่อทำการทดลองซ้ำ 14 ครั้ง พบว่า %RSD มีค่าต่ำกว่า 2.3%

ภาควิชา.....เคมี.....ลายมือชื่อนิสิต มารีสา วงษ์แก้ว
สาขาวิชา.....เคมี.....ลายมือชื่ออาจารย์ที่ปรึกษา.....
ปีการศึกษา.....2550.....

487 38413 23 : MAJOR CHEMISTRY

KEY WORD : PURPURIN / AMBERLITE XAD-2 / CHELATING RESIN / CEMENT-BASED STABILIZED WASTE

MARISA WONGKAEW: PURPURIN FUNCTIONALIZED AMBERLITE XAD-2 FOR EXTRACTION OF HEAVY METAL IONS IN LEACHATE FROM CEMENT-BASED STABILIZED WASTE. THESIS ADVISOR: ASST.PROF. APICHAT IMYIM, Ph.D., 111 pp.

A new chelating resin was synthesized by functionalizing the polymer support, Amberlite XAD-2 with the chelating ligand, purpurin through an azo linkage (-N=N-). The products were characterized by scanning electron microscopy, elemental analysis, Fourier transforms infrared and Raman spectroscopy and thermal gravimetric analysis. The optimum conditions for the extraction of Cd^{2+} , Cr^{3+} and Pb^{2+} in both matrices: leachate from cement-based material and DI water; were studied by batch and column methods. The determination of the metal ions was carried out by flame atomic absorption spectrometry. The optimum pH for the extraction of all the metal ions in both matrices was at 4.0. Their sorption equilibria were reached within 1 h. The sorbed Cd^{2+} and Pb^{2+} were desorbed by 1% HNO_3 within 10 min with the desorption recovery of >90%. For the elution of Cr^{3+} by 10% H_2O_2 in 0.1 M NaOH was achieved within 30 min with the desorption recovery of >80%. The sorption capacity of Cd^{2+} , Cr^{3+} and Pb^{2+} onto the resin was 75.0, 68.2, 82.7 $\mu\text{mol g}^{-1}$ resin in DI water and 54.1, 46.5 and 55.7 $\mu\text{mol g}^{-1}$ resin for the leachate, respectively. The column method has a limitation for this experiment, however, the extraction efficiency can be improved using the recirculation system. This new method gave a good accuracy in batch system at 86.5 and 89.9% recovery for Cd^{2+} and Pb^{2+} and %RSD less than 2.3% (n=14).

Department..... Chemistry..... Student's signature..... Marisa Wongkaew.....
 Field of study..... Chemistry..... Advisor's signature..... *Uthai*.....
 Academic year..... 2007.....

ACKNOWLEDGEMENTS

I wish to thank my advisor, Assistant Professor Dr. Apichat Imyim for suggestions, assistance, and encouragement. And extend my appreciation to Associate Professor Dr. Sirirat Kokpol; Associate Professor Dr. Thawatchai Tuntulani; Dr. Pakorn Varanusupakul; and Dr. Panya suninthaboon; for their valuable suggestions as my thesis committees.

This work cannot be completed without kindness and helps of many people. I would like to thank Dr. Wanlapa Aeungmaitrepirom, Assistant Professor Dr. Fuangfa Unob, and Lecturer Ponwason Eamchan for their suggestions teaching and helps. Next, I would like to thank all of many people in the Environmental Analysis Research Unit for their friendship and the good supports. Thesis Supporting Fund, Graduate School Chulalongkorn University, and the 90th Years Anniversary of Chulalongkorn University (Ratchadaphiseksomphot Endowment Fund) were acknowledged.

Finally, I am grateful to my family for their support, entirely care, encouragement and love. The usefulness of this work, I dedicate to my father, my mother and all the teachers who have taught me since my childhood.

สถาบันวิทยบริการ
จุฬาลงกรณ์มหาวิทยาลัย

CONTENTS

	page
ABSTRACT (IN THAI).....	iv
ABSTRACT (IN ENGLISH).....	v
ACKNOWLEDGEMENTS.....	vi
CONTENTS.....	vii
LIST OF TABLES.....	xii
LIST OF FIGURES.....	xiv
LIST OF SYMBOLS AND ABBREVIATIONS.....	xvi
CHAPTER I INTRODUCTION.....	1
1.1 Statement of the Problem.....	1
1.2 Scope of the Research.....	3
1.3 The Benefits of This Research.....	3
CHAPTER II THEORY AND LITERATURE REVIEW.....	4
2.1 Heavy Metals in Hazardous Waste.....	4
2.1.1 Toxicity of Heavy Metals.....	4
2.1.1.1 Cadmium.....	4
2.1.1.2 Chromium.....	4
2.1.1.3 Lead.....	5
2.1.2 Heavy Metals in Water.....	7
2.1.3 Solid Hazardous Waste.....	8
2.2 Leaching Procedure.....	10
2.2.1 Types of Leaching Tests.....	10
2.2.2 Regulatory Leaching Tests.....	11

	page
2.2.3 Assessment of Treated Waste from Solidification/Stabilization	
Process.....	15
2.3 Metal Determination.....	17
2.3.1 Atomic Spectroscopy.....	17
2.3.1.1 Atomic absorption spectroscopy (AAS).....	17
2.3.1.2 Atomic emission spectroscopy (AES).....	17
2.3.1.3 Atomic fluorescence spectroscopy (AFS).....	17
2.3.2 Elemental Mass Spectrometry.....	18
2.3.3 The Chromatography of Ions.....	18
2.4 Solid Phase Extraction.....	19
2.4.1 Objectives of Solid Phase Extraction	19
2.4.2 Four Steps of Solid Phase Extraction.....	20
2.4.3 Sorption Process.....	23
2.4.4 Sorbents in Solid Phase Extraction.....	26
2.4.4.1 Inorganic based sorbents.....	27
2.4.4.2 Organic based sorbents	28
2.5 Equilibrium Adsorption Models.....	30
2.5.1 The BET Adsorption Model.....	31
2.5.2 Langmuir Adsorption Isotherms.....	32
2.5.3 Freundlich Adsorption Isotherms.....	33
2.6 Characterization Techniques of Functionalized Polymers.....	34
2.6.1 Scanning Electron Microscope (SEM).....	34
2.6.2 Elemental Analysis (EA).....	34
2.6.3 Fourier Transforms Infrared Spectroscopy (FT-IR).....	35
2.6.4 Fourier Transforms Raman Spectroscopy (FT-Raman).....	35
2.6.5 Thermal Gravimetric Analysis (TGA).....	36
2.7 Literature Review.....	38

	page
2.8 Conclusion.....	40
CHAPTER III EXPERIMENTAL SECTIONS.....	42
3.1 Apparatus.....	42
3.2 Chemicals and Preparation of Reagents.....	44
3.2.1 Chemicals.....	44
3.2.2 Preparation of Reagents.....	45
3.3 Synthesis of Amberlite XAD-2 Functionalized with Purpurin.....	46
3.4 Characterization.....	47
3.4.1 Characterization of Resins.....	47
3.5 Appropriate Amount of Purpurin for XAD-P Synthesis.....	48
3.6 Influence of Leachate on Metal Ion Calibration Curve.....	48
3.7 Synthetic Sample (Leachate).....	48
3.8 Extraction and Desorption Studies.....	49
3.8.1 Batch Method.....	49
3.8.1.1 Effect of pH on metal extraction.....	50
3.8.1.2 Kinetics of metal extraction.....	50
3.8.1.3 Effect of eluent.....	51
3.8.1.4 Effect of elution time.....	51
3.8.1.5 Adsorption isotherm.....	51
3.8.2 Column Method.....	52
3.8.2.1 Effect of flow rate.....	52
3.8.2.2 Recirculation of sample solution.....	52
3.8.2.3 Desorption study.....	52
3.9 Method Validation.....	53

	page
CHAPTER IV RESULTS AND DISCUSSION.....	54
4.1 Synthesis of Amberlite XAD-2 Functionalized with Purpurin.....	54
4.2 Characterization of Amberlite XAD-2 Functionalized with Purpurin.....	57
4.2.1 Scanning Electron Microscopy.....	57
4.2.2 Elemental Analysis.....	58
4.2.3 Fourier Transforms Infrared Spectroscopy.....	60
4.2.4 Fourier Transforms Raman Spectroscopy.....	64
4.2.5 Thermal Gravimetric Analysis.....	66
4.3 Appropriate Amount of Purpurin for XAD-P Synthesis.....	69
4.4 Influence of Leachate on Metal Ion Calibration Curve.....	72
4.5 Extraction and Desorption Studies.....	75
4.5.1 Batch Method.....	75
4.5.1.1 Effect of pH on the metal extraction.....	75
4.5.1.2 Kinetics of metal extraction.....	80
4.5.1.3 Effect of eluent.....	83
4.5.1.4 Effect of elution time.....	86
4.5.1.5 Adsorption isotherm.....	87
4.5.2 Column Method.....	94
4.5.2.1 Effect of flow rate.....	94
4.5.2.2 Recirculation of sample solution.....	96
4.5.2.3 Desorption study.....	97
4.6 Method validation.....	98
CHAPTER V CONCLUSION.....	100
REFERENCES.....	103

VITA..... 111



สถาบันวิทยบริการ
จุฬาลงกรณ์มหาวิทยาลัย

LIST OF TABLES

Table	page
2.1 The various compounds of cadmium used in industrial.....	6
2.2 Drinking water quality standards.....	6
2.3 Comparisons of batch test with column test.....	11
2.4 The regulation of heavy metal founded in leachate.....	16
2.5 Hard and soft acids.....	24
2.6 Hard and soft bases.....	25
2.7 Differences and complementary power of Infrared and Raman Microscopy.....	37
3.1 Apparatus lists.....	42
3.2 Operating parameters in FAAS.....	43
3.3 Chemicals lists.....	44
3.4 Concentration of metal ion and amount of XAD-P for studying the effect of pH.....	50
4.1 Elemental composition of product in each synthesis step.....	58
4.2 Paired t-test between the determination of metal ion in leachate and DI water matrix.....	74
4.3 Comparison of pH solution after sorption.....	77
4.4 Summary the data from the Lagergren plot.....	81
4.5 Effect of EDTA and H ₂ O ₂ concentration for the Cr ³⁺ desorption.....	84
4.6 The relationship of R_L value and type of isotherm.....	89
4.7 Langmuir parameters for the adsorption of metal ions.....	91
4.8 Freundlich parameters for the adsorption of metal ions.....	91
4.9 Comparison of sorption capacities of XAD-P with other functionalized Amberlite XAD-2 in DI water.....	93

Table		page
4.10	Comparison of the percent stripping of metal ions by the column and batch methods.....	97
4.11	Recovery and precision of the proposed method.....	98
4.12	Analyte recovery and precision at different concentration.....	99
5.1	Optimum conditions for the sorption and desorption of metal ions on XAD-P.....	101



สถาบันวิทยบริการ
จุฬาลงกรณ์มหาวิทยาลัย

LIST OF FIGURES

Figure	page
2.1 Effect of solution pH toward the precipitation of metal ions.....	8
2.2 Method 1312 synthetic precipitation leaching procedure.....	13
2.3 Four typical steps of SPE.....	21
2.4 C ₁₈ activated with n-hexane.....	21
2.5 Sorbents based on inorganic supports.....	26
2.6 Sorbents based on organic support.....	27
2.7 Form of BET adsorption isotherm.....	31
2.8 Linear form of BET adsorption isotherm.....	31
2.9 Form of Langmuir adsorption isotherm.....	32
2.10 (a) Conventional linear form of Langmuir adsorption isotherm (b) Modified form of Langmuir adsorption isotherm emphasizing higher concentration data.....	32
2.11 Form of Freundlich adsorption isotherm.....	33
2.12 Linear form of Freundlich adsorption isotherm.....	33
2.13 Chemical structure of Amberlite XAD-2 polymeric sorbent.....	40
2.14 Structure of chelating ligand, purpurin.....	40
3.1 Reaction sequence of the synthesis of the chelating resin.....	46
4.1 Mechanism of the nitration.....	54
4.2 Mechanism of the diazotization.....	55
4.3 The proposed structure of XAD-P through the diazonium coupling reaction.....	56
4.4 SEM photographs.....	57
4.5 Carbon number of purpurin for the IR spectrum discussion.....	62
4.6 Electron withdraw effect of azo group through sigma bond.....	62

Figure	page
4.7 Infrared spectra.....	63
4.8 Raman spectra.....	63
4.9 Thermograms of XAD-P.....	67
4.10 Comparison thermograms.....	68
4.11 Comparison differentiate thermograms.....	68
4.12 The proposed structure of purpurin in basic medium after stirred with XAD-P.....	69
4.13 Reference absorption spectrum of purpurin in 50% ethanol.....	70
4.14 Absorption spectra of eluted purpurin.....	71
4.15 Comparisons of the amount of starting purpurin (in parenthesis), purpurin adsorbed on XAD-P and percent loading.....	71
4.16 Comparison of calibration curve between preparing standard in leachate and DI water matrix.....	73
4.17 Metal hydroxide solubility curve versus pH.....	74
4.18 Concentration of each metal ion before extraction at different pH.....	77
4.19 Effect of pH on metal extraction.....	78
4.20 Species distribution diagrams versus pH.....	79
4.21 Kinetics of metal extraction on XAD-P.....	82
4.22 Effect of HNO ₃ concentration on metal desorption.....	85
4.23 Effect of elution time.....	86
4.24 Proposed three chelation sites on XAD-P.....	90
4.25 Saturation adsorption and Langmuir adsorption isotherm fitting.....	92
4.26 Effect of solution flow rate on metal extraction.....	95
4.27 Effect of recirculation of sample solution.....	96

LIST OF SYMBOLS AND ABBREVIATIONS

EA	Elemental analysis
FAAS	Flame atomic absorption spectrometry
FT-IR	Fourier transforms infrared spectroscopy
FT-Raman	Fourier transforms Raman spectroscopy
LLE	Liquid liquid extraction
RSD	Relative standard deviation
SPE	Solid phase extraction
SEM	Scanning electron microscope
S/S	Solidification/stabilization
SPLP	Synthetic precipitation leaching procedure
TGA	Thermal gravimetric analysis
TCLP	Toxicity characteristic leaching procedure
XAD-2	Amberlite XAD-2
XAD-NO ₂	Amberlite XAD-2 after nitration
XAD-NH ₂	Amberlite XAD-2 after reduction
XAD-P	Amberlite XAD-2 functionalized with purpurin
ν	Stretching vibration
δ	Bending vibration

CHAPTER I

INTRODUCTION

1.1 Statement of the Problem

The cement-based solidification/stabilization (s/s) process is a well known method for the disposal of solid contaminated heavy metal hazardous wastes [1] because of its low price, ability to improve physical characteristics (solidification) and to reduce the toxicity and mobility of contaminants (stabilization). The product from s/s process can dispose to a landfill or use in a construction purpose. However the effectiveness of s/s treatment should be considered to prevent the release of heavy metals from the s/s waste to the environment, especially into water resources.

In 1997, the Ministry of Industry of Thailand announced the regulation for a testing of toxicity of the treated waste from the s/s process using the leaching extraction procedure, modified from the EPA method 1312. The leaching level of toxic heavy metals that has to be controlled in this regulation must not be more than 5.0, 100.0, 1.0, 5.0, 5.0, 0.2, 1.0 and 5.0 mg L⁻¹ for As, Ba, Cd, Cr, Pb, Hg, Se and Ag, respectively. If the concentration of the heavy metals leaching out from the treated waste using s/s process is equal or more than the regulatory level, the waste is identified to a leachable substance which must retreated before the disposal. The basic method for the determination of these metals is flame atomic absorption spectrometry (FAAS), due to its accuracy and precision, high sensitivity, good selectivity, low operation cost and its ability to determine various metals (more than 60 metals) [2].

The heavy metals in s/s products are dissolved in a leachant (extraction fluid), the solution becomes a complicated leachate that contains high concentration of calcium ions dissolved from the cement matrix and others elements such as Si, Al and Fe [3]. This matrix can affect the correct determination of heavy metals because their

concentration in the leachate is much less than that of calcium ions. In addition, the high concentration of calcium may cause a short life time of burner of FAAS and need to clean the burner often in order to gain correct results. An extraction of heavy metals from the leachate matrix before the determination is suggested to overcome those problems.

Several separation techniques of metal ions from the matrix interference consist of coprecipitation, liquid-liquid extraction or solid phase extraction. Processes involving solid-phase extraction show several advantages, such as selectivity, availability and easy recovery of sorbent, attainability of high preconcentration factors, facility of handling and eco-friendliness [4, 5].

To improve the selectivity towards metal ions, the chelating resin is very attractive. Chelating resin consists of two main parts, the first part is a solid support. Styrene-divinylbenzene commercially available as Amberlite XAD resin series has found to be a good solid support to load the chelating ligands due to its good physical and chemical properties such as porosity, high surface area, durability and purity [6]. The second part is a chelating ligand that is an important part to extract or chelate the metal ions onto the chelating resin. The nature of chelating ligand is a molecule that has donor atoms or binding site to form a complex with a metal ion. The selectivity can attribute to the size of the chelate ring and the metal atom, type of donor atoms (hard or soft), oxidation state of the metal ion and pH of the solvent system [7]. The two means for attaching the chelating ligand to the polymer solid support are impregnation through a physical adsorption and a functionalization which is a chemical bonding based on covalent coupling of the ligand with the polymer backbone through a spacer arm, generally an -N=N- group [7-11]. The functionalized sorbent is more stronger system and free from chelating ligand leaching problem [8].

This research focused on the synthesis and characterization of a chelating resin using Amberlite XAD-2 functionalized with purpurin (XAD-P) through -N=N- group followed by the studies on various parameters that operated in the process of

quantitative extraction of Cd^{2+} , Cr^{3+} and Pb^{2+} . These metals were selected from the list of toxic heavy metals in leachate since they were usually found in factory hazardous wastes [3, 12, 13]. The practical applicability of the new chelating resin to extract metal ions from the synthetic leachate has been tested.

1.2 Scope of the Research

The scope of this research was firstly a synthesis and characterization of the new chelating resin XAD-P through $-\text{N}=\text{N}-$ group. Scanning Electron Microscopy (SEM), Elemental Analysis (EA), Fourier Transforms Infrared Spectroscopy (FT-IR), Fourier Transforms Raman Spectroscopy (FT-Raman) and Thermal Gravimetric Analysis (TGA) were used for the characterization of the synthesized products. Moreover, the appropriate amount of purpurin for the synthesis of the chelating resin was investigated.

The influence of leachate on metal ion calibration curve was checked. Thereafter, optimum conditions in both batch and column methods were studied, i.e. the effect of pH on metal extraction, the kinetics of metal extraction, the effect of eluent (in batch method), the effect of elution time, the adsorption isotherm, the effect of flow rate, the recirculation of sample solution, and the desorption study (in column method). The optimum conditions for the extraction of metal ions were investigated in both leachate and deionized water matrix. The determination of the metal ions was accomplished using FAAS.

Finally, the proposed method for the extraction of Cd^{2+} , Cr^{3+} and Pb^{2+} from leachate matrix was validated.

1.3 The Benefits of This Research

A new chelating resin for extraction of heavy metal ions in leachate from cement-based stabilized waste was achieved

CHAPTER II

THEORY AND LITERATURE REVIEW

2.1 Heavy Metals in Hazardous Waste

Hazardous waste is a waste that can harmful to human, animal, or environment such as a water containing pesticides from agricultural activities and the by-products of manufacturing processes [14]. This research emphasizes the heavy metals contained hazardous waste that can be harmful to human or animal at a very low contamination level.

2.1.1 Toxicity of Heavy Metals

2.1.1.1 Cadmium

Cadmium is an extremely toxic metal commonly found in industrial workplaces, particularly where any ore is being processed or smelted. Cadmium is used extensively in electroplating and present in the manufacture of some types of batteries [15]. The target organ of cadmium toxicity is the kidney, other adverse effects may occur in the bones and stomach. This was observed in a syndrome known as "itai-itai" in Japan. It occurred as a result of consuming cadmium-contaminated rice. The various compounds of cadmium used in industrial are shown in Table 2.1 [16].

2.1.1.2 Chromium [17, 18]

Chromium enters the environment mostly in the chromium (III) and chromium (VI) forms. Chromium species can contaminate in the environment from the effluent discharge from steel industries, electroplating, tanning industries, oxidative dyeing, chemical industries and cooling water towers. They may also enter drinking water

supply systems from the corrosion inhibitors used in water pipes and containers or by contamination of the underground water from sanitary landfill leaching.

Chromium (III) Chromium (III) is an essential nutrient that helps the body use sugar, protein, and fat. Cr (III) is a very stable oxidation state for chromium. It is not a strong oxidizer and the human's natural body acidity is enough for the chrome to keep to this Cr (III) state.

Chromium (VI) Cr (VI), a very strong oxidizing agent, is more toxic than Cr (III). Uptake the Cr (VI) into the body can cause the irritation to the nose, stomach upsets, kidney liver and skin damage, and even death.

2.1.1.3 Lead

Lead is a toxic metal, which accumulates in the vital organs of human and animals. Although lead is absorbed very slowly into the body, its rate of excretion is even slower [19]. Lead can be emitted into the biosphere as a fuel additive, mainly as tetraethyllead and tetramethyllead and present in many industrial streams [17]. It causes the hematological damage, anemia, kidney malfunctioning or brain damage, etc.

To remark the toxicity of heavy metals, the drinking water quality standards is shown in Table 2.2. Their maximum acceptable concentrations are very low at trace level. Therefore, the determination of toxic metal at trace level is very important for human health.

Table 2.1 The various compounds of cadmium used in industrial

<i>Compounds of cadmium</i>	<i>Industrial uses</i>
Cadmium oxide	used in batteries as an intermediate and catalyst in electroplating
Cadmium sulphide	used as a pigment in paint
Cadmium sulphate	used as an intermediate in electroplating
Cadmium stearate	used as a plastic stabilizer
Cadmium chloride	used in photography and in dyes

Table 2.2 Drinking water quality standards [20]

<i>Properties</i>	<i>Parameters</i>	<i>standards</i>
		<i>Maximum Acceptable Concentration (mg L⁻¹)</i>
Toxic elements	1. Mercury (Hg)	0.001
	2. Lead (Pb)	0.05
	3. Arsenic (As)	0.05
	4. Selenium (Se)	0.01
	5. Chromium (Cr VI)	0.05
	6. Cyanide (CN)	0.2
	7. Cadmium (Cd)	0.01
	8. Barium (Ba)	1.0

2.1.2 Heavy Metals in Water

Heavy metal contamination in water resources is a major concern because it can diffuse easily to other sources. Their toxicity to human and animal draws attention towards finding suitable remediation technologies for these metals.

Various water treatment technologies such as conventional precipitation with hydroxide or sulfide; enhanced precipitation using dimethyl thiocarbamate, diethyl thiocarbamate, trimercapto-s-triazine or trisodium salt; ion exchange; and adsorption have been extensively used for the removal of heavy metal from the water.

Among of these techniques, the heavy metals removal using conventional precipitation as metal hydroxide is widely used since metal hydroxides are insoluble and easy to remove metals by this process. The main problem for this process is the precipitation as metal hydroxide of different metals is occurred at different pH (see Figure 2.1), i.e. some of the metal hydroxide will disassociate with the resulting metal ions going back into solution. The most common reagents used for hydroxide precipitation are caustic soda (NaOH), lime (CaO), and magnesium hydroxide (Mg(OH)₂)

Soluble metals can also be removed by precipitating them as a sulfide by the addition of sodium sulfide to the solution. This method yields more complete metal removal than hydroxide precipitation but can easily leave toxic sulfides in solution. This method is much more expensive than hydroxide precipitation since the excess sulfides are usually regulated and the resulting sludge may be difficult to landfill. Therefore, it is not as widely used as hydroxide precipitation [21].

After water treatment process using precipitation as metal hydroxide, the large amounts of sludge with high concentration of metals were produced. The treatment of these sludges is necessary before landfilling. The sludge treatment method will be explained in the next topic.

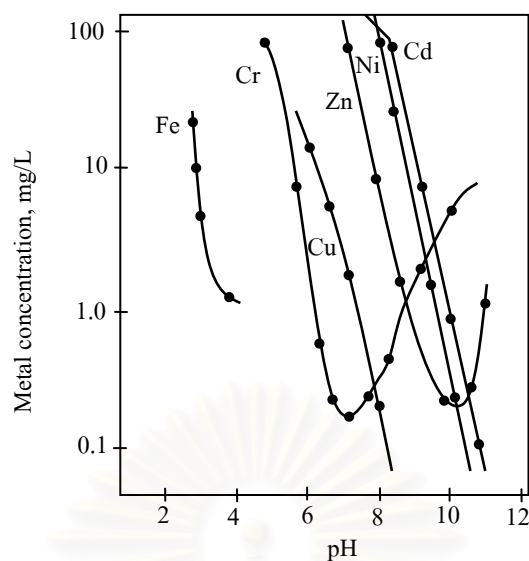


Figure 2.1 Effect of solution pH towards the precipitation of metal ions.

2.1.3 Solid Hazardous Waste

This topic will cover the information on solid hazardous waste containing heavy metals such as sludge generated from a water treatment process by precipitation of metal ions as metal hydroxides. This sludge cannot be disposed directly into a landfill due to the risk to underground water contamination. Therefore, the treatment of sludge before disposal to the landfill is required. One dominant method of sludge disposal is the cement-based solidification/stabilization process [3].

Solidification/stabilization (s/s) was used to treat nuclear wastes in the 1950s and then was widely applied to hazardous wastes in the early 1970s. Most applications of s/s are cement-based, Treatment by cement-based s/s combines two processes that occur simultaneously to produce a material that will have reduced environmental impact when disposed or reused. Two processes of s/s are discussed below [1].

a) Solidification

Solidification is the process that changes the physical properties of the waste material, so a solidified waste will reduce the free liquids composition and will have improved strength. Therefore, it will be much more easily handled. Furthermore, a

solidified waste will have less impact on the environment when disposed. The treated waste is reduced the permeability due to the liquid cannot flow through the waste directly.

b) Stabilization

Waste stabilization is the process about the chemical changes in contaminants and their environment that cause the contaminants to be less mobile or less toxic. Changes in mobility are due to a contaminant being converted from the dissolved phase to a solid phase. In the dissolved phase, a contaminant is free to diffuse to the external environment. In a solid phase, the contaminant is less mobile. Precipitation is a major reaction that results in immobilization during cement-based s/s. The high pH resulting from cement hydration will cause many metal contaminants forming hydroxide.



สถาบันวิทยบริการ
จุฬาลงกรณ์มหาวิทยาลัย

2.2 Leaching Procedure

Batchelor B. (2006) [1] claimed that characterization of the effectiveness of waste treatment should be based on the evaluation of their environmental impact after disposal or reuse. The simplest approach to characterize the treated waste for its potential to release contaminants to the environment is to measure the total amount of contaminant that can be expected to be released. Leaching test is one of the means of assessing the risk of the solid waste to human and health or the environment. Describing leaching by a very simple equation is shown below.



2.2.1 Types of Leaching Tests [22]

Common batch leaching tests include Extraction Procedure Toxicity (EP-Tox; US EPA Method 1310, 2001), Synthetic Precipitation Leaching Procedure (SPLP; US EPA Method 1312, 2001), Waste Extraction Test (WET; California Code of Regulations, 1985), American Society for Testing and Materials extraction test (ASTM D 3987-85, 2001), and Multiple Extraction Procedure (MEP; US EPA Method 1320). The batch tests typically involve mixing size-reduced waste with extraction solution and then agitating the mixture. These tests generally are performed for a short period of time (typically for hours or days). The main differences among these tests are leaching solution, liquid to solid (L/S) ratio, and number and duration of extraction.

A column test has been used for simulation of leaching from waste. This test involves the placement of waste material in a column and then the addition of leaching solution to the material to produce leachate. Unlike the batch leaching tests, the leaching solution is under continuous flux. However, controlling experimental conditions for this test is not easy. Some operational problems, such as channeling and clogging of the column, may result in a non-reproducible problem. A comparison of batch test with column test is shown in Table 2.3.

Table 2.3 Comparison of batch test with column test

<i>Parameters</i>	<i>Batch Test</i>	<i>Column Test</i>
Testing period	Short-term (hours to days)	Long-term (days to months)
Operation	Easy to operate	Difficult to operate (channeling due to non-uniform packing of waste or clogging of column)
Cost	Relatively low	Relative high
Application of results	Depending on type of batch test	More specific scenario
L/S ratio	Relatively high (To estimate maximum amounts of pollutants to be leached)	Relatively low (close to field conditions)
pH control	Easy to control pH with appropriate chemical	Material dictates its own chemical environment

A batch leaching test was chosen in this research due to a short experiment time and a low cost. Moreover, it is much easier to operate than the column test.

2.2.2 Regulatory Leaching Tests

Two of the most frequently used leaching procedures are Toxicity Characteristic Leaching Procedure (TCLP) and Synthetic Precipitation Leaching Procedure (SPLP), these require that solid waste shall be mixed with an appropriate extraction fluid and shaken for 18 hours in a rotary agitator. The liquid is then filtered, acid digested on a hot plate, and analyzed for metal concentration by Inductively Coupled Plasma-Atomic Emission Spectroscopy (ICP-AES) and for mercury by cold

vapor atomic spectroscopy. The other inorganic parameters are analyzed according to appropriate analytical methods.

Toxicity Characteristic Leaching Procedure, TCLP

TCLP (EPA Method 1311) is used to evaluate metal mobility in a sanitary landfill. The primary extraction fluid is a buffered organic acid solution at pH 4.98. If the waste is highly alkaline, a different extraction fluid at pH 2.88 is used. This combination of highly alkaline waste and a weak organic acid produces a buffered solution similar to the first fluid.

Synthetic Precipitation Leaching Procedure (SPLP)

SPLP (EPA Method 1312) is used to evaluate the potential for leaching metals into ground and surface waters. This method provides a more realistic assessment of metal mobility under actual field conditions, i.e., what happens when it rains (or snows). The extraction fluid is intended to simulate precipitation.

In summary, the sample processing and extraction process of SPLP is identical to the TCLP. The difference is the extraction fluid used. While the TCLP fluid are highly buffered and mildly acidic using acetic acid, SPLP uses an extraction fluid based on the physical location of the site to be characterized and it is an unbuffered solution of sulfuric and nitric acids, at a slightly more acidic pH.

The objective of this research is the determination of metal ions released from the cement-based stabilized waste by the groundwater or acid rain. Therefore, the SPLP was selected because the simulated extraction fluid is closer to real leachate such as groundwater than that used in the TCLP. The SPLP flow chart is shown in Figure 2.2 [23].

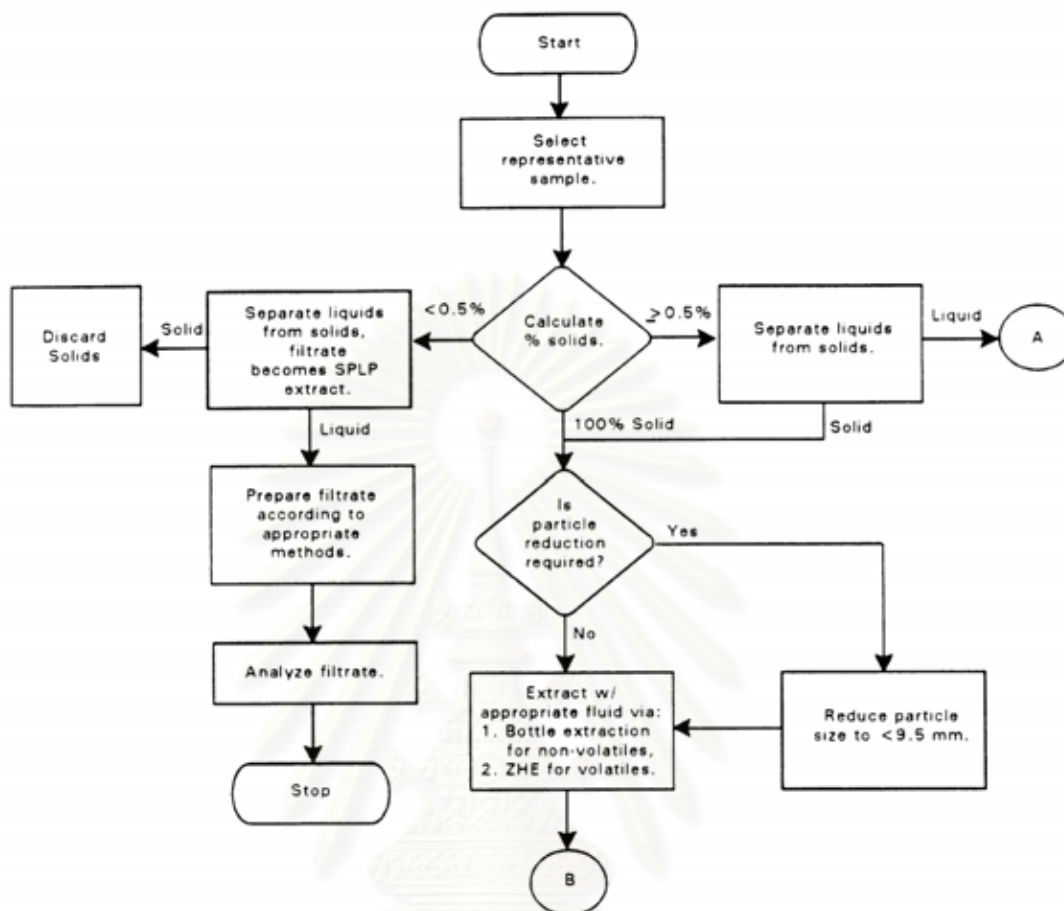


Figure 2.2 Method 1312 Synthetic Precipitation Leaching Procedure.

สถาบันวิทยบริการ
จุฬาลงกรณ์มหาวิทยาลัย

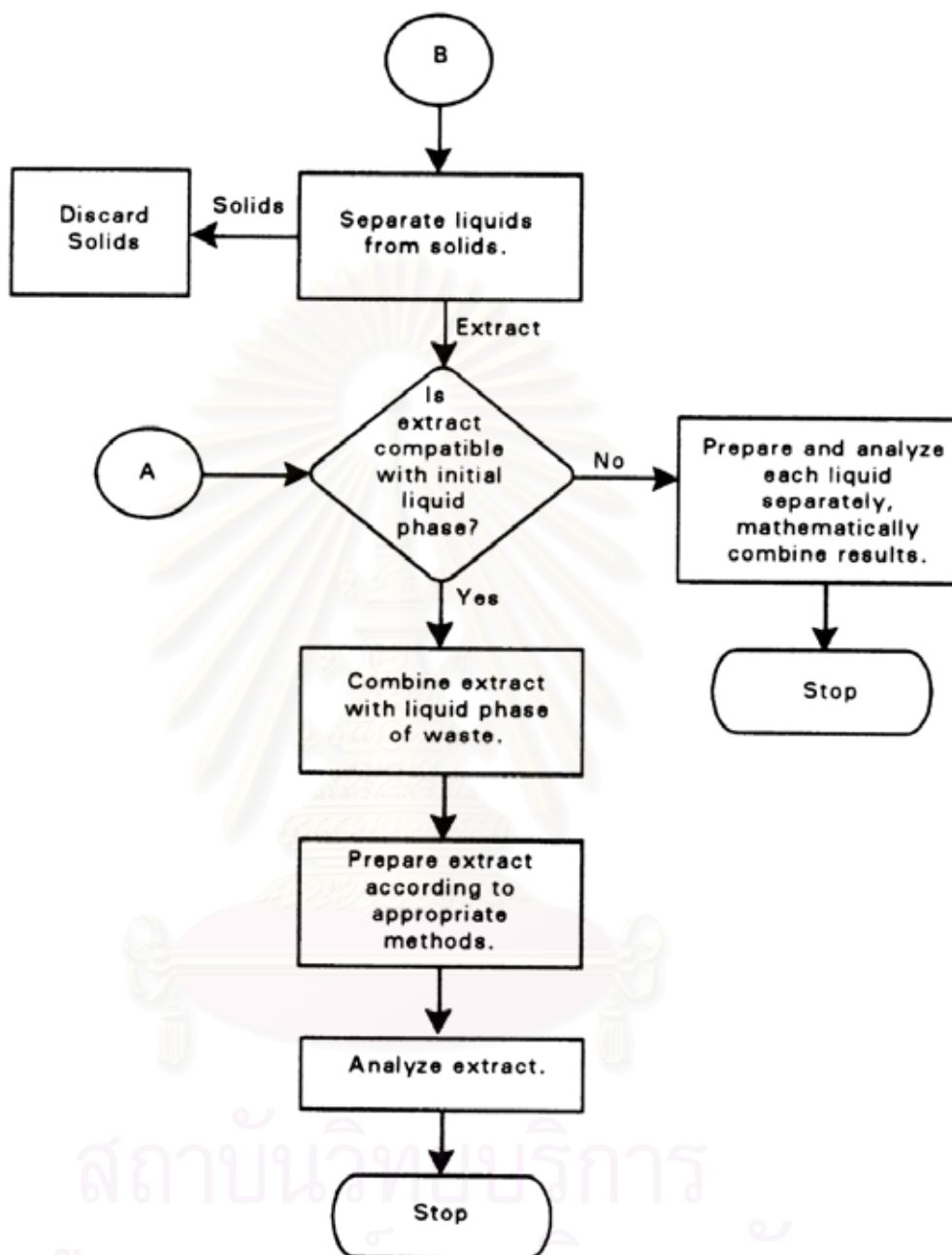


Figure 2.2 (continued) Method 1312 Synthetic Precipitation Leaching Procedure.

2.2.3 Assessment of Treated Waste from Solidification/ Stabilization Process

According to the notification of the Ministry of Industry of Thailand [24], after the treatment of hazardous wastes using s/s process, the treated waste must have the properties following the legal regulation before disposal to a landfill or use in a building construction. These properties are:

- tolerance with unconfined compressive strength following ATSM D-1633 and D-2166 more than $3.5 \text{ kg (cm}^2)^{-1}$ or tolerance with the pressure of the weight above the secured landfill;
- the density of product from s/s process is more than $1.15 \text{ ton (m}^3)^{-1}$;
- the concentration of toxicants in leachate should be lower than the legal regulation.

The latter properties can be tested by using the following leaching extraction procedure;

- a) The sample was crushed and sieved to a particle size less than 9.5 mm.
- b) 100 g of the sample was extracted with 2 L of leachant using synthetic acid rain extraction fluid prepared from mixing of sulfuric acid with nitric acid (80: 20 w/w) and deionized water. The final pH is adjusted to about 5. (ratio of liquid (mL)/solid (g) was controlled at 20:1)
- c) The mixture is shaken using a rotary agitator at 30 rpm at 25°C for 18 hours
- d) The leachate was filtered using 0.6-0.8 μm glass membrane filter
- e) The leached toxicant concentration in the filtrated leachate is determined by the US EPA SW 846 or Thailand standard method for determination of industry wastewater [25]. If the concentration of toxicant is more than the limit of legal regulation, as shown in Table 2.4, the retreatment process is necessary.

For heavy metal that is the main point of this research, its concentration can be determined using the direct aspiration to a flame atomic absorption spectrometer (FAAS) or an inductively coupled plasma atomic emission spectroscopy (ICP-AES).

Table 2.4 Regulatory level of heavy metals founded in leachate [25]

<i>Heavy metal</i>	<i>Regulatory Level (mg L⁻¹)</i>
Arsenic (total)	5.0
Barium	100.0
Cadmium (total)	1.0
Chromium (total)	5.0
Lead (total)	5.0
Mercury (total)	0.2
Selenium	1.0
Silver	5.0

2.3 Metal Determination [26]

The most common techniques for metal determination are shown below:

2.3.1 Atomic Spectroscopy

A recent survey showed that atomic spectroscopy accounts for over one-third of the applications in the field of inorganic trace analysis. The relative contributions from the four main modes of atomic spectroscopy were as follows:

Atomic Absorption Spectroscopy (AAS)	63%
Atomic Emission Spectroscopy (AES)	23%
X-Ray Fluorescence Spectroscopy (XRF)	12%
Atomic Fluorescence Spectroscopy (AFS)	2%

2.3.1.1 Atomic Absorption Spectroscopy (AAS)

The most of AAS procedures can use for single element analysis. The three different forms are flame AAS (FAAS), electrothermal AAS (ETAAS) and hydride generation (HGAAS) (include cold vapour AAS (CVAAS)). FAAS is the most commonly used technique due to its accuracy and precision, high sensitivity, good selectivity, low operation cost and its ability to determine various metals (more than 60 metals) [2].

2.3.1.2 Atomic Emission Spectroscopy (AES)

Of all the emission techniques the ICP ones now dominate the field. They compare well in terms of sensitivity with the various forms of FAAS but offer significant advantages for multi-element analysis.

2.3.1.3 Atomic Fluorescence Spectroscopy (AFS)

Atomic fluorescence can be applied to flame, plasma, and cold vapour systems. It has evolved to play a key role for certain specific elements. In particular, elements

suited to hydride generation or cold vapour treatments, have been successfully adapted to instruments based on fluorescence measurements.

2.3.2 Elemental Mass Spectrometry

Inductively coupled plasma mass spectrometry (ICP-MS) represents the state of the art in inorganic analytical chemistry. The technique is capable of producing semi-quantitative data for most of the elements in the periodic table, both in aqueous and in organic matrices, in under 2 min. The technique can be used for quantitative determinations with detection limits in the parts per trillion range (ng kg^{-1}) with typically a relative standard deviation of 5%.

2.3.3 Chromatography of Ions

Ion chromatography (IC) can be used for the analysis of many ions. There are several adequate methods for the determination of cations (*e.g.* AAS, ICP-MS), which are frequently used instead of IC. However, there are many anionic analytes for which no other suitable determination method exists. Examples include halides, nitrate, sulfate, and cyanide. Ion chromatography has become the standard technique for the analysis of such ions.

สถาบันวิทยบริการ
จุฬาลงกรณ์มหาวิทยาลัย

2.4 Solid Phase Extraction [17, 27]

Liquid-liquid extraction (LLE) is the early extraction method but it has many drawbacks such as using the toxic organic solvent for the extraction, high waste disposal cost, high extraction time and the formation of emulsion during the extraction method. Solid phase extraction (SPE) is a method that can overcome those problems with the additional advantage, allows the achievement of high recoveries along with possible elevated enrichment factor, easily automated and affords a broader range of applications than LLE due to the large choice of solid sorbents.

The short definition of SPE is a nonequilibrium, exhaustive removal of chemical constituents from a flowing liquid sample via retention on a contained solid sorbent and subsequent recovery of selected constituents by elution from the sorbent [28].

2.4.1 Objectives of Solid Phase Extraction

a) Concentration

Sometime the analyte concentration is lower than the detection limit of the instrument which causes an error of the determination. SPE can help to increase the concentration of analyte for accurate results. The three ways that can increase the analyte concentration are shown as the following.

- 1) Pass a large volume of sample through the smallest bed of sorbent that will complete retain all of the analyte.
- 2) Elute the analyte in the smallest volume of solvent possible.
- 3) Elute the analyte in a solvent that permits easy concentration, such as a volatile organic solvent.

b) Clean up

Clean up is the separation of the analyte from the interfering matrix before the analytical step. It may be achieved either by retaining the analyte on a solid phase sorbent or washing out interferences or by retaining the interferences and washing out the analyte.

c) Sample matrix removal/Solvent exchange

SPE can help to remove the sample matrix and convert the sample into a form compatible with each instrument.

Besides the main goal of SPE that mention above, SPE has others utilities that are preservation and storage of the analyte, high selectivity, automation and possible on-line coupling to analysis techniques such as SPE-liquid chromatography, SPE-atomic absorption spectrometry, SPE-ICP-AES or ICP-MS and SPE-spectrophotometry.

2.4.2 Four Steps of Solid Phase Extraction

A SPE technique consists of two methods, i.e. batch and column. A column SPE method is shown in Figure 2.3. The common and basic separation steps include three to four successive steps, as follows;

a) Conditioning

The first step of a SPE is the conditioning step that makes the sorbent compatible with sample solution. The conditioning solvent may be use the same solvent as the sample solvent. In addition, this step can remove the impurities initially contained in the sorbent, removes the air present in the column and fills the void volume with solvent. Typically, for reverse phase sorbent (such as octadecyl-bonded silica), n-hexane is used for activate C₁₈ chain, as shown in Figure 2.4.

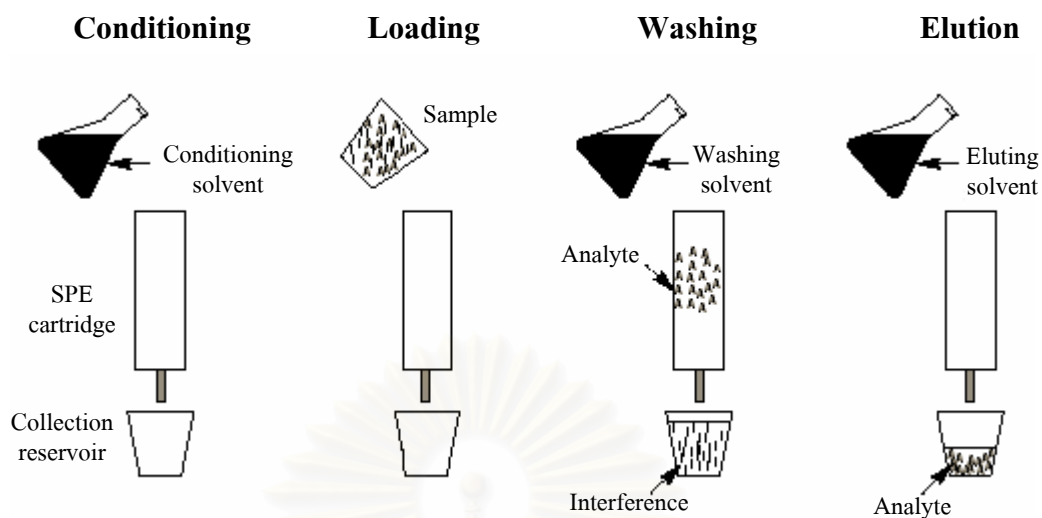


Figure 2.3 Four typical steps of SPE.

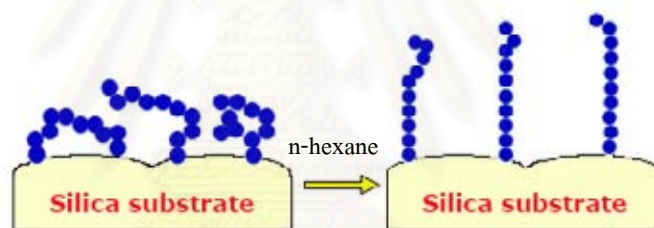


Figure 2.4 C_{18} activated with n-hexane.

b) Loading

The second step is the flow of sample solution through the solid sorbent. The sample flow rate through the sorbent should be low enough to enable efficient retention of the analytes, and high enough to avoid time consumption. Many loading parameters affect to the efficiency of the retention of analyte on solid sorbent, as follows;

- *Sample volume* should not be more than the breakthrough volume.

- *Sample flow rate* should be optimized to ensure quantitative retention along with minimization of the time required for sample processing.
- *Sample pH* is a very important parameter, especially for the retention of analyte based on chelation. The pH of sample solution influence with the basicity of the chelation site on solid sorbent if the pH is too low the basicity of the chelation site will be disrupted.
- *Sample matrix* is an obstruction for extracting analyte onto the solid sorbent. Because it may be formed a stronger complex with analyte or hinder the preconcentration step by overloading the sorbent or in some case the sample matrix can cause interferences during spectrophotometric analysis.

c) *Washing* (which is optional)

The third step may involve washing of the solid sorbent with an appropriate solvent. The washing solvent should elute only matrix components for cleaning up the analyte before desorption from the sorbent.

d) *Eluting*

The final step is the elution of the analyte by an appropriate solvent. The eluting solvent should be eluting only analyte and strong to completely removed adsorbed analyte from solid sorbent as small a volume as possible. The selection of the eluting solvent depends on the interactions of analyte and solid sorbent, for example, using a stronger chelating ligand (higher formation constant) to elute the metal ions from chelating sorbent, or if retention is due to ion exchange, the pH adjustment can be used to elute the analyte.

2.4.3 Sorption Process

The mechanism of analyte retention on the sorbent depends on the nature of the sorbent. There are many types of interactions, as follows.

Adsorption

Adsorption usually occurs with nonpolar sorbent such as C₁₈-silica. The interaction between analyte and solid sorbent occurs through *van der Waals* forces or hydrophobic interaction.

Chelation

Chelation interaction normally occurs between metal electron acceptor and ligand electron donator through a coordinate covalent bond. The ligand molecular structure frequently consists of oxygen, nitrogen or sulfur atoms which contain lone pair electrons that are ready to donate to the metal ion. The selectivity of ligand towards the metal ion can be explained by the hard soft acid base principle (HSAB).

Ralph Pearson [29] classified the cation Lewis acid and the anion Lewis base as hard, borderline or soft. The list of acids and bases in terms of their hardness or softness are shown in Table 2.5 and 2.6 [30]. His principle is that hard acids prefer to bind to hard bases and soft acids prefer to bind to soft bases. The interaction between hard acid and hard base preferentially reacts via electrostatic interactions whereas for soft acid and soft base, the interaction occurs through the covalent bond. The borderline acids have intermediate properties so they can react with both hard and soft base.

Chelating agent can be used to extract the metal ions in two ways. Firstly, if the solid sorbent is a nonpolar, metal extraction can be achieved by adding the chelating agent directly to the sample solution in order to form complex with the metal ion. The resulting neutral charge complex can be extracted onto the nonpolar sorbent. Secondly, the chelating agent was retained on the solid sorbent before use to extract the metal

ion. The three different means for attaching the chelating agent to the solid sorbent are the synthesis of new sorbents containing chelating agent (*new sorbent*), the chemical bonding of chelating agent on solid sorbents (*functionalized sorbents*) and the physical binding of the chelating agent on the sorbent by impregnating the solid matrix with a solution containing the chelating ligand (*impregnated, coated or loaded sorbents*). The latter is the easiest way to prepare but it has the main drawback that is the releasing of chelating agent during extraction or elution process.

The selectivity of chelating ligand towards metal ion depends on the HSAB principle. It also depends on nature, charge and size of the metal ion; nature of the donor atoms present in the ligand; pH of solution which favor certain metal extraction and binding to active donor or groups; and nature of the solid support (e.g. degree of cross-linkage for a polymer).

Table 2.5 Hard and soft acids

<i>Hard Acids</i>	<i>Borderline Acids</i>	<i>Soft Acids</i>
H ⁺ , Li ⁺ , Na ⁺ , K ⁺		
Be ²⁺ , Mg ²⁺ , Ca ²⁺ , Sr ²⁺		
BF ₃ , BCl ₃ , B(OR) ₃	B(CH ₃) ₃	BH ₃ , Tl ⁺ , Tl(CH ₃) ₃
Al ³⁺ , Al(CH ₃) ₃ , AlCl ₃ , AlH ₃		
Cr ³⁺ , Mn ²⁺ , Fe ³⁺ , Co ³⁺	Fe ²⁺ , Co ²⁺ , Ni ²⁺ , Cu ²⁺ , Zn ²⁺ , Pb ²⁺ , Rh ³⁺ , Ir ³⁺ , Ru ³⁺ , Os ²⁺	Cu ⁺ , Ag ⁺ , Au ⁺ , Cd ²⁺ , Hg ₂ ²⁺ , Hg ²⁺ , CH ₃ Hg ⁺ , the ³⁺ , Pd ²⁺ , Pt ²⁺ , Pt ⁴⁺ , Br ₂ , I ₂
Ions with oxidation states of 4 or higher		
HX (hydrogen-bonding molecules)		Metals with zero oxidation state π acceptors: e.q., trinitrobenzene, quinones, tetracyanoethylene

Table 2.6 Hard and soft bases

<i>Hard Bases</i>	<i>Borderline Bases</i>	<i>Soft Bases</i>
	Br^-	H^-
F^-, Cl^-		I^-
$\text{H}_2\text{O}, \text{OH}^-, \text{O}^{2-}$		$\text{H}_2\text{S}, \text{HS}^-, \text{S}^{2-}$
$\text{ROH}, \text{RO}^-, \text{R}_2\text{O}, \text{CH}_3\text{COO}^-$		$\text{RSH}, \text{RS}^-, \text{R}_2\text{S}$
$\text{NO}_3^-, \text{ClO}_4^-$	$\text{NO}_2^-, \text{N}_3^-$	$\text{SCN}^-, \text{CN}^-, \text{RNC}, \text{CO}$
$\text{CO}_3^{2-}, \text{SO}_4^{2-}, \text{PO}_4^{3-}$	SO_3^{2-}	$\text{S}_2\text{O}_3^{2-}$
$\text{NH}_3, \text{RNH}_2, \text{N}_2\text{H}_4$	$\text{C}_6\text{H}_2\text{NH}_2, \text{C}_5\text{H}_5\text{N}, \text{N}_2$	$\text{R}_3\text{P}, (\text{RO})_3\text{P}, \text{R}_3\text{AsC}_2\text{H}_4, \text{C}_6\text{H}_6$

Ion-pairing

The extraction of ionic species onto the nonpolar sorbent can be possible using the addition of an ion-pair reagent to the sorbent. Ion pairing reagent contained two parts; the first one is a nonpolar part which be attached to the nonpolar sorbent and another part is a polar part that can extract the ionic species.

Ion exchange

Ion-exchange sorbents can be used to extract both cation and anion. The extractive preference depends on the functional groups on the sorbent. Ion-exchange sorbent has two types of site which is strong and weak sites. Strong sites, such as sulfonic acid groups (cation-exchange) and quaternary amines (anion-exchange), are ion-exchangers that can exchange ions at any pH, while weak sites, such as carboxylic acid groups (cation-exchange) or primary, secondary and tertiary amines (anion-exchange), can exchange ions only at the pH value greater or less than the pK_a . The main drawback of ion-exchange sorbent is the lack of selectivity towards metal ions.

2.4.4 Sorbents in Solid Phase Extraction

Good properties of sorbent in SPE are wide working pH range, fast and quantitative sorption and elution, high sorption capacity, and reusability. To achieve fast kinetic rate of sorption, high surface area and hydrophilicity of sorbent are required. Sorbents can be divided as organic based and inorganic based ones as shown in Figure 2.5 and 2.6. The addition of organic compounds on the surface of the solid support is usually aimed at modifying the surface with the required functional groups for a higher selectivity of the extraction.

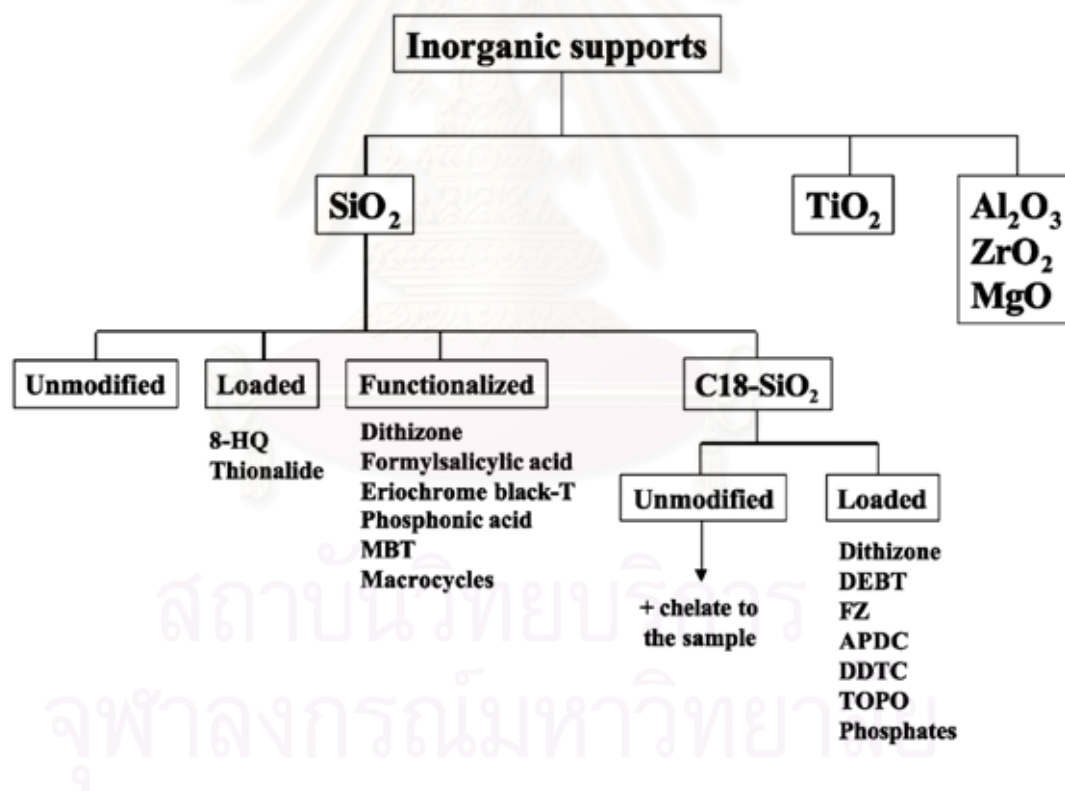


Figure 2.5 Sorbents based on inorganic supports.

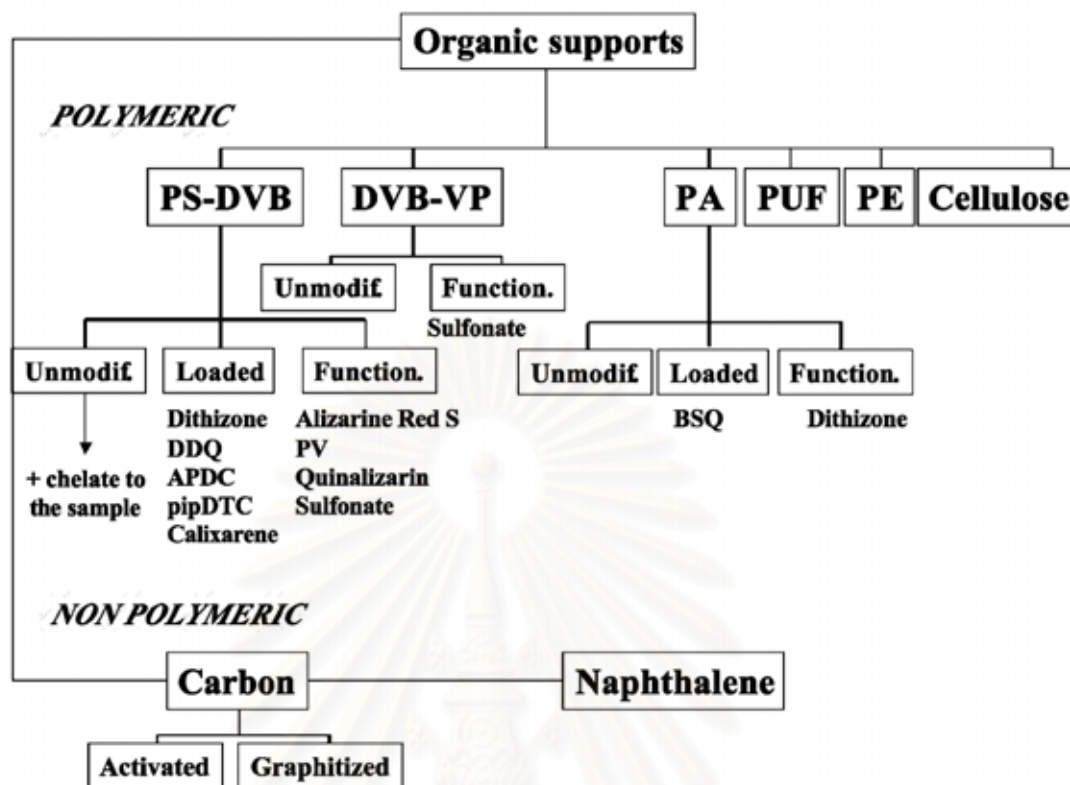


Figure 2.6 sorbents based on organic support.

2.4.4.1 Inorganic based sorbents

Inorganic based sorbents are mainly made of silica gel even though other inorganic oxides may be used. Some inorganic based sorbents are discussed below.

Silica gel

The advantages of silica gel sorbent are that it is not swell, has a good mechanical strength and can undergo heat treatment. In addition, chelating agents can be easily loaded on silica gel with high stability.

C₁₈-bonded silica gel

C₁₈-bonded silica gel can be used to extract metal ions by the silanol group that remains on its surface but it is not well suited for metal extraction because the hydrophobicity of the surface due to the C₁₈ that attach to silica sorbent. Therefore, the extraction of metal ions can be carried out using the addition of a chelating ligand to sample solution before extraction onto the C₁₈-bonded silica gel. The main drawback of this sorbent is a limited working pH in the range of 2-8, outside this range the hydrolysis may be occurred. As a consequence, polymeric sorbents may be preferred.

2.4.4.2 Organic based sorbents

Organic based sorbents may be divided into polymeric and non-polymeric sorbents. The advantage of polymeric sorbents over bonded silica is the ability to use in entire pH range. The selectivity of polymeric sorbent can be improved by chemically bonding chelating groups to the sorbent. The selection of chelating ligand should compromise between the solubility and the hydrophobicity for protecting the leaching out of the chelating ligand from the sorbent during extraction in aqueous solution and increase the mass transfer of metal ion to the sorbent. The efficiency of polymeric sorbents depends on various physicochemical parameters, such as particle size, surface area, pore diameter, pore volume, degree of crosslinking and particle size distribution. Some organic based sorbents are shown below.

Polystyrene-divinylbenzene based sorbents

Polystyrene-divinylbenzene (PS-DVB) is a macroporous hydrophobic resin. It is known as Amberlite XAD series such as Amberlite XAD-1, XAD-2, XAD-4 and XAD-16. PS-DVB is not suitable for extracting any metal ion due to its hydrophobicity. Therefore, the addition of a chelating ligand onto the sorbent can

modified its extraction property for metal ions. The chelating ligands are generally attached to this sorbent through a methylene or an azo spacer group.

Carbon sorbents

Carbon sorbent is an example for non-polymeric sorbent. This sorbent can extract both organic compounds and metal ions because it has two types of adsorption sites. The main drawback of this sorbent is their heterogeneous surface leading to low reproducibility and very reactive and can act as catalysts for oxidation and other chemical reactions.

As mentioned above, there are other kinds of organic based sorbents such as polyacrylate polymers, polystyrene polymers, polyethylene polymers, polyurethane polymers, polytetrafluoroethylene polymers, cellulose, naphthalene based sorbent, etc. Among the mentioned polymeric resins, PS-DVB has been widely used as a solid support for metal extraction in the SPE technique, due to its high porosity and ease of surface modification [31].

2.5 Equilibrium Adsorption Models [32]

The equilibrium adsorption models were used to describe adsorption processes. There are many equilibrium adsorption models such as Brunauer, Emmett, Teller (BET), Langmuir and Freundlich adsorption isotherms. These models explain different types of adsorption processes. However, these isotherms are simply relationships between the moles of the residual dissolved metal ion in solution at equilibrium at a constant (isothermal) temperature and a mass of sorbent. Experimental determination of an isotherm is usually accomplished by mixing a known amount of sorbent with a given volume of metal ion solutions whose initial concentration is known. The system is allowed to come to equilibrium at a selected temperature, and the residual dissolved metal concentration is measured. The concentration change is then used to calculate the moles of dissolved metal adsorbed.

$$\begin{aligned} x &= \text{moles of metal adsorbed} \\ &= (C_i - C)V \end{aligned} \quad 2-1$$

Where C_i, C = initial and equilibrium molar concentrations of dissolved metal, respectively

$$V = \text{liquid volume}$$

Moles adsorbed are then divided by the mass of sorbent m ($x/m = N_p$), and the result is plotted against the equilibrium concentration C .

Most equilibrium data can be fitted into one of three types of mentioned isotherms; BET; Langmuir or Freundlich. Both BET and Langmuir isotherms are based on theoretical developments, while the Freundlich isotherm is an empirical relationship. The BET isotherm is based on the concept of multi-layer adsorption, i.e. multiple layers of materials being adsorbed on the surface, while the Langmuir model assumes that only a single (mono) layer can be adsorbed.

2.5.1 BET Adsorption Model

The BET model assumes that layers of molecules are multi-layer adsorbed. Each layer adsorbs according to the same Langmuir-type model.

$$N_f = \frac{BCN_s}{(C_s - C)(1 + B - 1)(C/C_s)} \quad 2-2$$

where N_f = mole of metal adsorbed per gram of sorbent

N_s = value of N_f when mono layer has been completed

C_s = saturation concentration in the liquid

B = constant related to energy of interaction between sorbent and dissolved material

A plot of N_f versus C results in a curve of the form shown in Figure 2.7.

Theoretically, as C approaches the saturation value, the moles adsorbed become very large because the model does not constrain the number of layers adsorbed. A linear representation of the BET model can be obtained by plotting $C/[(C_s - C)N_f]$ versus C/C_s as shown in Figure 2.8.

In practice, the saturation concentration C_s can only be estimated. Initially, data would be plotted in the form of Figure 2.7, and a value of C_s would be approximated. The linear form would then be plotted.

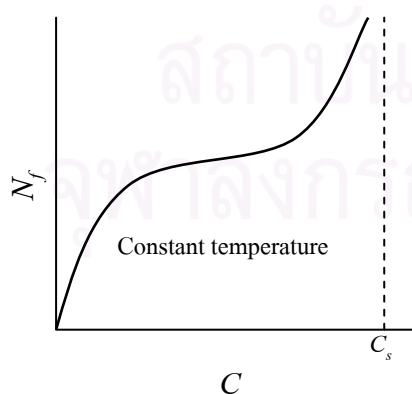


Figure 2.7
Form of BET adsorption isotherm.

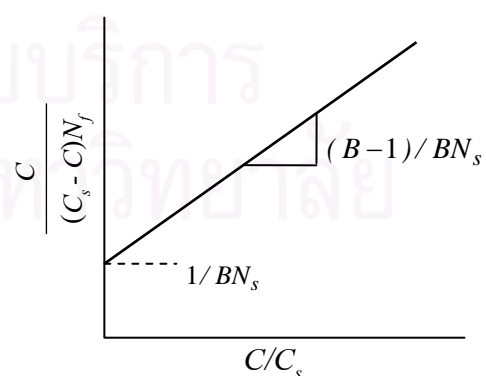


Figure 2.8 Linear form of BET
adsorption isotherm.

2.5.2 Langmuir Adsorption Isotherm

The Langmuir isotherm results from assuming that adsorption is reversible and occurs only for a monolayer on the sorbent surface.

$$N_f = \frac{bN_s C}{1 + bC} \quad 2-3$$

where b is an adsorption coefficient. Data are plotted either as shown in Figure 2.9 or in one of the two alternate linear forms shown in Figure 2.10. The second linear form gives extra weight to higher values of C and is useful because quite often these are more reliable due to poor analytical sensitivity at low concentrations.

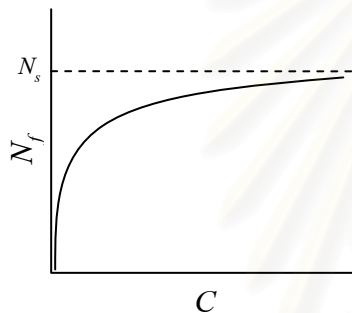


Figure 2.9

Form of Langmuir adsorption isotherm.

Approximation of the linear form is not necessary for the Langmuir isotherm, and the first plot of the data (assuming the data are of satisfactory quality) will demonstrate whether or not the model is applicable and also will allow determination of the coefficients. In many cases, a single model will not be satisfactory for a wide range of concentrations but will serve in narrow regions. An example of this can be seen by noting that at low concentrations ($C/C_s \ll 1$) the BET model reduces to a Langmuir isotherm-type expression.

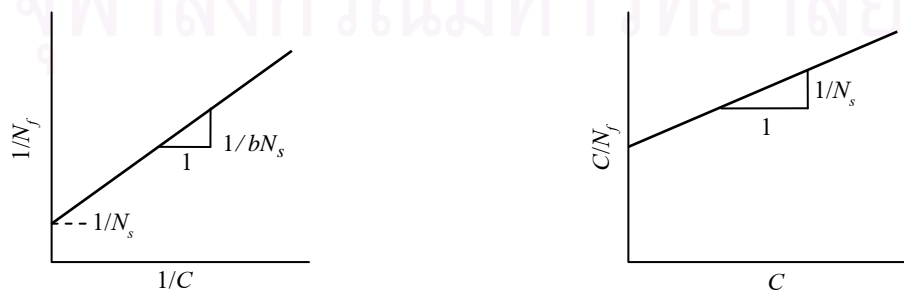


Figure 2.10 (a) Conventional linear form of Langmuir adsorption isotherm (b) Modified form of Langmuir adsorption isotherm emphasizing higher concentration data.

2.5.3 Freundlich Adsorption Isotherm

The Freundlich isotherm, an exponential model, is the third commonly used adsorption expression.

$$N_f = K_f C^{1/n} \quad 2-4$$

where K_f is the Freundlich adsorption coefficient. A plot of N_f versus C results in a curve of the form shown in Figure 2.11.

As noted earlier, Equation 2-4 is empirical but has been found to fit experimental data quite often. Usually the Freundlich isotherm is plotted on log-log paper (Figure 2.12) to facilitate determination of the model's validity and the values of the coefficients K_f and n .

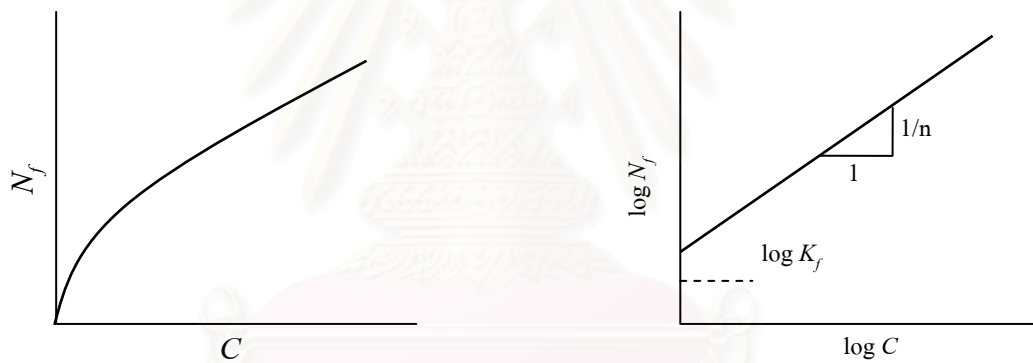


Figure 2.11
Form of Freundlich adsorption isotherm.

Figure 2.12 Linear form of Freundlich
adsorption isotherm.

2.6 Characterization Techniques of Functionalized Polymers

The characterization of functionalized polymer is necessary to confirm the achievement of product following the synthesis pathway. This research used many characterization techniques, i.e., SEM, EA, FT-IR, FT-Raman and TGA. The principles of these techniques are depicted below.

2.6.1 Scanning electron microscopy (SEM)

In this research, this technique is just used for considering the difference of surface image between unmodified and modified polymer. The operating principle starts at the electron source produces a stream of monochromatic electrons and focuses onto the part of the sample. When the beam strikes the sample, interactions occur inside the sample and are detected with various instruments. Before the beam moves to its next point, these instruments count the number of interactions and display a pixel on a CRT whose intensity is determined by this number (the more reactions the brighter the pixel) [33].

2.6.2 Elemental analysis (EA)

Elemental analysis on carbon, hydrogen and nitrogen is the most essential to investigate the elemental composition of functionalized polymer. The sample is operated by packing in a tin capsule and falls into a reactor chamber where excess oxygen has been beforehand introduced. At about 1000°C, the sample is mineralized or pyrolyzed. The resulting mixture should thus consist of CO₂, H₂O and NO_x. Then, the gas product mixture flows through a silica tube. In this zone held at about 500 C, remaining oxygen is bound and nitric/nitrous oxides are reduced. The leaving gas stream includes the analytically important species CO₂, H₂O and N₂. High purity helium is used as carrier gas. Finally, the gas mixture is passed to a gas chromatographic system. Separation of the species is done by so called zone

chromatography. In this technique a staircase type signal is used. Step height is proportional to the substance amount in the mixture [34].

2.6.3 Fourier Transforms Infrared Spectroscopy (FT-IR)

FT-IR is a powerful tool for identifying types of chemical bonds in a molecule by producing an infrared absorption spectrum. Each chemical bond has the individual vibration frequency in the infrared absorption spectrum. The vibration of bond can occur due to the interaction of infrared radiation with a sample molecule. Infrared spectrometry finds its widest applicability in the analysis of organic and polymeric materials, but it is also useful for polyatomic inorganic molecules and for organometallic compound [35]. Samples for FT-IR can be prepared in many ways. For liquid samples, the easiest is to place one drop of sample between two plates of sodium chloride (salt). Salt is transparent to infrared light. Solid samples can be milled with potassium bromide (KBr) to form a very fine powder. This powder is then compressed into a thin pellet which can be analyzed [36].

2.6.4 Fourier Transforms Raman Spectroscopy (FT-Raman)

Both results of FT-Raman and FT-IR are achieved from molecular vibrations. The difference between two techniques is mainly the interaction of light source and sample. For FT-IR, the interaction is absorption while for FT-Raman, the interaction is scattering. Raman spectroscopy provides information about molecular vibrations that can be used for functionalized polymer identification.

The Raman effect occurs when a monochromatic light (laser) irradiates onto a sample and excites molecules in the sample, which then scatter the light. While most of this scattered light is at the same wavelength as the monochromatic light, some ($\pm 0.0001\%$) is scattered at a different wavelength. This inelastically scattered light is called Raman scatter. The energy difference between the monochromatic light and the Raman scattered light is equal to the energy involved in changing the molecule's vibrational state. Several different Raman shifted signals will often be observed; each

being associated with different vibrational or rotational motions of molecules in the sample [37].

Raman and IR spectrometry should be viewed as complementary techniques, particularly for structural studies. The differences in the selection rules lead to different spectra for some types of molecules. In any case the combination of IR and Raman spectrometry is very powerful for achieving chemical structures. For organic functional group identification, IR spectrophotometry is usually used. Raman spectrometry is often the method of choice for inorganic and biological substance which their spectra are most obtained in aqueous solutions. The differences of IR and Raman techniques are shown in Table 2.7 [38].

2.6.5 Thermal Gravimetric Analysis (TGA)

TGA is a simple analytical technique that measures a weight loss (or weight gain) of a material as a function of temperature. After materials are heated, they can lose weight from a simple process such as drying, or from chemical reactions that release gasses. Some materials can gain weight by reacting with the atmosphere in the testing environment. For the characterization of functionalized polymer, TGA have two main utilities. Firstly, it is employed to study of thermal decomposition of polymer that can show the difference of polymer product. Secondly, it can show the hydrophilicity of functionalized polymer by losing of water molecule at temperature about 100°C [39].

Table 2.7 Differences and complementary power of Infrared and Raman spectroscopy

	<i>Infrared</i>	<i>Raman</i>
Physical effect	Absorption Changing of the dipole moment (strong: ionic bondings like O-H, N-H)	Scattering Changing of the polarisability (strong: covalent bondings like C=C, C-S, S-S)
Sample preparation	Optimal thickness (transmission mode) or sample contact (ATR) Mode necessary	No contact, no destruction, simple preparation (if only); water as solvent or glass as container do not disturb the measurement
Problems	Strong absorption of glass, water, CO ₂	Fluorescence
Materials	Mainly organic compounds	Nearly unlimited
Frequency range	4000-700 cm ⁻¹	4000-50 cm ⁻¹ (Stokes and Antistokes)

2.7 Literature Review: Determination of toxic elements in leachate

The important problem of the determination of toxic elements in leachate from cement-based stabilized waste is the high concentration of calcium that released from the main composition of cement (CaO or Ca(OH)_2). There were some reports that showed the interference effect of calcium toward the determination of metal. Stafilov et al. (2000) [40] determined the amount of Co, Cu, Pb and Ni in gypsum ($\text{CaSO}_4 \cdot 2\text{H}_2\text{O}$) by Zeeman electrothermal atomic absorption spectrometry (ETAAS). They found that Ca tended to decrease absorbance of investigated elements. Therefore, the investigated element was separated from solution obtained by dissolution of gypsum in HCl using liquid-liquid extraction before their determination. Another report of Stafilov et al. (2002) [41] also showed the interferences of Ca as matrix element in dolomite ($\text{MgCa(CO}_3)_2$) and gypsum on the decrease of Ag, Cd, Cr and Tl absorbances during their ETAAS determination. A flotation separation method was proposed to eliminate matrix interferences. These reports showing the necessary to separate the analyte from Ca matrix before their determination. Our research interested in the separation of toxic element from leachate using a solid phase extraction due to many advantages over other separation techniques such as good selectivity, eco-friendliness, reusability, high preconcentration factors and simple operation [5].

Chelating resin was one of the types of solid phase sorbent; it was used especially for metal extraction. Chelating resin was generally synthesized by functionalized a solid support with a chelating ligand through a methylene ($-\text{CH}_2-$) or an azo ($-\text{N}=\text{N}-$) spacer for protecting the ligand leaching problem [8]. Polystyrene-Divinylbenzene, PS-DVB resins (the structure is shown in Figure 2.13 [42]) were commercially available as Amberlite XAD series, which differ in their degree of crosslinkage, bead size, pore diameter, etc., directly influencing the rate and degree of metal ion sorption [43]. Several papers on Amberlite XAD series used as chelating solid support have been reported in the recent years. Amberlite XAD-2 functionalized

with many kinds of chelating agent had published. The examples of chelating agents are pyrocatechol [44], nitroso R salt [4], 2-(methylthio)aniline [45], thiosalicylic acid [46], tiron [9], *o*-aminophenol [8], 2-aminoacetylthiophenol [47], chromotropic acid [48] and pyrocatechol violet [49]. Amberlite XAD-4 functionalized with *o*-aminobenzoic acid [50], salicylic acid [51], succinic acid [52] and dithiocarbamates [53]; and Amberlite XAD-16 functionalized with 1,3-dimethyl-3-aminopropan-1-ol [43], (bis-2,3,4-trihydroxy benzyl) ethylene diamine [11], phthalic acid [54] and 2-{{1-(3,4-Dihydroxyphenyl)methylidene}amino}benzoic acid [5] were also used for metal extraction.

Amberlite XAD-2 was found to be the most suitable polymeric support, which has good physical and chemical properties such as porosity, high surface area, durability, purity [4] and it can be used over the wide pH range [17]. Moreover, Amberlite XAD-2 has only 4% crosslinkage, so it has many active sites on a benzene ring of polystyrene to functionalize with a small chelating ligand. This property of Amberlite XAD-2 can bring to a very high sorption capacity chelating resin [44].

Purpurin (1,2,4-trihydroxyanthraquinone) consists of five oxygen donor atom, as shown in Figure 2.14, so it can form complex with various metal ions. Arrebola et al. (1986) [55] studied La-Mg-Purpurin complex and its extraction with methyl isobutyl ketone (MIBK) for spectrophotometric determination. The results showed that the mixed-metal complex can be increased in sensitivity compared with the binary La-Purpurin complex. Another report of Arrobola et al. (1998) [56] continued the previous research for indirect determination of total yttrium and lanthanides by FAAS. They extracted the mixed metal complex La(or Y)-Mg-Purpurin complex using MIBK and determined the amount of Mg by FAAS, then stoichiometrically converted to the amount of La or Y. There were also some reports showing high selectivity of Purpurin towards some metal ions. Idriss et al. (1999) [57] described the highly selective complexation reaction of Mn^{2+} with Purpurin at pH 8.5 and the application for the direct spectrophotometric determination of MnO content of Portland cement was

satisfactorily achieved. This method has proved to be reliable, sensitive and highly selective. Two years later, Idriss et al. (2001) [58] showed the selectivity of Purpurin with Mg^{2+} at pH 9.5 and its application for selective determination of MgO in Portland cement that presence of high Ca^{2+} concentration using spectrophotometric determination was also succeeded. Two reports of Idriss et al. showed the selectivity of Purpurin that could be controlled by the solution pH. Beside the use of Purpurin in the form of solution to form complex with metal ion, Ahmad M. et al. (2002) [59] presented the utility of purpurin in the form of chelating agent immobilized on XAD-4. Purpurin was impregnated on XAD-4 through physical binding. The immobilized XAD-4 was contained into the tip of the optical fiber probe and used for Al^{3+} sensor.

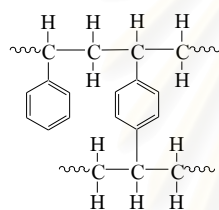


Figure 2.13 Chemical structure of Amberlite XAD-2 polymeric sorbent.

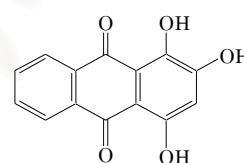


Figure 2.14 Structure of chelating ligand, purpurin.

2.8 Conclusion

According to the literature review above, the attraction of purpurin for the extraction of metal ions from cement-based leachate can be concluded. Firstly, it can form complex with various metal ions. Secondly, Purpurin was highly selective towards some metal ions in the presence of Ca^{2+} and the selectivity towards each metal ion can be controlled by adjusting the solution pH. Lastly, no research had been employed purpurin to prepare a chelating resin for the extraction of metal ions in a sample with interference matrix. In conclusion, an attempt of this work was to synthesize a new chelating resin; Amberlite XAD-2 functionalized with purpurin

through the covalent bond, $-N=N-$ group for the extraction of heavy metal ions in leachate from cement-based stabilized waste.



สถาบันวิทยบริการ
จุฬาลงกรณ์มหาวิทยาลัย

CHAPTER III

EXPERIMENTAL SECTIONS

3.1 Apparatus

The apparatuses used in this study are listed in Table 3.1.

Table 3.1 Apparatus lists

<i>Apparatus</i>	<i>Model (company)</i>	<i>Purpose</i>
1. CHNS/O analyzer	PE 2400 Series II (Perkin-Elmer)	elemental analysis of all polymer
2. Fourier transforms infrared spectrometer (FT-IR)	Impact 410 (Nicolet)	functional group identification on polymer surface
3. Fourier transform Raman spectrometer (FT-Raman)	Spectrum GX (Perkin-Elmer)	functional group identification on polymer surface
4. Flame atomic absorption spectrometer (FAAS)	AAAnalyst 100 (Perkin-Elmer)	metal ion determination (operating parameters are showed in table 3.2)
5. Mechanical shaker	SA-31 (Yamato shaker)	agitation of solutions for cement extraction
6. Scanning electron microscope (SEM)	JSM 5410LV (JEOL)	surface analysis of polymer

Table 3.1 Apparatus lists (continued)

<i>Apparatus</i>	<i>Model (company)</i>	<i>Purpose</i>
7. pH meter	pH 211 (Hanna instruments)	pH measurement
8. Peristaltic pump	REGLO Analog MS- 4/8 model ISM 827 (ISMATEC [®])	control of solution flow rate passing through the column
9. Thermal Analyzer	409 (Netzsch)	thermal decomposition and hydrophilicity studies
10. UV-Vis spectrophotometer	HP 8453 (Hewlett Packard)	absorbance measurement

Table 3.2 Operating parameters for FAAS

<i>Operating conditions</i>	<i>Cd</i>	<i>Cr</i>	<i>Pb</i>
Wavelength (nm)	228.8	357.9	283.3
Slit width (nm)	0.70	0.70	0.70
Lamp current (mA)	4	25	10
C ₂ H ₂ flow-rate (L min ⁻¹)	1.5	2	1.5
Air flow-rate (L min ⁻¹)	4	4	4

3.2 Chemicals and Preparation of Reagents

3.2.1 Chemicals

All chemicals were analytical reagent grade listed in Table 3.3.

Table 3.3 Chemical lists

<i>Chemicals</i>	<i>Supplier</i>
Amberlite XAD-2 (surface area 366.5 m ² /g dry resin)	SUPELCO
Ammonia solution 25%	MERCK
Ethanol	MERCK
Hydrochloric acid 37%	MERCK
Methanol	MERCK
Nitric acid 65%	MERCK
Purpurin	Fluka
Potassium bromide	MERCK
Single standard solution for Cd ²⁺ , Cr ³⁺ and Pb ²⁺ (1000 mg L ⁻¹)	BDH
Sodium hydroxide	MERCK
Sodium nitrite	MERCK
Stannous chloride 98%	NIHON KAGAKU SANGYO
Sulfuric acid 95%	MERCK

3.2.2 Preparation of Reagents

All solutions were prepared by using deionized (DI) water.

a) Working standard solutions

Working standard solutions of Cd^{2+} , Cr^{3+} and Pb^{2+} were prepared by dilution of 1000 mg L^{-1} stock standard solution to the required concentrations.

b) Nitric acid solution

Nitric acid solution (1% v/v) for pH adjustment was prepared by direct dilution from the concentrated solution.

c) Ammonia solution

Ammonia solution (5% v/v) for pH adjustment was prepared by direct dilution from the concentrated solution.

d) Sodium hydroxide solutions

Sodium hydroxide solutions (2 M and 10% w/v) were prepared daily by dissolving the appropriate amount of NaOH in DI water.

e) Hydrochloric acid solutions

Hydrochloric acid (1, 2 and 4 M) was prepared by direct dilution from the concentrated solution.

f) Sodium nitrite solutions

Sodium nitrite (1 M) was prepared daily by dissolving the appropriate amount of NaNO_2 in DI water.

g) Amberlite XAD-2

Before use, Amberlite XAD-2 was stirred with 4 M HCl for 12 h. It was then washed with DI water until free from acid and washed finally with a little amount of methanol and dried in air.

3.3 Synthesis of Amberlite-XAD-2 Functionalized with Purpurin

The procedure given by Kumar et al.[8] with some modifications was applied for the synthesis of the XAD-P chelating resin. Amberlite XAD-2 beads (10 g) were treated with 20 mL of concentrated HNO_3 and 50 mL of concentrated H_2SO_4 and the mixture was stirred at 60°C for 1 h on an oil bath. The nitrated mixture (XAD- NO_2) was poured into ice-cold water. It was further filtered, washed repeatedly with DI water until free from acid. Then it was reduced with SnCl_2 (40 g) in concentrated HCl (45 mL), ethanol (50 mL) and refluxed for 12 h at 90°C . The amino polymer (XAD- NH_2) was filtered and washed with DI water and 2 M NaOH .

The amino resin was firstly washed with 2 M HCl , then washed with DI water in order to remove excess of HCl and suspended in ice cold water and treated with 1 M HCl and 1 M NaNO_2 (add 1:1 mL each time until the reaction mixture showed a permanent dark blue color with starch-iodide paper). The diazotized resin was filtered, washed with ice cold water and finally reacted with purpurin (1 g in 250 mL of 10% NaOH) at $0-5^\circ\text{C}$ for 24 h. The resulting dark red beads were filtered and washed with DI water until the solution free from the red color of excess purpurin, then washed with methanol and air dried. The synthesis pathway is depicted in Figure 3.1

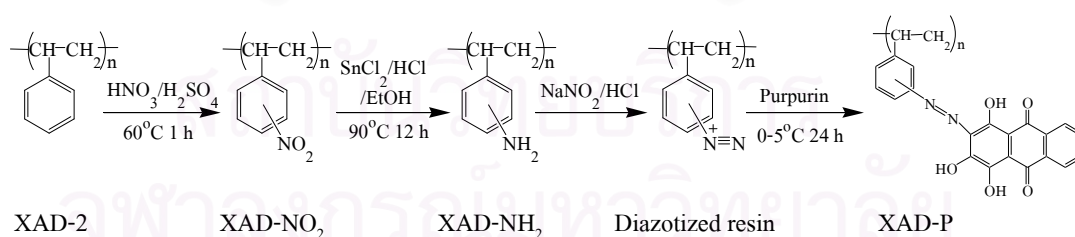


Figure 3.1 Reaction sequence of the synthesis of the chelating resin

3.4 Characterization

3.4.1 Characterization of Resins

The characterization was done in every synthesis step of the resin except for SEM the first and the last products were analysed.

a) Scanning electron microscopy (SEM)

XAD-2 and XAD-P were carefully cut into small pieces and exposed to gold vapor deposition to prepare photogenic sample, and put in an electron probe analyzer to give the SEM photographs of polymer surface. The accelerated voltage was 15 kV.

b) Elemental analysis (EA)

The samples were generated gaseous products freed by pyrolysis in high-purity oxygen and chromatographically separated by frontal analysis with quantitatively detected by thermal conductivity detector.

c) Fourier Transforms Infrared Spectrometer (FT-IR)

Infrared spectra were recorded from 400 to 4000 cm^{-1} in transmittance mode by KBr pellet technique.

d) Fourier Transforms Raman Spectrometer (FT-Raman)

Raman spectra were recorded from 200 to 3600 cm^{-1} with a 4 cm^{-1} resolution.

e) Thermal Gravimetric Analysis (TGA)

Thermogravimetric measurements were performed using Simultaneous Thermal Analyzer (STA) at a heating rate of 10°C/min under nitrogen atmosphere.

f) UV-Vis spectrophotometer

UV-Vis spectrophotometer was used for absorbance measurements of purpurin that was hydrolyzed from the chelating resin in the range of 200-700 nm.

3.5 Appropriate Amount of Purpurin for Synthesis

The appropriate amount of purpurin for the synthesis of chelating resins was studied by varying the amount of purpurin; 0.1, 0.5, 1 and 3 g in the last synthesis step for 10 g of XAD-P used. Thereafter, purpurin in those chelating resins was eluted by 50% v/v ethanol for determination of the adsorbed purpurin (purpurin is soluble in 50% v/v ethanol). The amount of released purpurin was determined by a UV-Vis spectrophotometer. Based on the covalent bond between purpurin and polymer support, the elution using DI water should not be observed. Consequently, the elution using DI water was compared with that of ethanol. A 5 mL of each eluent was stirred with 0.0300 g XAD-P for 1 h.

3.6 Influence of Leachate on Metal Ion Calibration Curve

To prove the effect of leachate on the determination of metal ions, experiments using two different matrices; leachate and DI water were compared by preparing standard solutions in each matrix at the concentration in the linear dynamic range that is 0.4-2.0 ppm for Cd, 1.0-5.0 ppm for Cr and Pb. Absorbance signals of each metal ion were detected using FAAS. The significance test between two different matrices was studied using paired *t*-test at the 95% confidence limit.

3.7 Synthetic Sample (Leachate)

The extraction of heavy metal ions in leachate from cement-based stabilized waste is the main objective for this research, so the experiment should be done in the leachate matrix which can be prepared by modified EPA Method 1312 (SPLP) [60] under the following procedure.

a) Preparation of blank cement-based mortar

A blank cement-based mortar was prepared by mixing cement and sand with a weight composition of 30:70. A small volume of DI water was added. The mixture was homogenized and the paste was molded in a plastic container.

b) Preparation of leachant (extraction fluid)

Simulated natural precipitation leachant was slightly acidified DI water. It was easily prepared by using a mixture of H_2SO_4 : HNO_3 (80:20 by weight) to adjust pH of DI water to pH 5.

c) Leachate extraction procedure

The blank cement-based mortar was crushed and sieved to particle size less than 9.5 mm. And then 25 g of the crushed solid was extracted using 500 mL of leachant (controlled ratio of liquid (mL)/solid(g) at 20:1) and the mixture was shaken using a mechanical shaker for 18 hours. The leachate was then filtered through a 0.45 μm membrane filter utilizing a pressure filtration unit. This filtrate was used as a representative synthetic sample for further experiments.

3.8 Extraction and Desorption Studies

The study of extraction was divided into two methods, batch and column. All experiments were performed in triplicate.

3.8.1 Batch Method

The extraction of metal ions was studied in both leachate and DI matrix, in order to compare the optimum conditions in both matrices that give useful data for application in the real sample.

3.8.1.1 Effect of pH on metal extraction

The effect of the solution pH on the metal ion extraction was investigated in the range of pH 1.0-6.0 using 5 mL of individual metal ion solution (pH more than 6.0 causes precipitates of metal ions). pH adjustments were made with 1% HNO₃ and 5% NH₃. The concentration of metal ion and the amounts of chelating resins were compromised to remain the metal in solution enough for determination.

In DI matrix, 5 mL of sample solution containing 5 ppm of Cd²⁺ at pH 1.0-6.0 was taken in a test tube (size 14 mL, diameter 15 mm) and 10 mg of XAD-P was added after that the mixture was stirred with small magnetic bar for 1 h. Thereafter, the residual metal ion concentration in the supernatant was determined by a FAAS.

The study of Cd²⁺ in leachate, Cr³⁺ and Pb²⁺ in both matrices was performed by the same procedure using the suitable concentration of metal ion and the amount of XAD-P shown in Table 3.4.

Table 3.4 Concentration of metal ion and amount of XAD-P for studying the effect of pH

<i>Metal</i>	<i>DI matrix</i>		<i>Leachate matrix</i>	
	<i>XAD-P (mg)</i>	<i>conc.(ppm)</i>	<i>XAD-P (mg)</i>	<i>conc.(ppm)</i>
Cd	10	5	30	1
Cr	30	5	30	5
Pb	5	5	20	5

3.8.1.2 Kinetics of metal extraction

In DI matrix, 10 mg of XAD-P was stirred with 5 mL of solution containing 5 ppm of Cd²⁺ after adjusting its pH to the optimum value at different time in the range of 2-60 min. Thereafter, the residual metal ion concentration in the supernatant was determined by a FAAS.

The study of Cd^{2+} in leachate, Cr^{3+} and Pb^{2+} in both matrices was performed by the same procedure using the suitable concentration of metal ion and the amount of XAD-P shown Table 3.4.

3.8.1.3 Effect of eluent

XAD-P containing adsorbed metal ions at the optimum pH and time was washed with DI water 2-3 times for removing unadsorbable metal ions and then stirred with 5 mL of various types and concentrations of eluent for 1 h. Metal ion concentration in eluates was determined by FAAS.

3.8.1.4 Effect of elution time

For decreasing the elution time, the optimum elution time should be studied under the following procedure.

The sorbed metal ion XAD-P was washed with DI water 2-3 times and then eluted with the suitable eluent at different time in the range of 2-60 min. Metal ion concentration in eluates was determined by FAAS.

3.8.1.5 Adsorption isotherm

Under the optimum pH for each metal, the adsorption isotherm can be studied by extracting the various concentrations of solution containing 5-150 ppm of metal ion at $25 \pm 1^\circ\text{C}$ with the suitable amount of XAD-P shown in Table 3.4 for 1 h. Thereafter, the residual metal ion concentration in the supernatant was determined by a FAAS. The results were treated with Langmuir and Freundlich adsorption isotherm to describe the mechanism at the solid-liquid interface and estimate the maximum sorption capacity of the chelating resin, XAD-P.

3.8.2 Column Method

A mini-column was prepared by using homemade columns with a Curity[®] stomach tube i.d. 0.4 cm. The experiments in column method were studied using leachate only. The suitable concentration of metal ion and the amount of XAD-P loaded column for the study of the effect of flow rate, the recirculation of sample solution and the desorption was the same with that of the batch method shown in Table 3.4. For all experiments, the XAD-P loaded column was conditioned by DI water at the suitable pH for extraction before passing sample solutions.

3.8.2.1 Effect of flow rate

For each metal ion, 5 mL of the suitable concentration of metal ion was adjusted to the optimum pH value. Thereafter it was passed through the appropriate amount of XAD-P loaded column at a flow rate varying between 0.5 and 5 mL min⁻¹. The unadsorbed metal ion was determined by FAAS.

3.8.2.2 Recirculation of sample solution

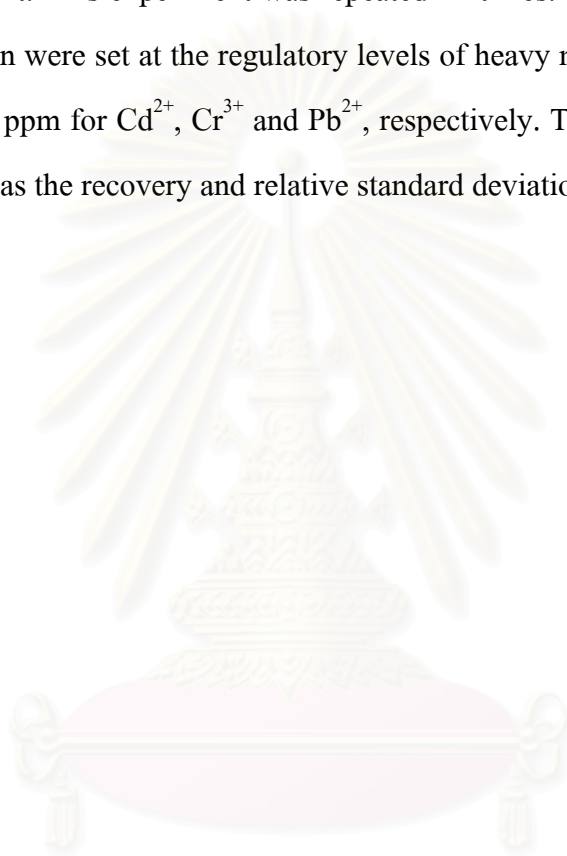
The recirculation of sample solution was adapted for higher extraction efficiency. After 5 mL of metal ion solution at optimum pH was passed through a XAD-P loaded column at a suitable flow rate, the remaining solution was recirculated by passing through a XAD-P loaded column at the same flow rate again and again in the range of 5-40 cycles. The remaining metal ion in the solution after the recirculation was determined by FAAS.

3.8.2.3 Desorption study

The study of desorption of metal ion from XAD-P column was carried out by using 5 mL of the same appropriate eluent for each metal ion from the batch method at a slow flow rate of 1 mL min⁻¹. Metal ion concentration in eluates was determined by FAAS.

3.9 Method Validation

Under the optimum conditions, the method validation was performed in batch method by extracting the metal ions spiked in leachate at the optimum pH (5 mL of sample solution) using 0.0500 ± 0.0002 g of XAD-P and eluting with 5 mL of the appropriate eluent. This experiment was repeated 14 times. The spiked concentrations of each metal ion were set at the regulatory levels of heavy metal in leachate that were 1.0, 5.0 and 5.0 ppm for Cd^{2+} , Cr^{3+} and Pb^{2+} , respectively. The accuracy and precision were calculated as the recovery and relative standard deviation (RSD).



สถาบันวิทยบริการ
จุฬาลงกรณ์มหาวิทยาลัย

CHAPTER IV

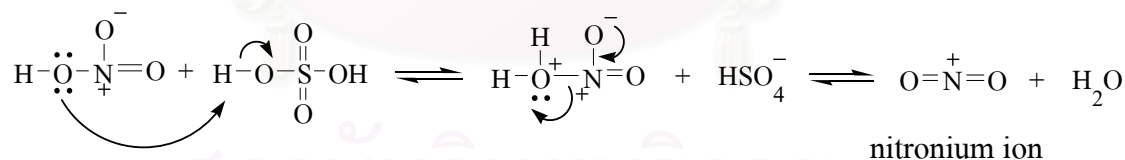
RESULTS AND DISCUSSION

4.1 Synthesis of Amberlite XAD-2 Functionalized with Purpurin

The three steps of the synthesis of XAD-P consist of nitration, reduction, and diazotization for coupling with purpurin. In each step, the color of resin beads changed obviously. At the beginning, Amberlite XAD-2 was white, after the nitration and reduction, the white beads turned yellow and then brown, respectively. For the last step, the resin became dark red that was the color of purpurin.

The nitration is an addition reaction of nitro group to benzene ring of the polystyrene backbone, the reaction mechanism is shown in Figure 4.1. A nitronium ion was initially generated by HNO_3 and H_2SO_4 and then subsequently attacked the aromatic ring, resulting in a nitro benzene derivative, called XAD- NO_2 .

Generation of nitronium ion



Electrophilic aromatic substitution

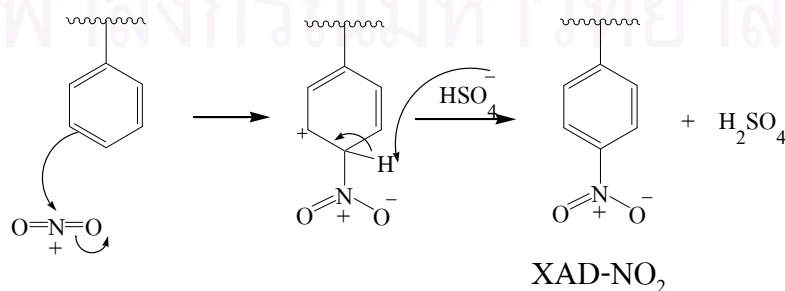


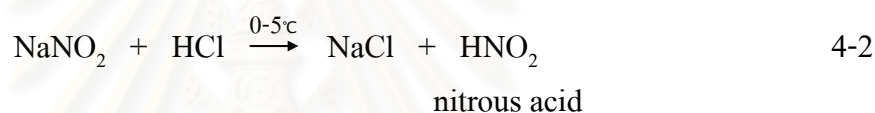
Figure 4.1 Mechanism of the nitration.

The nitro group was then reduced to an amine using the SnCl_2 reduction. After this reaction, the product was washed with 2 M NaOH for producing the free amino polymer according to the following equation [10]:

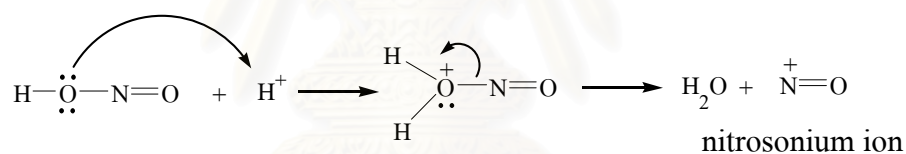


The next step was a diazotization and coupling reaction with purpurin. The mechanism has many steps, as shown in Figure 4.2. Nitrous acid was firstly generated from the reaction between sodium nitrite and HCl. It is unstable and decomposes to nitrosonium ion (NO^+) that is a good electrophile for the diazotization.

Generation of nitrous acid



Generation of nitrosonium ion



Diazotization

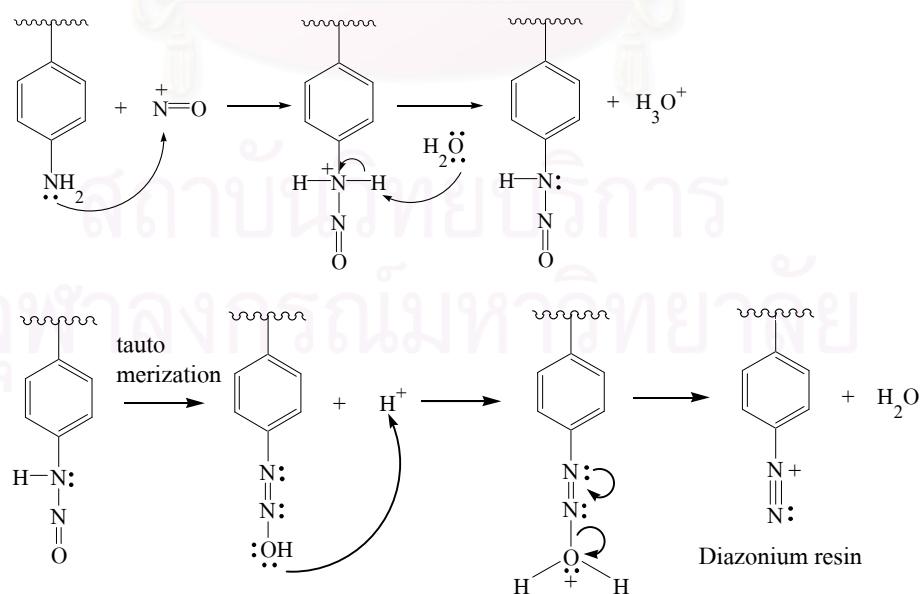
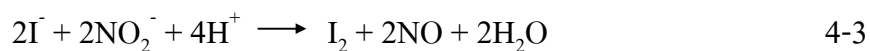


Figure 4.2 Mechanism of the diazotization.

This step needed to have an excess nitrous acid to generate the diazonium resin as much as possible. The excess nitrous acid was checked using starch-iodide paper which was changed to the dark blue color due to generated free iodine. The reaction was shown in Equation 4-3.



In basic condition using 10% NaOH, the generated diazonium resin reacted with purpurin through the electrophilic aromatic substitution (coupling reaction). The diazonium resin is a poor electrophile however it can react with purpurin because the benzene ring of purpurin has three donating hydroxyl groups, consequently the electron density of benzene ring is increased and highly reactive towards electrophile. A diazo coupling often takes place in basic solution because deprotonation of the hydroxyl groups help to activate the aromatic rings towards an electrophilic aromatic substitution. The proposed structure of XAD-P is shown in Figure 4.3.

Diazo coupling

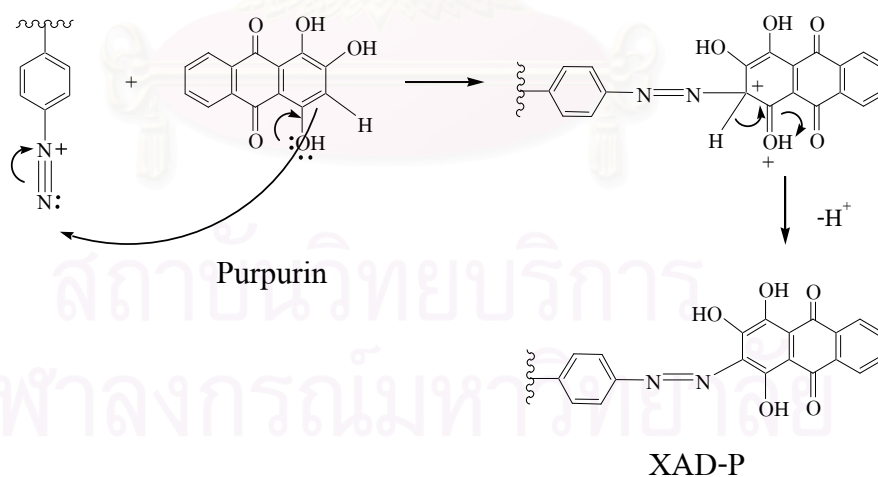


Figure 4.3 Proposed structure of XAD-P through the diazonium coupling reaction.

4.2 Characterization of Amberlite XAD-2 Functionalized with Purpurin

The synthesis of Amberlite XAD-2 functionalized with purpurin comprised three steps. Therefore, the characterization was necessary to identify and confirm the product from each step of the synthesis pathway. The functionalized resin was characterized by SEM, EA, FT-IR, FT-Raman and TGA before sorption studies. The results were illustrated in the following.

4.2.1 Scanning Electron Microscopy

The SEM micrographs, as shown in Figure 4.4, exhibit the difference between XAD-2 and XAD-P surface. The XAD-2 surface is rougher than XAD-P surface, implying that the substrate surface was changed after the functionalization with purpurin.

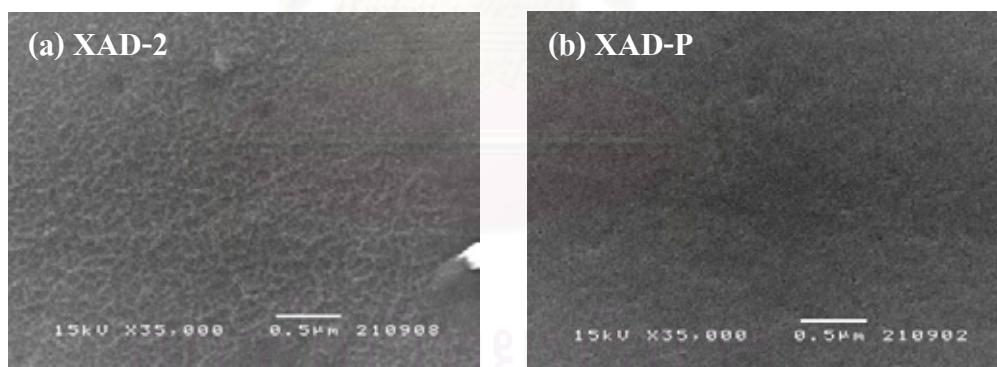


Figure 4.4 SEM photographs of (a) XAD-2 (b) XAD-P surface.

4.2.2 Elemental Analysis

The EA results were illustrated in Table 4.1.

Table 4.1 Elemental composition of the product in each synthesis step

<i>Sample</i>		<i>%C</i>	<i>%H</i>	<i>%N</i>	<i>%N/%C</i>	<i>%conversion</i>
XAD-2	exp	90.63	7.93	nd	-	-
	cal	92.31	7.69	-	-	
XAD-NO ₂	exp	61.15	5.75	8.53	0.139	95
	cal	64.43	4.70	9.40	0.146	
XAD-NH ₂	exp	67.24	7.14	6.47	0.096	66
	cal	80.67	7.56	11.76	0.146	
XAD-P	exp	71.56	7.63	6.71	0.094	89
	cal	68.39	3.63	7.25	0.106	

nd = not detectable, exp = experimental value, cal = calculated value based on one repeat unit of Amberlite XAD-2, i.e., C₈H₈, C₈H₇NO₂, C₈H₉N, C₂₂H₁₄N₂O₅.

The EA results of XAD-2 showed that the starting material consisted of only carbon and hydrogen, corresponding to the structure of XAD-2. The experiment value was slightly different from the calculated value. This difference may be due to a crosslink in their structure. If the structure of XAD-2 has the crosslink, a benzene ring will lose from the repeating unit. The results agree with this assumption, i.e., %C_{exp} (90.63) < %C_{cal} (92.31) and %H_{exp} (7.93) > %H_{cal} (7.69). From these results, the degree of crosslink can be estimated using the following equation;

$$\%crosslink = 100 - \left(\frac{(\%C / \%H)_{exp}}{(\%C / \%H)_{cal}} \times 100 \right) \quad 4-4$$

The estimation of the crosslink of XAD-2 structure was 5%. After nitration, the nitrogen content appeared, giving the value about 8.53%. This showed the successful synthesis of the XAD-NO₂. The experimental value was less than the calculated one because the letter was obtained by considering that there is no crosslink in the XAD-2 structure. But actually, XAD-2 has 5% crosslink, so some of active sites that can react with nitronium ions were reduced. The %conversion to XAD-NO₂ product was estimated using the following equation;

$$\%conversion = \frac{(\%N / \%C)_{exp}}{(\%N / \%C)_{cal}} \times 100 \quad 4-5$$

The estimation of the conversion was 95% for the nitration step. After reduction, the nitrogen content was found to be 6.47% which decreased from the previous step. Actually, the nitrogen content in this step should increase but the result opposed to the theoretical value. It indicated the incompleteness of the conversion from XAD-NO₂ to XAD-NH₂. However, the %conversion of the reduction was estimated using Equation 4-5, giving approximately 66%. The last step was the diazotization and coupling with purpurin. The result was different from the calculations which assume that the complete reaction was occurred in every step. The incompleteness of the reduction was the main cause for the low %conversion to XAD-P (89%) because of the small amount of the starting material for generating the azo (-N=N-) spacer arm attaching with purpurin.

In conclusion, although the EA result cannot completely confirm the success of the modification of the XAD-2 with purpurin, it can reveal the elemental composition of the products and help to estimate the %conversion in each synthesis step.

4.2.3 Fourier Transforms Infrared Spectroscopy

The IR spectra were illustrated in Figure 4.7.

The IR spectra of the resins were recorded using the potassium bromide technique. The IR spectrum of XAD-2 showed three characteristic peaks of aromatic ring as follows: $\nu(\text{C-H})$ at 3017 cm^{-1} and $\nu(\text{Ar C=C})$ at 1600 and 1448 cm^{-1} which correspond to the aromatic network structure of the polymer backbone. After nitration, the IR spectrum of XAD-NO₂ exhibited peaks at 1526 and 1348 cm^{-1} due to $\nu(\text{N=O})$ asymmetric and $\nu(\text{N=O})$ symmetric, respectively. To confirm these two N=O peaks, the difference in wavenumber should not be more than 200 cm^{-1} , the result gave only 178 cm^{-1} . Therefore, the XAD-NO₂ resin was successfully synthesized. The appearance of a broad band in the spectrum of XAD-2 and XAD-NO₂ at $3600\text{-}3200\text{ cm}^{-1}$ was possibly due to $\nu(\text{O-H})$ of the adsorbed water in the pore of resin.

The next step was the reduction of XAD-NO₂ to XAD-NH₂, the IR spectrum of XAD-NH₂ (see Figure 4.7(c)) showed peaks at 3430 , 1626 and 1383 cm^{-1} , which may be assigned to $\nu(\text{N-H})$, $\delta(\text{N-H})$ and $\nu(\text{=C-NH}_2)$, respectively. The primary amine in XAD-NH₂ resin should theoretically show two peaks in the range of $3500\text{-}3200\text{ cm}^{-1}$ but the obtained spectrum showed only one peak, probably due to the overlap with the $\nu(\text{O-H})$ band of adsorbed water. Although the signal of $\nu(\text{O-H})$ and $\nu(\text{N-H})$ appeared at the same frequencies range, we can distinguish these signals using the difference of the peak intensity of the signal of $\nu(\text{N-H})$ that was stronger than $\nu(\text{O-H})$ as shown in Figure 4.7(b) and 4.7(c). Moreover, the presence of weak intensity peaks at 1517 and 1348 cm^{-1} in the XAD-NH₂ spectrum exhibited the remaining of nitro group on the resin surface after reduction, corresponding to the EA result that showed the incomplete reaction which gave about 66% conversion for reduction step.

The final step involved the addition of purpurin into the diazotized resin. The characteristic peaks of purpurin are concerned to $\nu(\text{O-H})$, $\nu(\text{C=O})$ (2 peaks), $\nu(\text{Ar C=C})$ (2 peaks), $\nu(\text{C-O})$ and carbonyl C-C-C, which appeared at 3396 ; 1670 and

1622; 1583 and 1443; 1287; and 1174 cm^{-1} , respectively (see Figure 4.7(e)). To easily discuss, the additional numbering in the purpurin structure indicating carbon numbers was assigned in Figure 4.5. The peaks of $\nu(9\text{-C=O})$ at 1665 cm^{-1} and $\nu(10\text{-C=O})$ at 1622 cm^{-1} appeared at lower frequency than $\nu(\text{C=O})$ of simple ketone that normally occurs around 1710 cm^{-1} . Since the conjugation effects of the purpurin structure, the delocalization of π -electrons reduced the electron density of C=O bonds, weakening it and lowering the stretching frequency. In addition, intramolecular hydrogen bonding between 9-C=O and 1-OH and 10-C=O and 4-OH also affected the reduction of electron density between C=O bonds. These effects (conjugation and hydrogen bonding effect) lead to the very lower stretching frequency of 9-C=O and 10-C=O bonds than the simple ketone. The peaks of $\nu(9\text{-C=O})$ and $\nu(10\text{-C=O})$ separately appeared, possibly due to a resonant donation involving the electron donating of 2-OH group through π -bonding that more influences to near 9-C=O than far 10-C=O groups, therefore, the electron density at 9-C=O was slightly higher than that of 10-C=O one and appeared at higher stretching frequency. The band of carbonyl C-C-C at 1174 cm^{-1} means stretching and bending modes of three carbons in the middle of purpurin anthraquinone skeleton. After functionalization with purpurin (see Figure 4.7(d)), the IR spectrum of XAD-P was compared with that of previous XAD-NH₂. There are two additional peaks at 1704 and 1347 cm^{-1} which may be assign to $\nu(\text{C=O})$ and $\nu(\text{C-O})$, respectively, ensuring the presence of the chelating ligand purpurin attached to the polymer support. The slightly higher frequency of $\nu(\text{C=O})$ and $\nu(\text{C-O})$ after attachment of purpurin to the polymer support through the azo (-N=N-) spacer, possibly due to an inductive effect involving the electron withdrawing of azo spacer group through the sigma bond, as shown in Figure 4.6. The nitrogen atoms in the azo group have strong electronegativity, they can withdraw electrons from the vicinal 4-C-OH and 2-C-OH and consequently the C-O bond distance was reduced so it can stretch at higher frequency. This situation slightly influenced with the farther 10-C=O that we can see the blue shift of $\nu(\text{C=O})$ frequency (+39 cm^{-1}) that is less than the blue

shift of $\nu(\text{C-O})$ frequency ($+60 \text{ cm}^{-1}$). Furthermore, the presence of peaks $\nu(\text{N-H})$ at 3439 cm^{-1} , $\delta(\text{N-H})$ at 1626 cm^{-1} and $\nu(\text{N=O})$ at 1522 cm^{-1} in Figure 4.7(d) showed the remaining of amino and nitro group on the XAD-P surface which caused the difference between the experimental and calculated values of the EA results of the final product.

In conclusion, FT-IR characterization showed the success of the synthesis following the pathway and confirmed the attachment of purpurin on the polymer support. Moreover, the data from the EA results were supported by the observation of FT-IR technique.

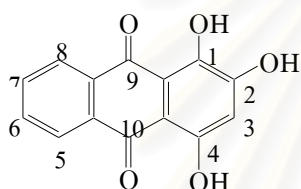


Figure 4.5

Carbon number assignment of purpurin for the IR spectrum discussion.

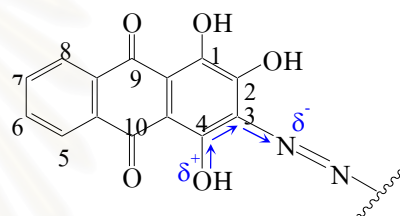


Figure 4.6

Electron withdrawing effect of the azo group through a sigma bond.

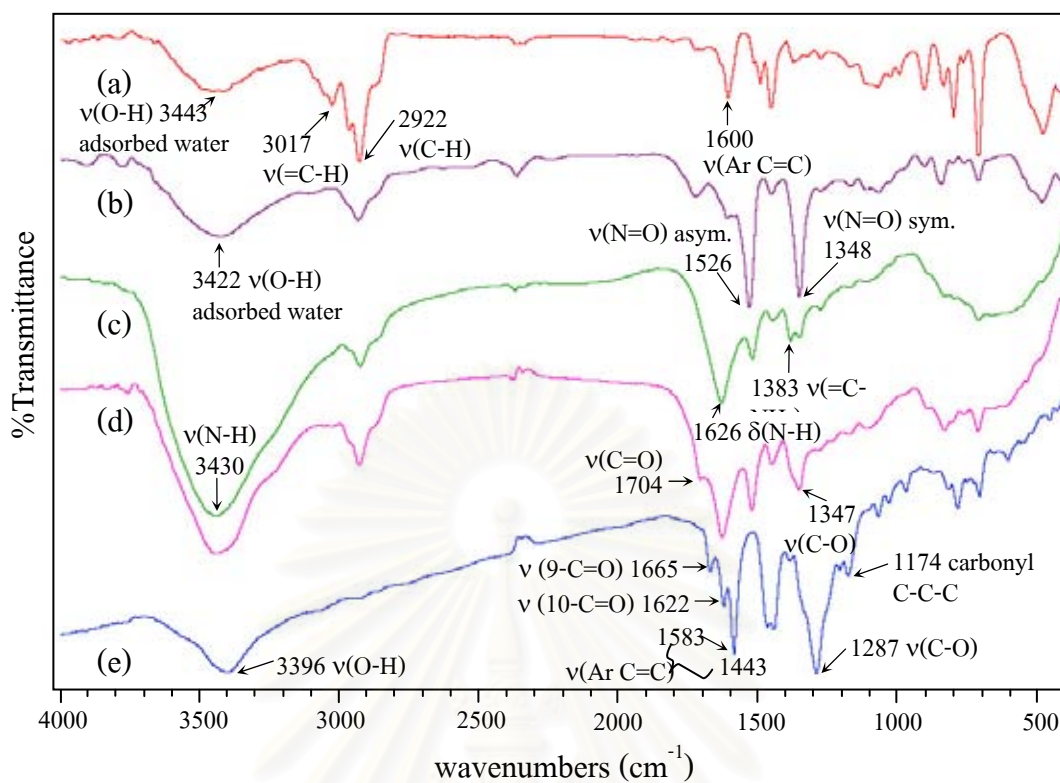


Figure 4.7 Infrared spectra of (a) XAD-2, (b) XAD-NO₂, (c) XAD-NH₂, (d) XAD-P and (e) Purpurin

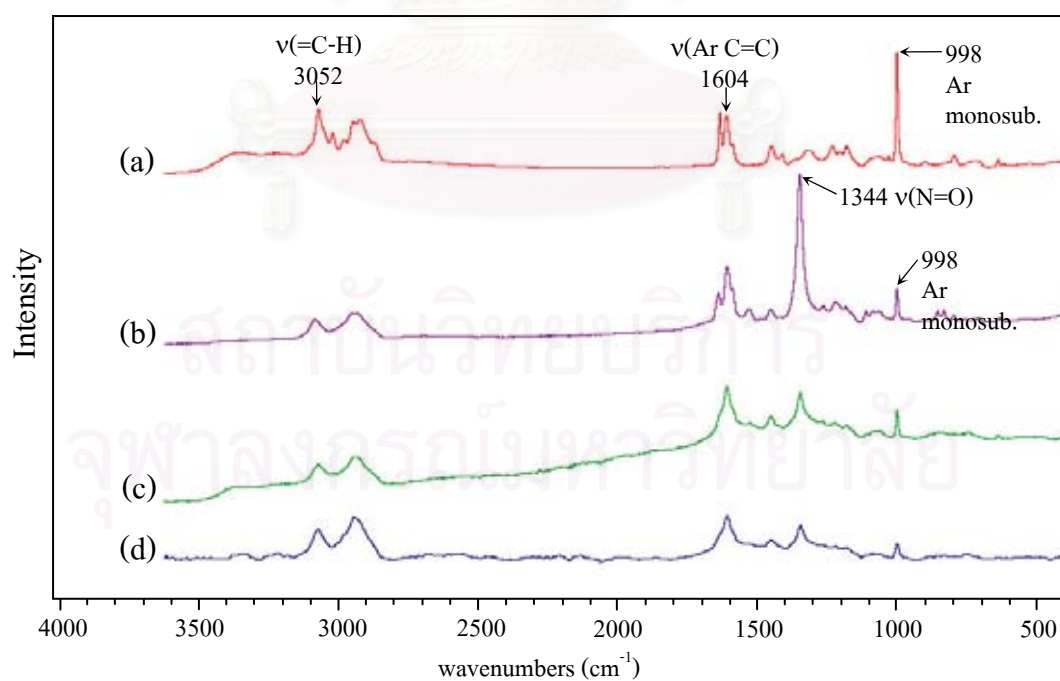


Figure 4.8 Raman spectra of (a) XAD-2, (b) XAD-NO₂, (c) XAD-NH₂ and (d) XAD-P

4.2.4 Fourier Transforms Raman Spectroscopy

The Raman spectra were illustrated in Figure 4.8.

Another way to identify the functional groups on the resin surface was a Raman spectroscopy. FT-Raman has many advantages over FT-IR. Therefore, this research used Raman spectroscopy in order to get more information about the resin structure and we expected to get easier interpretation of the spectrum because the Raman spectra are usually much simpler than IR spectra.

The Raman spectrum gave sharper peaks and combination bands are not very intense, so we got the very simple spectrum than IR ones, as shown in Figure 4.8. The Raman spectrum of XAD-2 has three characteristic peaks at 3052, 1604 and 998 cm^{-1} , which may be assigned to $\nu(\text{=C-H})$, $\nu(\text{Ar C=C})$ and aromatic monosubstituted. The latter peak was not previously found in the IR spectrum. This peak showed a monosubstitution of aromatic ring in the network structure of polystyrene. In fact, some parts of network structure are disubstituted aromatic at the crosslink position (divinylbenzene) but this characteristic does not appear in the spectrum because XAD-2 polymer has only 5% crosslink. After nitration, the strong intensity of $\nu(\text{N=O})$ was observed at 1344 cm^{-1} together with the decreasing intensity of the peak at 998 cm^{-1} . The decrease of peak intensity showed the change of monosubstituted to disubstituted one due to the addition of nitro group to the aromatic ring. This result confirmed a successful nitration. Moreover, the appearance of a small peak at 998 cm^{-1} indicated an incomplete nitration (If the reaction was complete, this peak would have absolutely disappeared because no monosubstituted content on the resin surface). The observation is in accordance with the EA results that showed 95% conversion for the nitration step. Considering the Raman spectrum in Figure 4.8(a) and 4.8(b), no peak appeared at the frequency more than 3100 cm^{-1} , this confirmed that the band in the range of 3600-3200 cm^{-1} in Figure 4.7(a) and 4.7(b) of IR spectra was the $\nu(\text{O-H})$ of adsorbed water, since water molecule is inactive in Raman spectroscopy. After

reduction, no additional peak showed in the Raman spectrum (see Figure 4.8(c)) but we can see the decrease of $\nu(\text{N}=\text{O})$ intensity inferred the conversion of XAD-NO₂ to XAD-NH₂. In the last step, purpurin was attached to the resin. The Raman spectrum of the XAD-P was compared with the previous product. The spectra are mostly similar, as shown in Figure 4.8(d), because of the detection limits for Raman spectrometry are often inferior to those obtained with IR spectrometry. Therefore, it cannot detect a few amount of purpurin which attached to the resin.

Although Raman spectroscopy cannot confirm the successful synthesis of the XAD-P, but it provided the additional information, such as, the number of the substitution groups on aromatic ring and supported the hypothesis of incomplete conversion XAD-2 to XAD-NO₂ from the EA result.



สถาบันวิทยบริการ
จุฬาลงกรณ์มหาวิทยาลัย

4.2.5 Thermal Gravimetric Analysis

The different TGA curves of the product from each synthesis step, as illustrated in Figures 4.10 and 4.11, showed the different decomposition temperature of the synthesized functional polymers.

The starting material XAD-2 was decomposed in the range of 350-500°C. After nitration, XAD-NO₂ was decomposed at lower temperature (250-350°C) than XAD-2, possibly due to the effect of an electron withdrawing nitro group. The strength of π -conjugate system of XAD-2 was diminished, so it can decompose easier. For the reduction, XAD-NO₂ was reduced to XAD-NH₂ where amine is the electron donating group, so the strength of π -conjugate system of XAD-2 returned and the decomposition temperature was back to the range of 350-500°C. Moreover, the 19.09% mass loss at up to 150°C was observed, showing the sorbed water in the pores of XAD-NH₂.

The TGA curve of the final product XAD-P (see Figure 4.9) showed two stages of mass loss up to 500°C. In the first stage, a mass loss of 10.16% at 130°C seems to be due to sorbed water evaporation and suggested that approximately two and a half water molecules per repeat unit of resin was present. The second mass loss started after 200°C, corresponding to the first decomposition stage of purpurin that began around 250°C (see the arrow in Figure 4.11) and then gradually decomposed up to 500°C that corresponded to the finished decomposition of polymer support (see Figure 4.11(a)). Therefore, the second mass loss of XAD-P was attributed to the decomposition of the functionalized purpurin together with the polymer support. After 500°C, the TGA curve showed a very slow but steady mass loss until 800°C. The presence of water molecule in this resin showed that XAD-P was more hydrophilic than the starting solid support (XAD-2). Consequently, the rate of metal ion phase transfer from solution onto the chelating resin will be increased.

The TGA results can confirm the presence of purpurin on the XAD-2 surface and showed the hydrophilicity of XAD-P. In addition, higher thermal stability of the functionalized resin was observed.

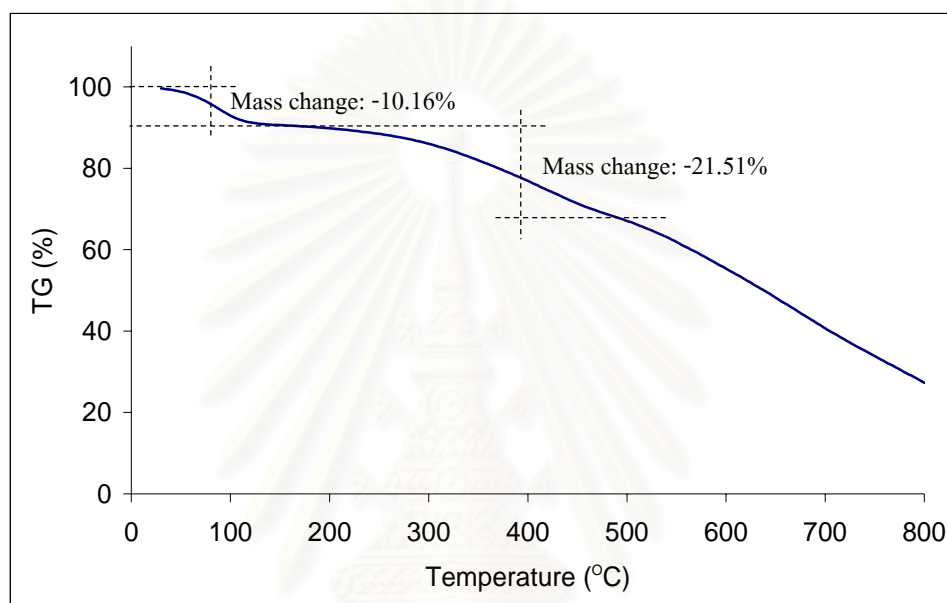


Figure 4.9 Thermograms of XAD-P.

สถาบันวิทยบริการ
จุฬาลงกรณ์มหาวิทยาลัย

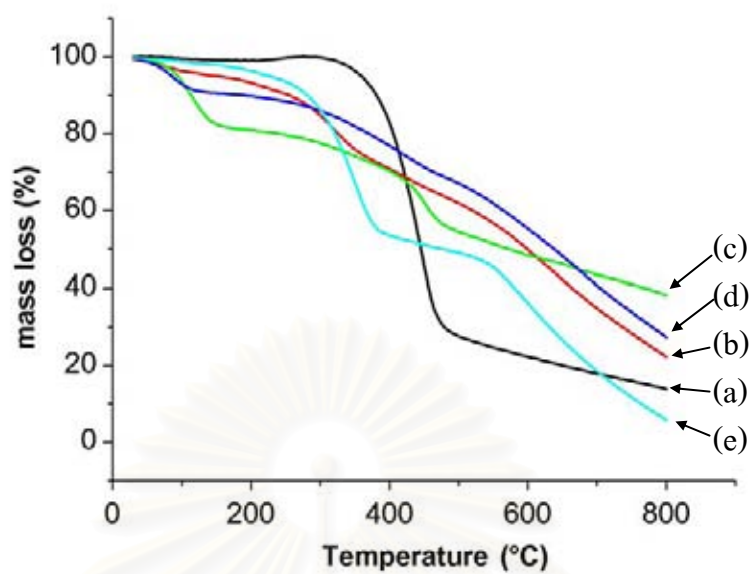


Figure 4.10 Comparison thermograms of (a) XAD-2 (b) XAD-NO₂ (c) XAD-NH₂ (d) XAD-P and (e) purpurin.

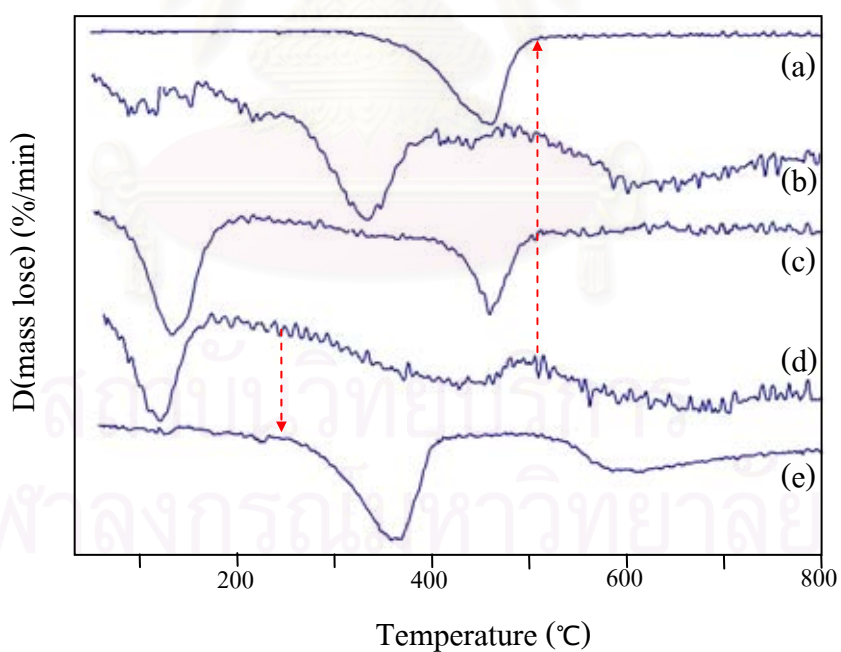


Figure 4.11 Comparison differentiate thermograms of (a) XAD-2 (b) XAD-NO₂ (c) XAD-NH₂ (d) XAD-P (e) purpurin.

excess amount of physisorbed purpurin (noncovalent bond) that remained on the resin surface. From this result, we can infer that 3 g of purpurin was too much for the synthesis of XAD-P.

The selection of the appropriate amount of purpurin based on the use of the smallest starting amount of purpurin to achieve the highest amount of purpurin adsorbed on XAD-P or the highest of percent loading. Figure 4.15 showed that 3 g of starting purpurin (Batch No.1) was too much for XAD-P synthesis because it gave a very low percent loading. For Batch No.4, 0.1 g of starting purpurin was not enough for XAD-P synthesis since it gave a little amount of purpurin adsorbed on XAD-P. Therefore, we can infer that the use of 3 and 0.1 g purpurin was not suitable for the synthesis of XAD-P. Thus 0.5 g of starting purpurin (Batch No.3) gave the maximum percent loading so this amount should be the most suitable for XAD-P synthesis. However, 1 g of starting purpurin (Batch No.2) slightly gave the amount of purpurin adsorbed more than Batch No.3.

Therefore, 1 g of purpurin per 10 g XAD-2 used was selected for XAD-P synthesis to ensure the high amount of purpurin adsorbed on the solid support. At this amount, XAD-P contained with purpurin about 0.14 mg g^{-1} resin.

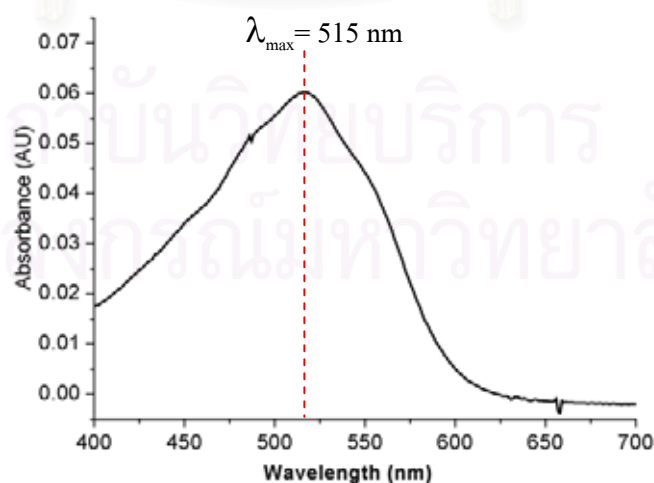


Figure 4.13 Reference absorption spectrum of purpurin in 50% ethanol.

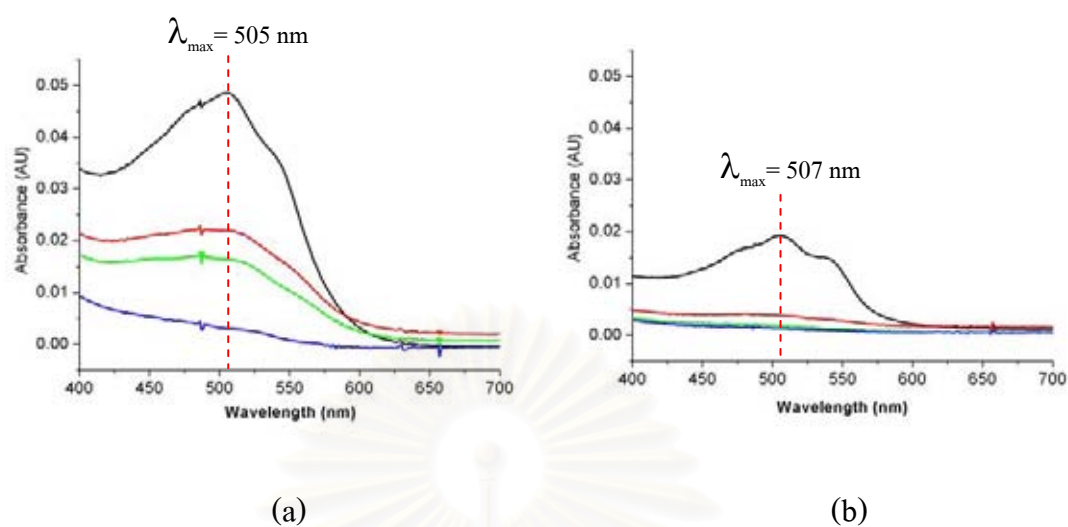


Figure 4.14 Absorption spectra of eluted purpurin using (a) 50% ethanol (b) DI water.

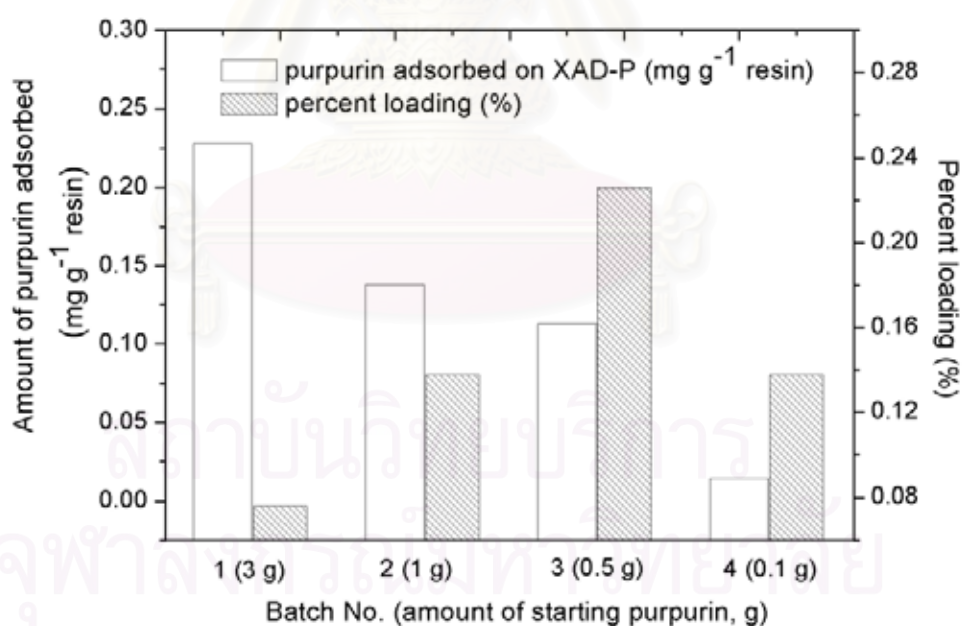


Figure 4.15 Comparisons of the amount of starting purpurin (in parenthesis), purpurin adsorbed on XAD-P and percent loading.

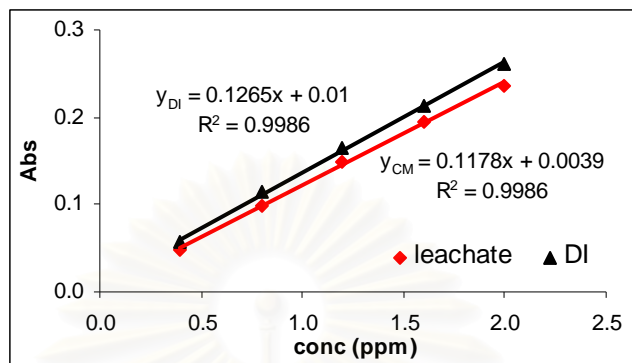
4.4 Influence of Leachate on Metal Calibration Curve

To prove the effect of leachate on the determination of metal ions, the comparison of calibration curves in two different matrices; leachate and DI water was studied and the significance test was accomplished using paired t -test at 95% confidence limit.

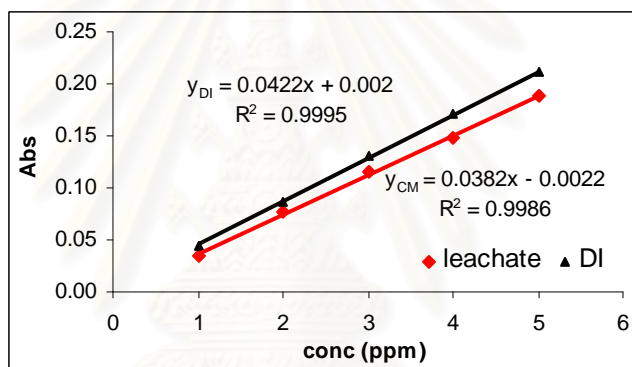
Considering Figure 4.16, in leachate, the sensitivity (slope of calibration equation) of the determination of all the metal ions was lower comparing with in DI water. The significance test result, as shown in Table 4.2, showed that the determination of metal ions in both matrices gave significantly different results for Cd and Cr since the calculated value of $|t_{stat}|$ is more than $t_{critical}$ whereas no significantly different results was observed for Pb. This can be explained by the very high pH of leachate at about 12 that induced the precipitation of metal ion as metal hydroxide. The metal hydroxide solubility curve is illustrated in Figure 4.17, it shows that the solubility of some metal hydroxide can increase in high pH, especially for $Pb(OH)_2$. The $Pb(OH)_2$ can completely dissolve at pH 12, thus the absorbance of Pb in the high pH leachate was not significantly different from that in DI water. In addition, a P -value (probability) was used to determine how much the result of the metal determination in both matrices differs. The P -value of Cd^{2+} and Cr^{3+} (Table 4.2) is much less than 0.05. This indicates that the results from both matrices are much different. For Pb^{2+} , the P -value is greater than 0.05 that means the results do not differ significantly at $P = 0.05$.

From this observation, the extraction of metal ions from leachate matrix should be done before their determination using FAAS in order to get better sensitivity. Even though in the case of Pb, the decrease of sensitivity is not significantly different but the extract of Pb from leachate before determination is still important to prolong the lifetime of AAS burner and reduce the interferences during spectrophotometric analysis. Particularly, if an electrothermal AAS is subjected to be used for the determination, since calcium and other concomitants are the main background

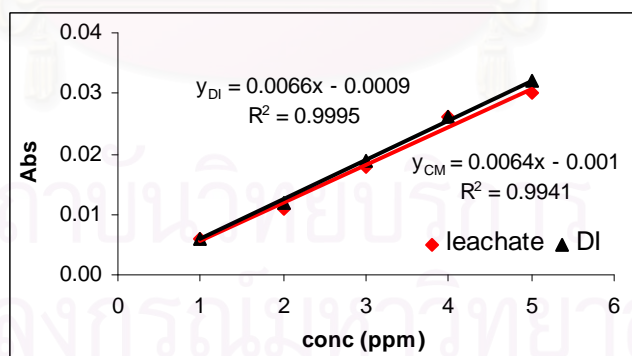
interferences. The cleaner the sample solution, the longer the lifetime of a graphite furnace, as well as the better the result.



(a) Cd



(b) Cr



(c) Pb

Figure 4.16 Comparison of calibration curve between preparing standard in leachate and DI water matrix.

Table 4.2 Paired t -test between the determination of metal ion in leachate and DI water matrix

<i>metal</i>	t_{stat}	$t_{critical} (n-1=4)$	$P(T \leq t_{stat})$
Cd	-6.16	2.78	0.004
Cr	-6.43	2.78	0.003
Pb	-2.13	2.78	0.099

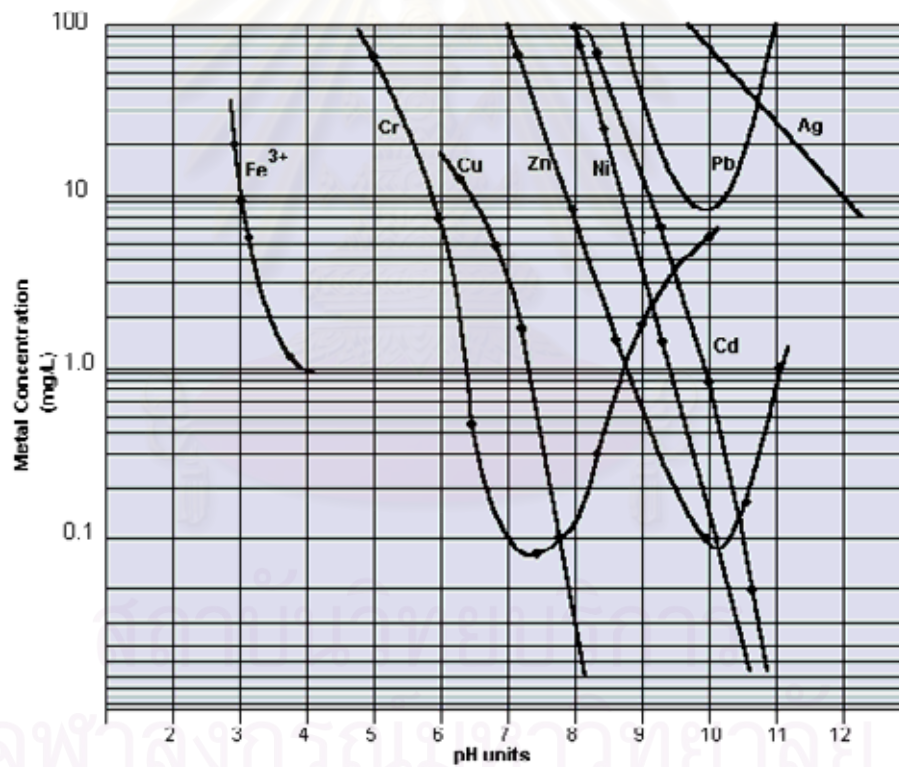


Figure 4.17 Metal hydroxide solubility curve versus pH [61].

4.5 Extraction and Desorption Studies

4.5.1 Batch Method

4.5.1.1 Effect of pH on metal extraction

Binding sites of ligand can be controlled by solution pH. In acid medium, binding sites may be protonated, so the ligand cannot form complex with any metal ion. In basic medium, binding sites should be ready to complex with metal ion(s) but sometime the metal ions cannot be extracted because many hydroxide ions in solution caused the precipitation of these metal ions. Therefore, the effect of pH on metal extraction should be preliminary studied.

The results were illustrated in Figure 4.19. The sorption capacity (mg g^{-1} resin) of each metal ion was determined by Equation 4-7.

$$\text{sorption capacity} = \frac{mg_{bef} - mg_{aft}}{g_{sorbent}} \quad 4-7$$

where mg_{bef} = the amount of metal in the solution before extraction

mg_{aft} = the amount of metal remaining in the solution after extraction

$g_{sorbent}$ = mass of resin, XAD-P (g)

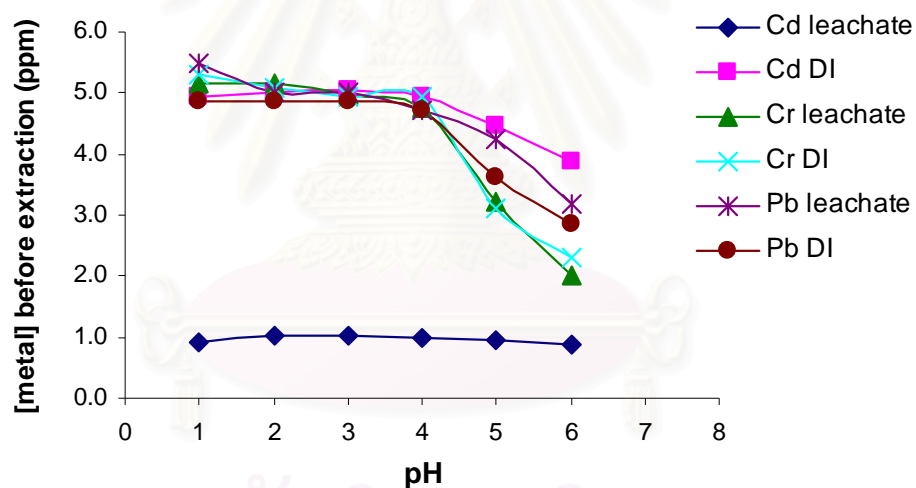
The maximum sorption capacity for Cd^{2+} , Cr^{3+} and Pb^{2+} was observed at pH 4.0 in both matrices. The pH less than 4.0 was not suitable for the extraction because the binding site of purpurin was possibly protonated. At pH more than 4.0, the sorption capacity decreased gradually. This situation can be explained by the decrease of metal ion concentration before extraction (see Figure 4.18). This indicated that the absorbance of all the metal ions at 5 ppm began decreasing after pH 4.0. According to the species distribution versus pH, as illustrated in Figure 4.20, some metals might be precipitated at high pH, for example Pb^{2+} . Moreover at pH more than 4.0, the metals are difficulty atomized caused by hydrated or hydroxide species such as $\text{Cr}_3(\text{OH})_4^{5+}$.

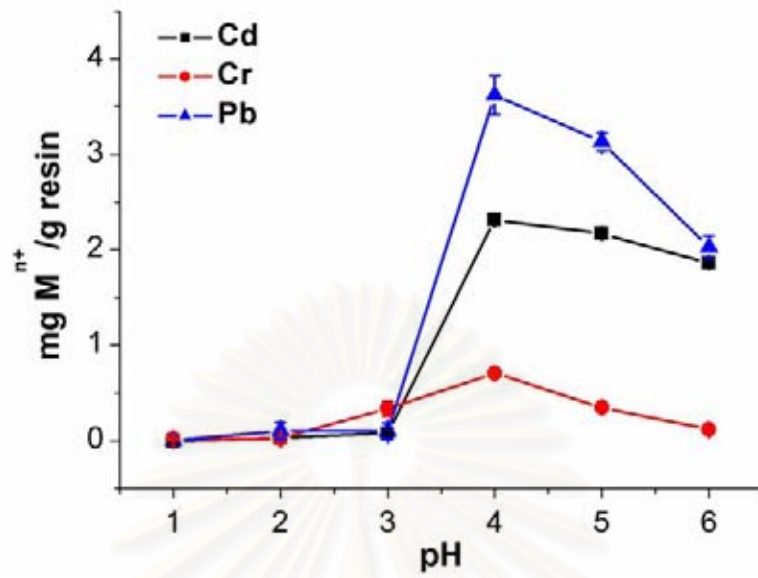
In addition, the pH of solution after extraction was measured, as shown in Table 4.3. It was observed that the pH of DI water /XAD-P increased up to 9.75, possibly due to the use of 10%NaOH in the last step of XAD-P synthesis. Comparing with that of DI water /XAD-P containing 1 ppm of Cd, it was found that the pH of solution decreased to 8.65. This indicated that the sorption process involved the proton exchange mechanism of the complexation of metal ions. When the leachate spiked with 1 ppm of Cd was used, the pH of the solution after sorption was observed at 7.15. This indicated that Ca^{2+} in the leachate can also adsorbed onto XAD-P and the release of H^+ to the solution took place. In addition, the leachate has a buffer property, the pH of the solution was kept more constant.

In summary, the appropriate pH for making the purpurin moiety ready to form complex with the metal ions in both matrices was ≥ 4.0 . Since all the metal ions in this research begin to precipitate after pH 4.0, the optimum pH all the metal ions was selected at 4.0.

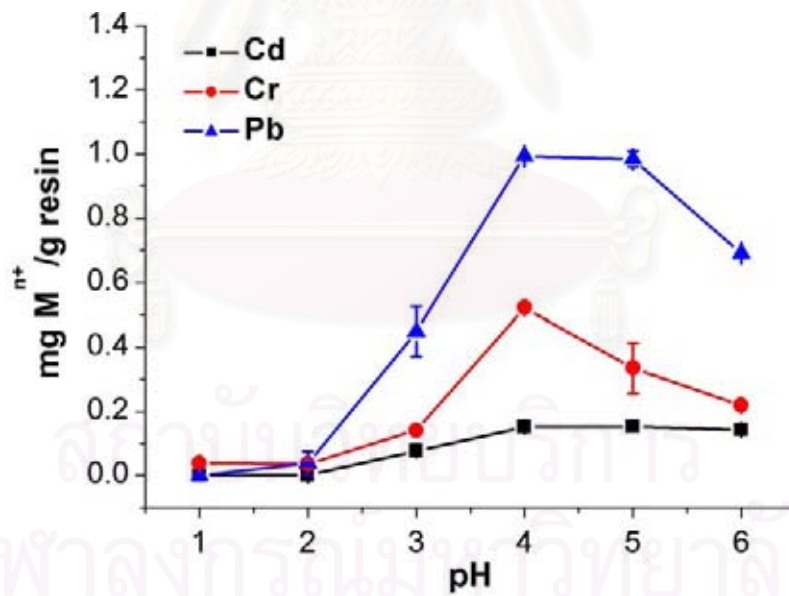
Table 4.3 Comparison of pH solution after sorption

XAD-P stir with	Solution pH	
	Before extraction	After extraction
DI	5.59	9.75
DI + Cd ²⁺ 1 ppm	5.96	8.65
Leachate + Cd ²⁺ 1 ppm	5.83	7.15

**Figure 4.18** Concentration of each metal ion before extraction at different pH.



(a) Cd²⁺ 1 ppm, Cr³⁺ 5 ppm and Pb²⁺ 5 ppm in DI matrix



(b) Cd²⁺, Cr³⁺ and Pb²⁺ 5 ppm in leachate matrix

Figure 4.19 Effect of pH on metal extraction.

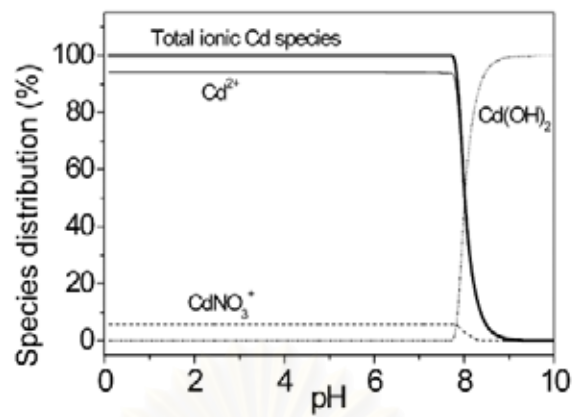
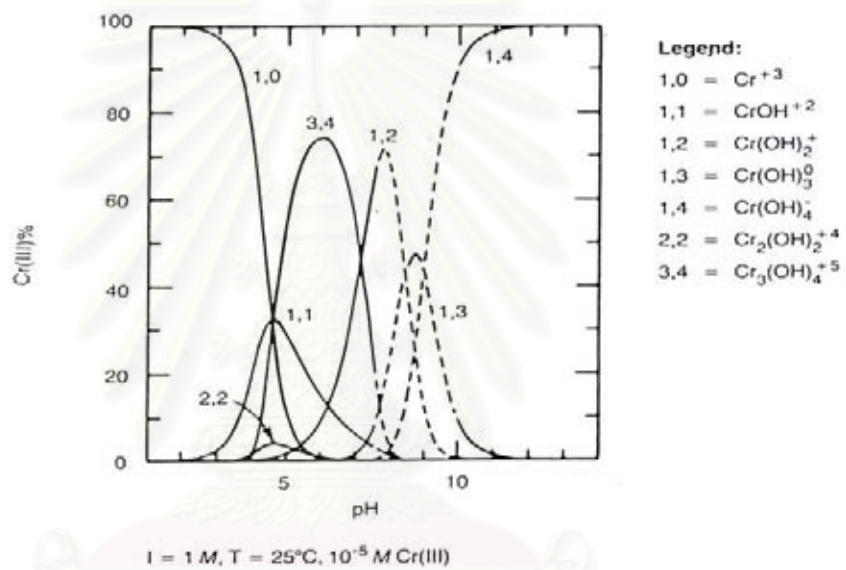
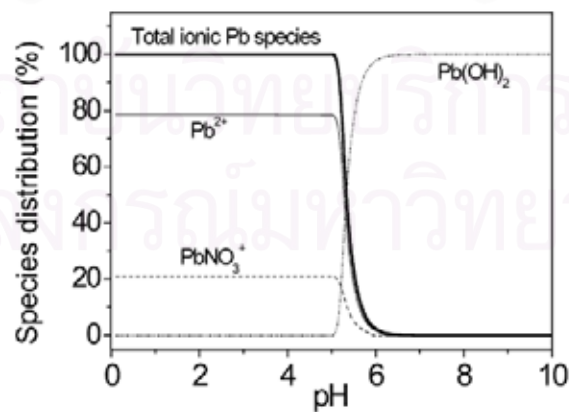
(a) Cd^{2+} (b) Cr^{3+} (c) Pb^{2+}

Figure 4.20 Species distribution diagrams versus pH [62, 63].

4.5.1.2 Kinetics of metal extraction

The variation of sorption as a function of time for all the metal ions at pH 4.0 is shown in Figure 4.21, it was observed that an equilibrium time of about 30 min and 20 min was required for Pb^{2+} and Cd^{2+} , respectively, in both matrices and that of about 10 min for Cr^{3+} in DI and 40 min for Cr in leachate.

To determine the rate constant of each metal ion, the Lagergren equation (Equation 4-8) was applied by plotting $\log(q_e - q_t)$ versus time [64].

$$\log(q_e - q_t) = \log q_e - \frac{kt}{2.303} \quad 4-8$$

where q_e = the sorbed concentration of metal ions onto sorbent at equilibrium (mol g^{-1})

q_t = the sorbed concentration of metal ions at any time t (mol g^{-1})

t = extraction time (min)

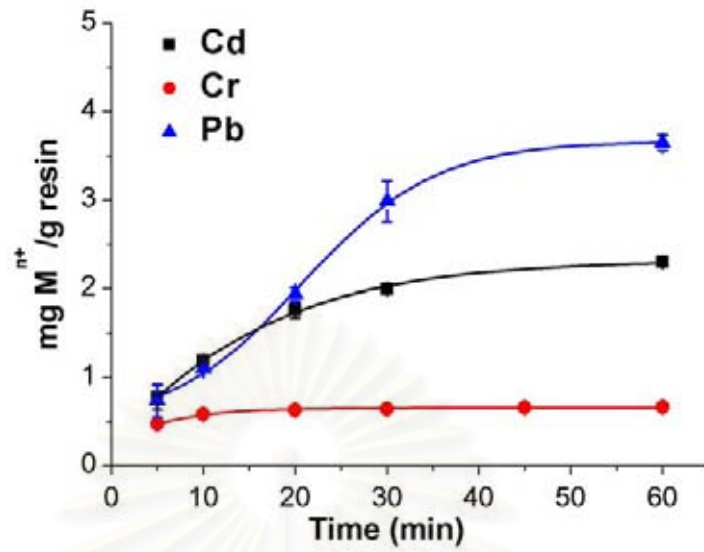
k = rate constant (min^{-1})

The rate constants are shown in Table 4.4 and the order was observed that $\text{Cr}^{3+} > \text{Cd}^{2+} > \text{Pb}^{2+}$ in DI water and $\text{Cd}^{2+} > \text{Pb}^{2+} > \text{Cr}^{3+}$ in leachate. In leachate, the matrix contained calcium ions at very high concentration, so the competition of the sorption onto XAD-P between Ca^{2+} and the analyte metal ions occurred. The order of rate constant in leachate can be explained by HSAB principle. The soft cation Cd^{2+} prefers to bind at a soft base site (O, N), namely B site in Figure 4.24 and the borderline Pb^{2+} prefers to bind at a borderline site (O, O), namely A and C site in Figure 4.24; (the detail of hardness and softness of binding site will be discussed in 4.5.1.5), while hard cation Cr^{3+} has no favorite site to bind on XAD-P. Ca^{2+} in leachate extremely affected the sorption of Cr^{3+} because both of them are hard cations that can bind with purpurin at the same binding site. This corresponds to the order of the rate constants in leachate in Table 4.4 that Cr^{3+} had the slowest rate constant whereas the rate constants of Cd^{2+} and Pb^{2+} was still the same in both matrices, indicated that Ca^{2+} ions do not disturb the rate of sorption of these two metal ions.

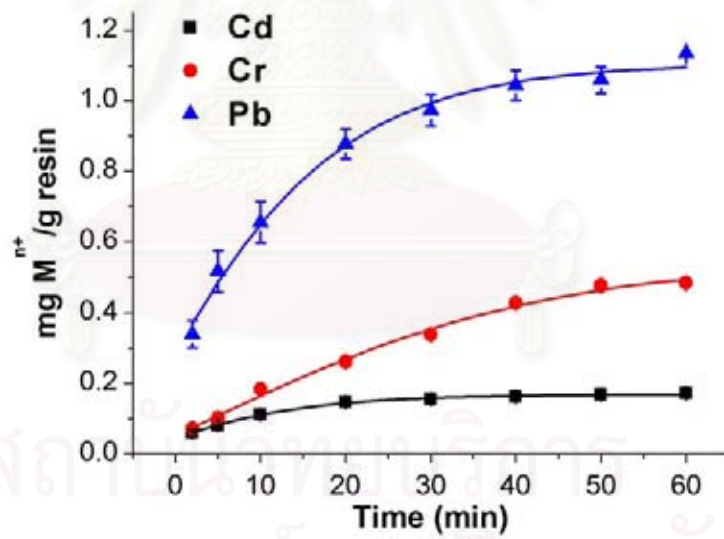
In conclusion, the experiment showed that Ca^{2+} in leachate do not interfere the rate of sorption of Cd^{2+} and Pb^{2+} onto XAD-P surface but it greatly reduce the rate of Cr^{3+} sorption. And the equilibrium time of one hour was fixed for the further extraction of all the metal ions.

Table 4.4 Summary the data from the Lagergren plot

<i>metal</i>	<i>equation</i>	R^2	<i>Rate constant (min^{-1})</i>
In DI water			
Cd	$y = -0.0283x - 4.7295$	0.9974	0.0652
Cr	$y = -0.0668x - 5.0812$	0.9723	0.1538
Pb	$y = -0.0254x - 4.5642$	0.9354	0.0585
In leachate			
Cd	$y = -0.0282x - 5.9757$	0.9902	0.0649
Cr	$y = -0.0161x - 5.0646$	0.9945	0.0371
Pb	$y = -0.0244x - 5.3913$	0.9973	0.0562



(a) Cd²⁺ 1 ppm, Cr³⁺ 5 ppm and Pb²⁺ 5 ppm at pH 4 in DI matrix



(b) Cd²⁺, Cr³⁺ and Pb²⁺ 5 ppm at pH 4 in leachate matrix

Figure 4.21 Kinetics of metal extraction on XAD-P.

4.5.1.3 Effect of eluent

The effect of eluent was investigated to recover the adsorbed metal ions on XAD-P.

Nitric acid, which is compatible with the determination using FAAS, was firstly selected as an eluent. The selection criterion was based on the result of the effect of pH observed that XAD-P could not extract any metal ions at pH 1.0-2.0. The concentration of nitric acid was varied in the range of 1-5% v/v in order to achieve the enough of proton for protonating chelation sites (proton exchange mechanism was purposed). The results were plotted between the %strip that was calculated from Equation 4-9, versus the concentration of nitric acid, as shown in Figure 4.22.

$$\%strip = \frac{mg_{strip}}{mg_{adsorbed}} \times 100 \quad 4-9$$

Where $mg_{adsorbed}$ = the amount of metal ion adsorbed on resin (mg)

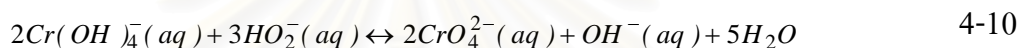
mg_{strip} = the amount of metal ion eluted from resin (mg)

1% v/v HNO_3 was sufficient for quantitative elution with more than 90%strip of all the metal ions, except for Cr^{3+} . The similar results for the elution of Cr^{3+} using nitric acid was previously reported by Wuttinun L. [63]. We try to explain this situation using the charge density of metal ion. Cr^{3+} has the highest charge density. It sorbs strongly onto the resin, therefore is difficult to elute from XAD-P surface by a simple acid solution.

The alternative way for desorption is an elution by a chelating agent that should form stronger complex with Cr than purpurin. EDTA, which is a well known complexing agent and has a high formation constant with many metal ions, was selected for eluting Cr from XAD-P. The results are shown in Table 4.5. The results showed that EDTA cannot quantitatively elute Cr from XAD-P.

Cr^{3+} might form complex with purpurin using the difference between its positive charge and the negative charge of the ligand. If the metallic positive charge is

changed to negative charge, the complexation will be disrupted. Based on this assumption, H₂O₂ in 0.1 M NaOH was selected to elute Cr³⁺ because it can act as an oxidizing agent following Equation 4-10 [65], so Cr³⁺ on XAD-P might be oxidized to Cr⁶⁺. The dominant species of Cr⁶⁺ is chromate ion (CrO₄²⁻) [63] which has a negative charge and cannot rather be retained on XAD-P. Therefore, Cr should be eluted. This hypothesis could be elucidated by observing the yellow color of CrO₄²⁻ presented in the eluate. The results of various concentrations of H₂O₂ in 0.1 M NaOH are shown in Table 4.5. It was found that the quantitative elution of Cr was achieved by using more than 5 %H₂O₂ in 0.1 M NaOH.



(This equation, Cr³⁺ stays in the form of Cr(OH)₄⁻ due to the basic medium of eluent)

In conclusion, the selected eluents for the metal desorption from XAD-P were 1%HNO₃ for Cd²⁺ and Pb²⁺ and 10%H₂O₂ in 0.1 M NaOH for Cr³⁺.

Table 4.5 Effect of EDTA and H₂O₂ concentration for the Cr³⁺ desorption

<i>eluent</i>	<i>concentration</i>	<i>%strip (Mean value ± SD, n=3)</i>
EDTA (M)	0.01	7 ± 0.32
(at pH 5.0)	0.05	11 ± 0.58
	0.1	12 ± 0.26
H ₂ O ₂ (%)	5	89 ± 0.20
(in 0.1 M NaOH)	10	93 ± 1.60
	15	91 ± 0.61

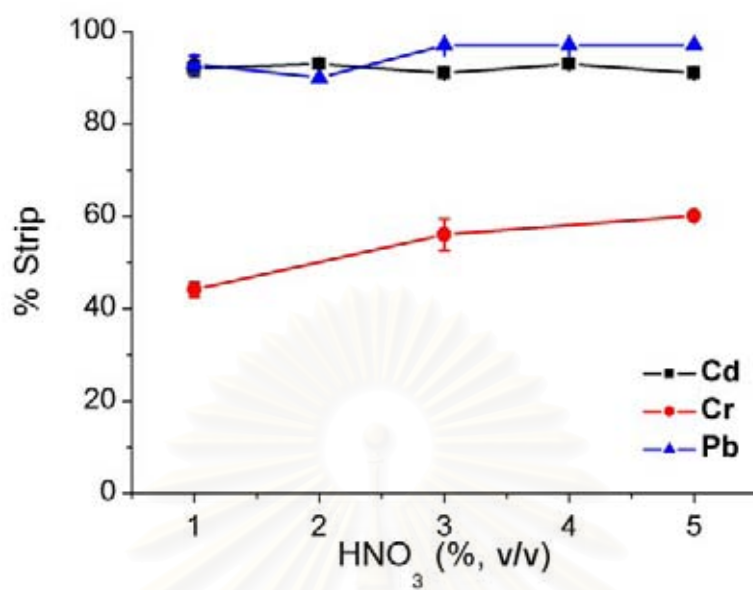


Figure 4.22 Effect of HNO₃ concentration on metal desorption.

สถาบันวิทยบริการ
จุฬาลงกรณ์มหาวิทยาลัย

4.5.1.4 Effect of elution time

To test the kinetics of desorption, %strip was investigated as a function of time. The results, Figure 4.23, showed that the desorption of Cd^{2+} and Pb^{2+} by 1% HNO_3 occurred rapidly with more than 90%strip within 10 min. For Cr^{3+} , H_2O_2 in 0.1 M NaOH solution was used as the eluent. The redox reaction required longer time than those of Cd^{2+} and Pb^{2+} . About 80%strip was obtained within 30 min.

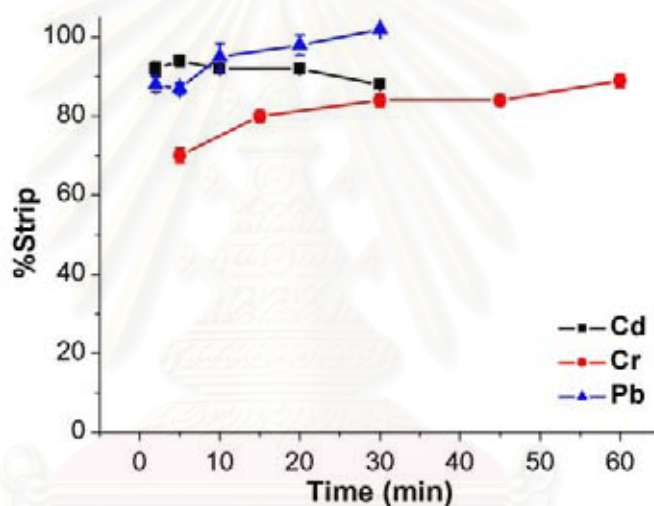


Figure 4.23 Effect of elution time.

4.5.1.5 Adsorption isotherm

The distribution of metal ions between liquid and solid phases can be described by several adsorption isotherms. The earliest and simplest adsorption isotherms are Langmuir and Freundlich isotherms. Langmuir isotherm is based on these assumptions; metal ions are chemically adsorbed at a fixed number of well defined sites; each site can hold only one ion (monolayer adsorption); all sites are energetically equivalent (homogenous surface) and; there is no interaction between the ions [66, 67]. Whereas, Freundlich isotherm is based on the assumption that the uptake of metal ions occurs on a heterogeneous surface by monolayer adsorption [66] or a multi-layer adsorption if the adsorption isotherm lacks a plateau [67].

The experiments were performed for both adsorption isotherms. The linearized Langmuir isotherm allows the calculation of adsorption capacities and the Langmuir constant and the model is described by Equation 4-11.

$$\frac{C}{N_f} = \frac{1}{bN_s} + \frac{C}{N_s} \quad 4-11$$

where C = the metal residual concentration in solution at equilibrium
(mol dm⁻³)

N_f = the amount of metal ions adsorbed per gram of sorbent (mol g⁻¹)

N_s = the maximum sorption capacity of the sorbent (mol g⁻¹)

b = Langmuir constant related to energy of adsorption (L mol⁻¹)

And the linearized form of Freundlich isotherm is shown in Equation 4-12.

$$\log N_f = \log K_f + \left(\frac{1}{n}\right) \log C \quad 4-12$$

where K_f = Freundlich constant related to adsorption capacity (mol g⁻¹)

n = the numerical value of Freundlich constant
 (n values between 1 and 10 represent beneficial adsorption [67] and $1/n < 1$ shows the sorption capacity is only slightly suppressed at lower equilibrium concentrations [64])

The experiment was carried out by using a fixed amount of XAD-P suspended in various initial concentrations of each metal ion at $25 \pm 1^\circ\text{C}$. The equilibrium had to be attained, the remained concentration of the metal ions in solution was determined using FAAS. The data gathered from Langmuir and Freundlich equations are shown in Table 4.7 and 4.8, respectively. It was observed that the correlation coefficients (r^2) of the linear regression line of Langmuir isotherm were more than 0.99 for all the metal ions in both matrices while those of Freundlich isotherm were between 0.8680 and 0.9845. This indicated that the sorption of the metal ions onto XAD-P was more agreeable with the Langmuir model than the Freundlich one.

For Langmuir isotherm, the treated data were shown in both Figure 4.25 (left) and (right). The first one was plotted to illustrate the saturation of binding sites on the resin after increasing the metal ion concentration. And the second one presented the linearity of the regression line in order to confirm the applicability of Langmuir adsorption isotherm.

The essential characteristics of Langmuir isotherm model can be explained in term of a dimensionless constant separation factor of equilibrium parameter, R_L , given by [64, 68]

$$R_L = \frac{1}{1 + bC_0} \quad 4-12$$

where b = Langmuir constant related to energy of adsorption (L mol^{-1})

C_0 = the initial concentration of metal ion (mol L^{-1})

The parameter R_L indicated the shape of isotherm as follows.

Table 4.6 The relationship of R_L value and type of isotherm

<i>Value of R_L</i>	<i>Type of isotherm</i>
$R_L > 1$	Unfavorable
$R_L = 1$	Linear
$0 < R_L < 1$	Favorable
$R_L = 0$	Irreversible

The calculated R_L values (see Table 4.6) were between 0.01 and 0.80, indicating highly favorable sorption of all the metal ions on XAD-P in both matrices whose the data fitted reasonably well with the Langmuir isotherm.

According to the N_s Langmuir parameter, the sequence of the maximum sorption capacities on XAD-P was $Pb^{2+} > Cd^{2+} > Cr^{3+}$ in both matrices. The comparison of sorption capacities of XAD-P with other functionalized XAD-2 in DI water is shown in Table 4.9 (no report investigated the sorption capacity of sorbent towards Cr^{3+} was found). This comparison showed that XAD-P has a high sorption capacity, especially for Pb^{2+} . The availability of multiple binding sites on the XAD-P resin, as exhibited in Figure 4.24, is probably responsible for the good sorption capacity.

The selectivity of XAD-P towards metal ions is in the same direction to the sequence of the maximum sorption capacity that is $Pb^{2+} > Cd^{2+} > Cr^{3+}$. The different selectivity for each metal ion can be explained by the Hard Soft Acid Base principle (HSAB) that is hard acids prefer to coordinate to hard bases and soft acids prefer to coordinate to soft bases [29]. Three effective binding sites in the purpurin structure can be separated in two types that is (O, O) and (O, N). The oxygen atom normally acts as hard base but in this molecule, it acts as borderline base because the delocalized electron on the coplanar structure of anthraquinone reduces the ability to donate the electron to the coordinated cation. For nitrogen atom, normally acts as hard base but in

the azo group, it acts as borderline base and when attaching to purpurin molecule, it extends the coplanar conjugated system where lone pair electrons from N atoms can delocalize into the anthraquinone coplanar structure. This phenomenon should reduce the donation ability of N atoms. So N atoms at the azo linkage in the XAD-P act as soft base. Consequently, purpurin has two binding sites, namely A and C sites which are suitable for borderline acids and one binding site, namely B site which is suitable for soft acids (see Figure 4.24). According to HSAB principle, the selectivity of purpurin should be the highest with Pb^{2+} which is a borderline acid, followed by a soft acid; Cd^{2+} , and finally by Cr^{3+} (hard acid). Beside the HSAB principle, the low selectivity of purpurin toward Cr^{3+} also may be caused by the very slow sorption rate of Cr^{3+} in leachate matrix (see topic 4.5.1.2).

Considering the N_s of XAD-P in two matrices, the results showed that the N_s in leachate were lower than in DI water. This can be explained by the reducing of the binding site due to the possession of the high calcium content in leachate.

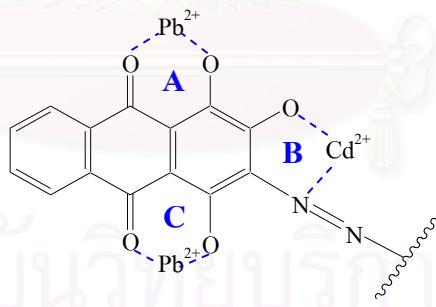


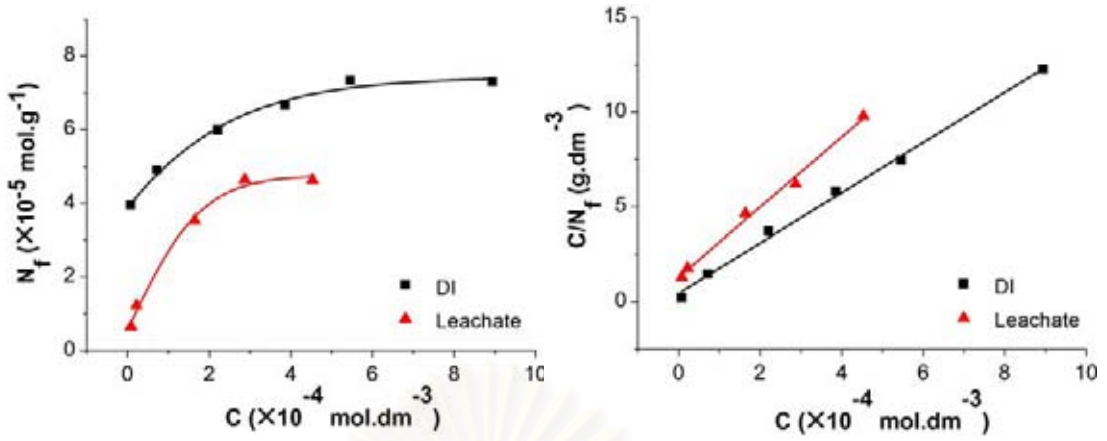
Figure 4.24 Proposed three chelation sites on XAD-P (A, B and C indicate the name of the binding sites).

Table 4.7 Langmuir parameters for the adsorption of metal ions at 25±1°C

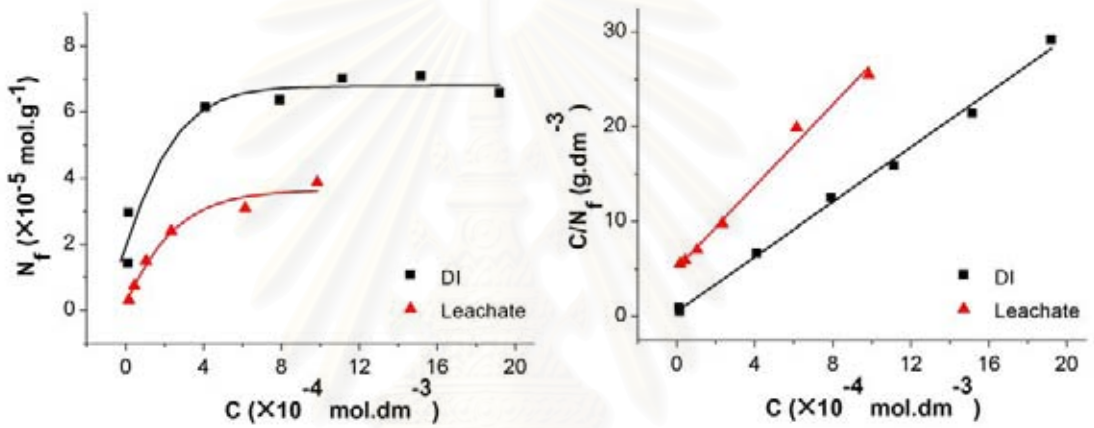
<i>Metal</i>	<i>Matrix</i>	<i>Equation</i>	r^2	$b \times 10^4$ ($L mol^{-1}$)	N_s ($\mu mol g^{-1}$)	R_L
Cd ²⁺	DI	y = 13342x + 0.4436	0.9966	3.01	75.0	0.03-0.27
	Leachate	y = 18497x + 1.2998	0.9933	1.43	54.1	0.09-0.61
Cr ³⁺	DI	y = 14672x + 0.5073	0.9957	2.89	68.2	0.01-0.26
	Leachate	y = 21506x + 5.1648	0.9904	0.42	46.5	0.17-0.80
Pb ²⁺	DI	y = 12095x + 0.3188	0.9988	3.79	82.7	0.05-0.35
	Leachate	y = 17966x + 0.7063	0.9976	2.01	55.7	0.11-0.34

Table 4.8 Freundlich parameters for the adsorption of metal ions at 25±1°C

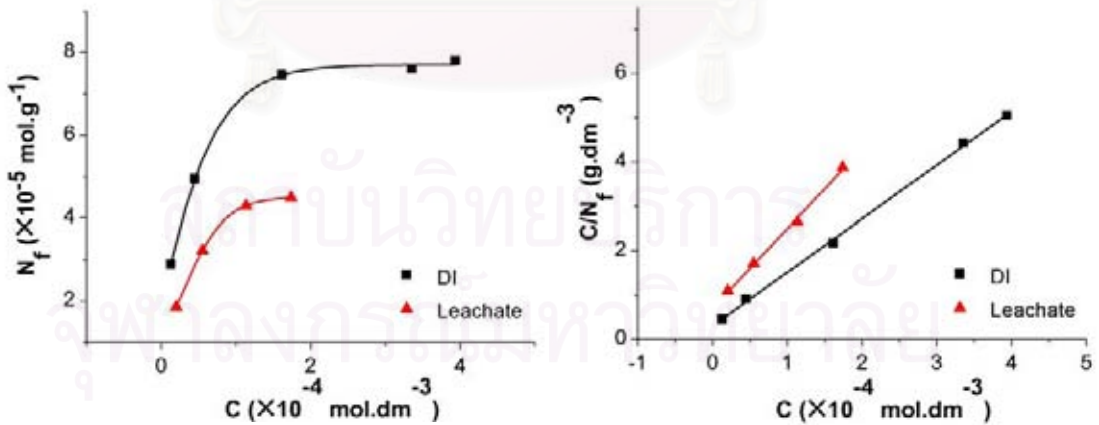
<i>Metal</i>	<i>Matrix</i>	<i>Equation</i>	r^2	K_f ($mmol g^{-1}$)	$1/n$
Cd ²⁺	DI	y = 0.1416x - 3.6972	0.9719	0.20	0.14
	Leachate	y = 0.5109x - 2.5589	0.9845	2.76	0.51
Cr ³⁺	DI	y = 0.2692x - 3.3766	0.8680	0.42	0.27
	Leachate	y = 0.6064x - 2.5150	0.9549	3.05	0.61
Pb ²⁺	DI	y = 0.2873x - 3.0961	0.9414	0.80	0.29
	Leachate	y = 0.4234x - 2.7211	0.9644	1.90	0.42



(a) Cd



(b) Cr



(c) Pb

Figure 4.25 Saturation adsorption (left) and Langmuir adsorption isotherm fitting (right) at pH 4 and $25 \pm 1^\circ\text{C}$.

Table 4.9 Comparison of sorption capacities of XAD-P with other functionalized Amberlite XAD-2 in DI water (only azo spacer linkage)

<i>chelating ligand</i>	<i>sorption capacity ($\mu\text{mol g}^{-1}$)</i>		
	<i>Cd</i>	<i>Cr</i>	<i>Pb</i>
Purpurin [this work]	75.0	68.2	87.7
<i>o</i> -aminophenol [8]	30.4	-	16.0
2-aminoacetylthiophenol [47]	190.4	-	-
Thiosalicylic acid [46]	197.5	-	-
Tiron [9]	84.5	-	60.3
Alizarin Red-S [10]	1.1	-	1.5
Pyrocatechol [44]	40.9	-	-
<i>o</i> -vanillinthiosemicarbazone [7]	-	-	9.7

4.5.2 Column Method

In column method, the experiment was progressed only in leachate matrix using a homemade column (i.d. 0.4 cm) packed with XAD-P.

4.5.2.1 Effect of flow rate

The difference the column method from the batch method is a flow of sample solution passed through packed resin. Therefore, the flow rate of sample solution should be optimized. The degree of sorption was studied at different flow rates and reported by %extraction, as illustrated in Figure 4.26. The %extraction was calculated using the following equation.

$$\%extraction = \frac{mg_{adsorbed}}{mg_{bef}} \times 100 \quad 4-13$$

Where $mg_{adsorbed}$ = the amount of metal ion adsorbed on resin (mg)

mg_{bef} = the amount of metal ion before extraction (mg)

The results showed that the %extraction was very low even though a very slow flow rate at 0.5 mL min^{-1} was applied. Moreover, at flow rates greater than 0.5 mL min^{-1} , the %extraction decreased. This can be explained by the slow kinetics of metal-purpurin complex in leachate and the equilibrium time was previously found at around 1 hour for all the metal ions. Therefore, the dynamic system in the column method was not recommended for XAD-P.

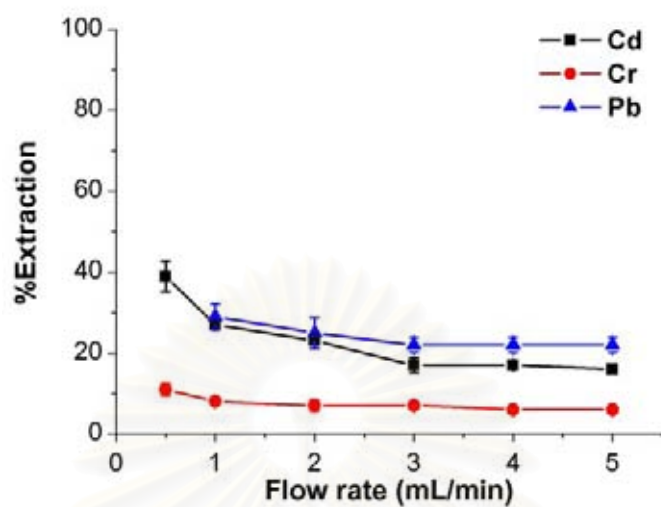


Figure 4.26 Effect of solution flow rate on metal extraction (1, 5 and 5 ppm for Cd^{2+} , Cr^{3+} and Pb^{2+} , respectively, pH 4).

4.5.2.2 Recirculation of sample solution

From the latter topic, the results showed the very low percent extraction of metal ions. To improve the degree of metal ion sorption on XAD-P, the recirculation of sample solution was applied. To reduce the experiment time, the flow rate at 5 mL min^{-1} was chosen. The results are shown in Figure 4.27.

The result showed that the recirculation system could raise the percent extraction. The percent extraction was a directly proportional to the cycle number. The percent extraction of Cd and Pb increased up to 80% when using 30 cycles of sample solution recirculation. As well as the percent extraction of Cr could be improved but it still low around 50% after 40 cycles of recirculation.

Although the percent extractions could be improved using the recirculation system, time consumption is a main drawback for this system. Therefore, the use of XAD-P in the column method needs to be further developed.

In addition, the increase of the amount of XAD-P together with the recirculation of sample solution may be used for improving the extraction efficiency.

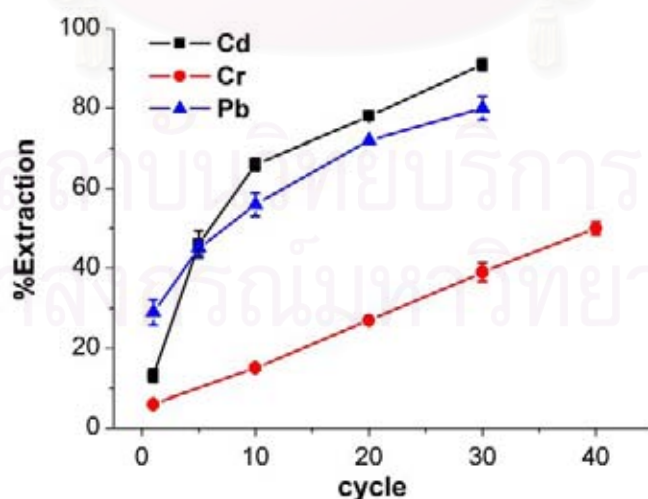


Figure 4.27 Effect of recirculation of sample solution at pH 4

(1, 5 and 5 ppm for Cd^{2+} , Cr^{3+} and Pb^{2+} , respectively).

4.5.2.3 Desorption study

Since the rate of metal desorption using 1% HNO_3 and 10% H_2O_2 in 0.1 M NaOH were rapid (see topic 4.5.1.4), they might be applied to the column system. Therefore, we attempted to use the suitable eluents to elute the metal ions in the column system using a slow flow rate at 1 mL min^{-1} . The results are shown in Table 4.10.

The results showed that the desorption using the column system gave a percent stripping less than those previously obtained from the batch system because the contact time between the eluents and the sorbed metal ions might not be sufficient .

Table 4.10 Comparison of the percent stripping of metal ions by the column and batch methods

<i>metal</i>	<i>suitable eluent</i>	<i>%strip (Mean value \pm SD, n=3)</i>	
		Column	Batch
Cd	1% HNO_3	84 ± 2.01	92 ± 1.74
Cr	10% H_2O_2 (in 0.1 M NaOH)	68 ± 4.39	93 ± 4.39
Pb	1% HNO_3	72 ± 2.63	93 ± 1.80

4.6 Method Validation

After the optimum condition for the extraction of Cd^{2+} , Cr^{3+} and Pb^{2+} in leachate from cement-based stabilized waste using XAD-P was achieved, the method validation should be investigated in order to check the accuracy and precision of the new proposed extraction method. The experiment was carried out in batch method by extracting metal ion spiked leachate at 1, 5 and 5 ppm for Cd^{2+} , Cr^{3+} and Pb^{2+} , respectively using 0.0500 ± 0.0002 g of XAD-P. The pH of the solutions was fixed at pH 4.0 and the extraction time was 1 hour. These levels of spiked concentration refer to the regulatory level of heavy metal found in leachate [24]. After sorption, the sorbed metal ions were eluted with 1% HNO_3 for Cd^{2+} and Pb^{2+} and 10% H_2O_2 in 0.1 M NaOH for Cr^{3+} using elution time of 30 min for Cd^{2+} and Pb^{2+} and 60 min for Cr^{3+} .

The results, as shown in Table 4.11, showed that the accuracy (%recovery) and precision (%RSD) of this method were acceptable for Cd^{2+} and Pb^{2+} , according to the criteria of analyte recovery and precision at different concentration [69], as shown in Table 4.12. Therefore, XAD-P resin was suitable to extract Cd^{2+} and Pb^{2+} from leachate without interfering from high content of calcium ions.

Table 4.11 Recovery and precision of the proposed method

<i>Metal</i>	<i>Spiked concentration (ppm)</i>	<i>Recovery^a (%)</i>	<i>RSD^a (%)</i>
Cd^{2+}	1	86.5	2.1
Cr^{3+}	5	56.9	4.8
Pb^{2+}	5	89.9	2.3

^aMean value (n=14)

Table 4.12 Analyte recovery and precision at different concentration

Analyte, %	Analyte ratio	Unit	Mean recovery, %	RSD, %
100	1	100%	98-102	1.3
10	10^{-1}	10%	98-102	2.8
1	10^{-2}	1%	97-103	2.7
0.1	10^{-3}	0.1%	95-105	3.7
0.01	10^{-4}	100 ppm	90-107	5.3
0.001	10^{-5}	10 ppm	80-110	7.3
0.0001	10^{-6}	1 ppm	80-110	11
0.00001	10^{-7}	100 ppb	80-110	15
0.000001	10^{-8}	10 ppb	60-115	21
0.0000001	10^{-9}	1 ppb	40-120	30

สถาบันวิทยบริการ
จุฬาลงกรณ์มหาวิทยาลัย

CHAPTER V

CONCLUSION

Concomitants such as calcium ions in the leachate from cement-based stabilized waste cause the important problem for the determination of leached toxic heavy metal ions because it can reduce metal ion analytical signals and lead to short lifetime of instruments used. Therefore, the extraction of heavy metal ions from leachate matrix should be done before the detection. In this work, a new chelating resin, Amberlite XAD-2 functionalized with purpurin through azo spacer linkage (XAD-P) was synthesized and used for the extraction of Cd^{2+} , Cr^{3+} and Pb^{2+} from the leachate before their determination using FAAS.

The synthesis of XAD-P was accomplished using three steps that are nitration, reduction, and *in situ* diazotization-coupling with purpurin. The product from each synthesis step was characterized by scanning electron microscopy (SEM), elemental analysis (EA), Fourier transforms infrared (FT-IR) and Raman (FT-Raman) spectroscopy and thermal gravimetric analysis (TGA). SEM photographs showed the difference between XAD-2 and XAD-P surface. The results of EA indicated the C, H and N composition in each step and the percent conversions for nitration, reduction and diazotization-coupling with purpurin were estimated to be 95, 66 and 89%, respectively. FT-Raman confirmed the structure of the polymeric products. The attachment of purpurin onto the Amberlite XAD-2 was confirmed by FT-IR and TGA. FT-IR spectrum of XAD-P showed $\nu(\text{C}=\text{O})$ and $\nu(\text{C}-\text{O})$ of purpurin at 1704 and 1347 cm^{-1} , respectively and TGA showed the decomposition of purpurin on XAD-P that began at 250°C. Therefore, the results from all characterization techniques exhibited the success of the XAD-P synthesis.

From the study of the appropriate amount of purpurin for XAD-P synthesis, 1 g of purpurin per 10 g XAD-2 was recommended. The influence of the matrix of the leachate on metal ion calibration curves was studied. The results indicated that the leachate matrix could reduce the absorbance signal of the metal ions.

The optimum conditions had been investigated before using XAD-P for the extraction and desorption of Cd^{2+} , Cr^{3+} and Pb^{2+} . The experiments were done in both batch and column methods and the experimental results of the extraction of metal ions from leachate and DI water matrices were compared. The optimum conditions for batch method are summary in Table 5.1.

Table 5.1 Optimum conditions for the sorption and desorption of metal ions on XAD-P

<i>Experimental parameters</i>	Cd^{2+}	Cr^{3+}	Pb^{2+}
Solution pH ^a	4.0	4.0	4.0
Equilibrate time (min)			
DI water	20	10	30
Leachate	20	40	30
Eluent	1% HNO_3	10% H_2O_2 ^b	1% HNO_3
Elution time (min)	10	30	10
sorption capacity ($\mu mol g^{-1}$)			
DI water	75.0	68.2	82.7
Leachate	54.1	46.5	55.7
%recovery ^c	86.5	56.9	89.9
%RSD ^c	2.1	4.8	2.3

^a in both matrices: leachate and DI water

^b in 0.1 M NaOH

^c in leachate only (n=14)

For column method, the experiment was carried out only in leachate matrix, the slowest flow rate (0.5 mL min^{-1}) could not efficiently extract all metal ions. Nevertheless, the extraction efficiency could be improved by the recirculation of sample solution. The desorption of sorbed metal ions could be succeeded using the same eluents as those used in batch method but the percent stripping was lower.

For the method validation in batch method, it gave a good accuracy at 86.5 and 89.9% recovery for Cd^{2+} and Pb^{2+} and %RSD less than 2.3% ($n=14$).

This newly developed chelating resin, Amberlite XAD-2 functionalized with purpurin was successfully applied for the extraction of Cd^{2+} and Pb^{2+} from leachate matrix in batch method. Many advantages have been concluded as follows, the resin was easily synthesized and exhibited high sorption capacity and high selectivity towards for Pb^{2+} and Cd^{2+} and the elution was successful using 1% HNO_3 within 10 min. However, the main disadvantage of XAD-P is the slow extraction kinetics in leachate matrix, so the application in column method is limited.

Suggestions for Future Work

This research aimed at the extraction of Cd^{2+} , Cr^{3+} and Pb^{2+} in leachate from cement-based stabilized waste, thus the effect of other interference ions on heavy metal ion sorption was not investigated. If XAD-P is applied for the extraction of metal ions from other samples such as tap water, sea water or industrial waste water, the effect of various interference ions on the metal sorption should be further studied. In addition, to increase the attraction of XAD-P, the reuse of this resin shall be also investigated.

REFERENCES

- [1] Batchelor, B. Overview of waste stabilization with cement. Waste Management 26 (2006): 689-698.
- [2] Amonsit, M.; and Petchsom, A. Principle and techniques of instrumental analysis. Bangkok: chuanpim, 1991.
- [3] Shawabkeh, R. A. Solidification and stabilization of cadmium ions in sand-cement-clay mixture. Journal of Hazardous Materials 125 (2005): 237-243.
- [4] Lemos, V. A.; Santos, J. S.; Nunes, S. L.; Carvalho, M. B.; Baliza, P. X.; and Yamaki, R. T. Amberlite XAD-2 functionalized with Nitroso R salt: synthesis and application in an online system for preconcentration of cobalt. Analytica Chimica Acta 494 (2003): 87-95.
- [5] Venkatesh, G.; and Singh, A. K. 2-{{[1-(3,4-Dihydroxyphenyl)methylidene]amino}benzoic acid immobilized Amberlite XAD-16 as metal extractant. Talanta 67 (2005): 187-194.
- [6] Lemos, V. A.; Silva, D. G.; Carvalho, A. L.; Santana, D. A.; Novaes, G. S.; and Passos, A. S. Synthesis of amberlite XAD-2-PC resin for preconcentration and determination of trace elements in food samples by flame atomic absorption spectrometry. Microchemical Journal 84 (2006): 14-21.
- [7] Jain, V. K.; Sait, S. S.; Shrivastav, P.; and Agrawal, Y. K. Application of chelate forming resin Amberlite XAD-2-o-vanillinthiosemicarbazone to the separation and preconcentration of copper(II), zinc(II) and lead(II). Talanta 45 (1997): 397-404.
- [8] Kumar, M.; Rathore, D. P. S.; and Singh, A. K. Amberlite XAD-2 functionalized with o-aminophenol: synthesis and applications as extractant for copper(II), cobalt(II), cadmium(II), nickel(II), zinc(II) and lead(II). Talanta 51 (2000): 1187-1196.

- [9] Kumar, M.; Rathore, D. P. S.; and Singh, A. K. Metal ion enrichment with Amberlite XAD-2 functionalized with Tiron: analytical applications. The Analyst 125 (2000): 1221-1226.
- [10] Saxena, R.; Singh, A. K.; and Sambhi, S. S. Synthesis of a chelating polymer matrix by immobilizing Alizarin Red-S on Amberlite XAD-2 and its application to the preconcentration of lead(II), cadmium(II), zinc(II) and nickel(II). Analytica Chimica Acta 295 (1994): 199-204.
- [11] Prabhakaran, D.; and Subramanian, M. S. Selective extraction and sequential separation of actinide and transition ions using AXAD-16-BTBED polymeric sorbent. Reactive and Functional Polymers 57 (2003): 147-155.
- [12] Jing, C.; Liu, S.; Korfiatis, G. P.; and Meng, X. Leaching behavior of Cr(III) in stabilized/solidified soil. Chemosphere 64 (2006): 379-385.
- [13] Yang, C. Y.; Shaaban, M. G.; and Mahmud, H. B. Stabilization/solidification of lead-contaminated soil using cement and rice husk ash. Journal of Hazardous Materials 137 (2006): 1758-1764.
- [14] Hazardous waste[Online]. U.S. Environmental Protection Agency. Available from: <http://www.epa.gov/epaoswer/osw/hazwaste.htm>[2007, August 14]
- [15] Cadmium[Online]. U.S. Department of Labor : Occupational Safety & Health Administration. Available from: <http://www.osha.gov/SLTC/cadmium/> [2007, August 15]
- [16] Lajis, R. The effects of cadmium[Online]. National Poison Centre, University Sains Malaysia, Penang. Available from: <http://www.prn2.usm.my/mainsite/bulletin/sun/1995/sun36.html>[2007, August 15]
- [17] Camel, V. Solid phase extraction of trace elements. Spectrochimica Acta Part B 58 (2003): 1177-1233.
- [18] Chromium toxicity[Online]. (n.d.). Available from: <http://www.corrosion-doctors.org/Pollution/chromiumtoxicity.htm>[2007, August 15]

- [19] The toxicity of Lead[Online]. (n.d.). Available from: <http://www.macslab.com/toxic.html>[2007, August 15]
- [20] Water Quality standards[Online]. Pollution control Department, Ministry of Natural Resources and Environment. Available from: http://www.pcd.go.th/Info_serv/en_reg_std_water01.html[2007, August 16]
- [21] Cyanide and heavy metal removal[Online]. Advanced Chemical Technilogy. Available from: http://www.actglobal.net/products_wastewater_heavy_metals.htm[2007, August 16]
- [22] Townsend, T.; Jang, Y. C.; and Tolaymat T. A Guide to the Use of Leaching Tests in Solid Waste Management Decision Making[online]. The Florida Center for Solid and Hazardous Waste Management, (2003). Available from: [http://www.hinkleycenter.com/publications/0301\(A\)_A%20Guide%20to%20Leaching%20Tests-Final.pdf](http://www.hinkleycenter.com/publications/0301(A)_A%20Guide%20to%20Leaching%20Tests-Final.pdf)[2007, August 17]
- [23] Method 1312: Synthetic precipitation leaching procedure[Online]. (n.d.). Available from: http://www.accustandard.com/asi/pdfs/epa_methods/1312.pdf[2007, August 1]
- [24] The Ministry of Industry of Thailand. The notification of the Ministry of Industry No.6 [B.E.2540 (1997)] issued pursuant to the factory act B.E. 2535(1992) subject: disposal of wastes or unusable materials. 1997.
- [25] The Ministry of Industry of Thailand. The notification of the Ministry of Industry No.2 [B.E.2539 (1998)] issued pursuant to the factory act B.E. 2535(1992) subject: waste water industry regulations. 1998.
- [26] Prichard, E.; MacKay G. M.; and Point, J. Trace analysis. Bodmin, UK: Great Britain by Hartnolls, 1996.
- [27] Simpson, N. J. K. Solid-phase extraction principle, technique, and applications. New york: Marcel Dekker, 2000.
- [28] Wells, M. J. M. Essential guides to method development in solid-phase extraction. Encyclopedia of Separation Science 10 (2000): 4636-4643.

- [29] Pearson, R. G. Hard and soft acids and bases-the evolution-the evolution. Coordination Chemistry Reviews 100 (1990): 403-425.
- [30] Gary, L.; and Miessler, D. A. T. Inorganic Chemistry. 3rd ed. New Jersey: Pearson Prentice Hall, Pearson Education, 2004.
- [31] Akelah, A.; and Moet, A. Functionalized polymers and their applications. Great Britain: Chapman and Hall, 1990.
- [32] Schroeder, E.D. Water and wastewater Treatment. Tokyo, Japan: Tosho, 1977.
- [33] Scanning Electron Microscope (SEM)[Online]. (n.d.). Available from: <http://www.unl.edu/CMRAcfe/semoptic.htm>[2007, August 17]
- [34] Theiner, J. C/H/N-analysis[Online]. Microanalysis Laboratory, University of Wien. Available from: http://www.univie.ac.at/Mikrolabor/chn_eng.htm [2007, August 17]
- [35] Ingle, J. D., Jr.; and Crouch, S. R. Spectrochemical analysis. United states of America: Prentice-Hall International, 1988.
- [36] Fourier Transform Infrared Spectroscopy[Online]. West Coast Analytical Service. Available from: <http://www.wcaslab.com/tech/tbftir.htm>[2007, August 17]
- [37] Spectrometer applications Raman measurement[Online]. avantes. Available from: <http://www.avantes.com/news/raman.pdf>[2007, August 17]
- [38] Infrared & Raman Microspectrometry[Online]. (n.d.). Available from: http://www.felmi-zfe.tugraz.at/research_raman.html[2007, August 17]
- [39] Thermal Gravimetric Analysis[Online]. orton. Available from: <http://www.si-mex.com.mx>[2007, August 17]
- [40] Stafilov, T.; and Zendelovska, D. Determination of cobalt, copper, lead and nickel in gypsum by zeemzn electrothermal atomic absorption spectrometry. Acta Chimica Slovenica 47 (2000): 381-388.

- [41] Stafilov, T.; Zendelovska, D.; Pavlovska, G.; and Cundeveva, K. Determination of trace elements in dolomite and gypsum by atomic absorption spectrometry: overcoming the matrix interference by flotation separation. Spectrochimica Acta Part B 57 (2002): 907–917.
- [42] Product data sheet: Amberlite XAD-16[Online]. Rohm and Haas Company. Available from: http://www.advancedbiosciences.com/Bioprocessing_doc/english/xad16.PDF[2007, August 18]
- [43] Prabhakaran, D.; and Subramanian, M. S. A new chelating sorbent for metal ion extraction under high saline conditions. Talanta 59 (2003): 1227-1236.
- [44] Tewari, P. K.; and Singh, A. K. Synthesis, characterization and applications of pyrocatechol modified amberlite XAD-2 resin for preconcentration and determination of metal ions in water samples by flame atomic absorption spectrometry (FAAS). Talanta 53 (2001): 823–833.
- [45] Guo, Y.; Din, B.; Liu, Y.; Chang, X.; Meng, S.; and Tian, M. Preconcentration of trace metals with 2-(methylthio)aniline-functionalized XAD-2 and their determination by flame atomic absorption spectrometry. Analytica Chimica Acta 504 (2004): 319-324.
- [46] Tewari, P. K.; and Singh, A. K. Thiosalicylic acid-immobilized Amberlite XAD-2: metal sorption behaviour and applications in estimation of metal ions by flame absorption spectrometry. The Analyst 125 (2000): 2350-2355.
- [47] Guo, Y.; Din, B.; Liu, Y.; Chang, X.; Meng, S.; and Liu, J. Preconcentration and determination of trace elements with 2-aminoacetylthiophenol functionalized Amberlite XAD-2 by inductively coupled plasma-atomic emission spectrometry. Talanta 62 (2004): 209-215.
- [48] Tewari, P. K.; and Singh, A. K. Preconcentration of lead with Amberlite XAD-2 and Amberlite XAD-7 based chelating resins for its determination by flame atomic absorption spectrometry. Talanta 56 (2002): 735–744.

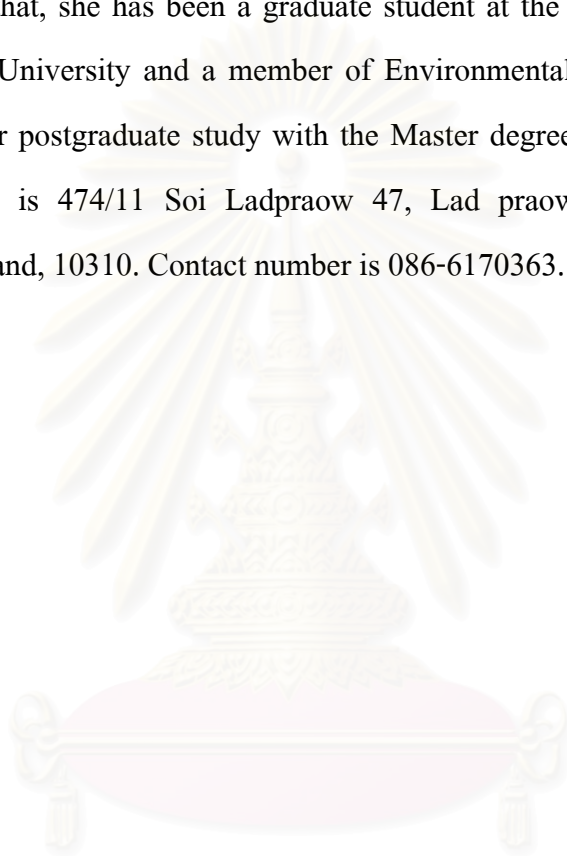
- [49] Saxena, R.; and Singh, A. K. Pyrocatechol Violet immobilized Amberlite XAD-2: synthesis and metal-ion uptake properties suitable for analytical applications. *Analytica Chimica Acta* 340 (1997): 285-290.
- [50] Cekic, S. D.; Filik, H.; and Apak, R. Use of an o-aminobenzoic acid-functionalized XAD-4 copolymer resin for the separation and preconcentration of heavy metal(II) ions. *Analytica Chimica Acta* 505 (2004): 15-24.
- [51] Vanloot, P.; Boudenne, J. L.; Brach, P. C.; Sergent, M.; and Coulomb, B. An experimental design to optimize the flow extraction parameters for the selective removal of Fe(III) and Al(III) in aqueous samples using salicylic acid grafted on Amberlite XAD-4 and final determination by GF-AAS. *Journal of Hazardous Materials* 147 (2007): 463-470.
- [52] Metilda, P.; Sanghamitra, K.; Mary, G. J.; Naidu, G. R. K.; and Prasada, R. T. Amberlite XAD-4 functionalized with succinic acid for the solid phase extractive preconcentration and separation of uranium(VI). *Talanta* 65 (2005): 192-200.
- [53] Ramesh, A.; Mohan, K. R.; and Seshaiyah, K. Preconcentration of trace metals on Amberlite XAD-4 resin coated with dithiocarbamates and determination by inductively coupled plasma-atomic emission spectrometry in saline matrices. *Talanta* 57 (2002): 243-252.
- [54] Memon, S.Q.; Hasany, S. M.; Bhangar, M. I.; and Khuhawar, M. Y. Enrichment of Pb(II) ions using phthalic acid functionalized XAD-16 resin as a sorbent. *Journal of Colloid and Interface Science* 291 (2005): 84-91.
- [55] Ramirez, A. A.; Linares, C. J.; Barrero, F. A.; and Ceba, M. R. Study of the mixed-metal lanthanum-magnesium-purpurin complex: spectrophotometric determination of yttrium and lanthanides. *Talanta* 33(12) (1986): 1021-1025.

- [56] Arrebola, A.; Bagur, M. G.; Vinas, M. S.; Gazquez, D.; Romero, R.; and Camino, M. Indirect determination of total yttrium and lanthanides by flame atomic absorption measurement of magnesium after extraction of their ternary complexes with purpurin (1,2,4-trihydroxyanthraquinone) and magnesium into isobutyl methyl ketone. Journal of Analytical Atomic Spectrometry 13 (1998): 765-768.
- [57] Idriss, K.A.; Sedaira, H.; Abdel-Aziz, M.S.; and Ahmad, H. M. Rapid test methods for minor components analysis of hydraulic cement. Spectrophotometric determination of manganese oxide content of Portland cement and cement raw meal. Talanta 50 (1999): 913-919.
- [58] Idriss, K.A., Sedaira, H.; and Ahmad, H. M. An insight into the solution equilibria of magnesium(II) with purpurin and spectrophotometric determination of magnesium. Talanta 54 (2001): 369-375.
- [59] Ahmad, M.; and Narayanaswamy, R. Optical fiber Al (III) sensor based on solid surface fluorescence measurement. Sensors and Actuators B 81 (2002): 259-266.
- [60] Hageman P. L.; Briggs, P. H.; Desborough, G. A.; Lamothe, P. J.; and Theodorakos, P. J. Synthetic precipitation leaching procedure (SPLP) leachate chemistry data for solid minewaste composite samples from southwestern new mexico, and leadville, colorado. Available from: http://pubs.usgs.gov/of/2000/0033/pdf/of00-33_508.pdf[2007, August 20]
- [61] Hydroxide Precipitation[Online]. Hoffland Environmental. Available from: <http://www.hoffland.net/src/tks/3.xml>[2007, August 19]
- [62] Mei Peng Hor, L. L; Su, F.; and Zhao, X. S. Competitive adsorption of Pb^{2+} , Cu^{2+} , and Cd^{2+} ions on microporous titanosilicate ETS-10. Journal of Colloid and Interface Science 287(1) (2005): 178-184.

- [63] Lerkmangkorn, W. Speciation analysis and preconcentration of chromium using chemically modified silica. Master's Thesis, Department of Chemistry, Science, Chulalongkorn University, 2006.
- [64] Memon, S. Q.; Bhanger, M. I.; Hasany, S. M.; Khuhawar, M. Y. Sorption behavior of impregnated Styrofoam for the removal of Cd(II) ions. Colloids and Surfaces A: Physicochem. Eng. Aspects 279 (2006): 142-148.
- [65] Andersen, J. E. T. Introduction of hydrogen peroxide as an oxidant in flow injection analysis: speciation of Cr(III) and Cr(VI). Analytica Chimica Acta 361 (1998): 125-131.
- [66] Zhai, Y.; Wei, X.; Zeng, G.; Zhang, D.; and Chu, K. Study of adsorbent derived from sewage sludge for the removal of Cd²⁺, Ni²⁺ in aqueous solutions. Separation and Purification Technology 38(2) (2004): 191-196.
- [67] Igwe, J. C.; and Abia, A. A. Adsorption isotherm studies of Cd (II), Pb (II) and Zn (II) ions bioremediation from aqueous solution using unmodified and EDTA-modified maize cob. Ecletica Quimica 32(1) (2007): 33-42.
- [68] Kumar, K. V.; and Porkodi, K. Batch adsorber design for different solution volume/adsorbent mass ratios using the experimental equilibrium data with fixed solution volume/adsorbent mass ratio of malachite green onto orange peel. Dyes and Pigments 74(3) (2007): 590-594.
- [69] Mark, R.L. Validation and qualification in analytical laboratories. Illinois: Interpharm Press, 1999.

VITA

Miss Marisa Wongkaew was born on March 10, 1983 in Roi-Et, Thailand. She received her Bachelor degree of Science in Chemistry from Chulalongkorn University in 2005. After that, she has been a graduate student at the Department of Chemistry Chulalongkorn University and a member of Environmental Analysis Research Unit. She finished her postgraduate study with the Master degree of Science in 2008. The present address is 474/11 Soi Ladpraow 47, Lad praow Road, Wongtonghlang, Bangkok, Thailand, 10310. Contact number is 086-6170363.



สถาบันวิทยบริการ
จุฬาลงกรณ์มหาวิทยาลัย